LAND VEHICLE NAVIGATION WITH GPS/INS SENSOR FUSION USING KALMAN FILTER

A THESIS SUBMITTED TO
THE GRADUATE SCHOOL OF NATURAL AND APPLIED SCIENCES
OF
MIDDLE EAST TECHNICAL UNIVERSITY

BY

MUSTAFA EMRE AKÇAY

IN PARTIAL FULFILLMENT OF THE REQUIREMENTS
FOR
THE DEGREE OF MASTER OF SCIENCE
IN
MECHANICAL ENGINEERING DEPARTMENT

DECEMBER 2008

Approval of the thesis

"**LAND VEHICLE NAVIGATION WITH GPS/INS SENSOR FUSION USING KALMAN FILTER**"

Submitted by **MUSTAFA EMRE AKÇAY** in partial fulfillment of the requirements for the degree of **Master of Science in Mechanical Engineering Department, Middle East Technical University** by,

Prof. Dr. Canan Özgen _____
Dean, Graduate School of **Natural and Applied Sciences**

Prof. Dr. Süha Oral _____
Head of Department, **Mechanical Engineering**

Assist. Prof. Dr. E. İlhan Konukseven _____
Supervisor, Mechanical Engineering Dept., METU

Prof. Dr. M. Kemal Özgören _____
Co-Supervisor Mechanical Engineering Dept., METU

Examining Committee Members:

Prof. Dr. Reşit Soylu _____
Mechanical Engineering Dept., METU

Assist. Prof. Dr. E. İlhan Konukseven _____
Mechanical Engineering Dept., METU

Prof. Dr. M. Kemal Özgören _____
Mechanical Engineering Dept., METU

Prof. Dr. M. Kemal Leblebicioğlu _____
Electrical Engineering Dept., METU

Prof. Dr. Ozan Tekinalp _____
Aerospace Engineering Dept., METU

Date: 04 / 12 / 2008

I hereby declare that all information in this document has been obtained and presented in accordance with academic rules and ethical conduct. I also declare that, as requires by thesis rules and conduct, I have fully cited and referenced all material and results that are not original to this work.

Name, Last Name : Mustafa Emre AKÇAY

Signature :

ABSTRACT

LAND VEHICLE NAVIGATION WITH GPS/INS SENSOR FUSION USING KALMAN FILTER

Akçay, Mustafa Emre

M.S. Department of Mechanical Engineering

Supervisor: Assist. Prof. Dr. E. İlhan Konukseven

Co-Supervisor: Prof. Dr. M. Kemal Özgören

December 2008, 115 Pages

Inertial Measurement Unit (IMU) and Global Positioning System (GPS) receivers are sensors that are widely used for land vehicle navigation. GPS receivers provide position and/or velocity data to any user on the Earth's surface independent of his position. Yet, there are some conditions that the receiver encounters difficulties, such as weather conditions and some blockage problems due to buildings, trees etc. Due to these difficulties, GPS receivers' errors increase. On the other hand, IMU works with respect to Newton's laws. Thus, in stark contrast with other navigation sensors (i.e. radar, ultrasonic sensors etc.), it is not corrupted by external signals. Owing to this feature, IMU is used in almost all navigation applications. However, it has some disadvantages such as possible alignment errors, computational errors and instrumentation errors (e.g., bias, scale factor, random noise, nonlinearity etc.). Therefore, a fusion or integration of GPS and IMU provides a more accurate navigation data compared to only GPS or only IMU navigation data.

In this thesis, loosely coupled GPS/IMU integration systems are implemented using feed forward and feedback configurations. The mechanization equations, which convert the IMU navigation data (i.e. acceleration and angular velocity components) with respect to an inertial reference frame to position, velocity and orientation data with respect to any desired frame, are derived for the geographical frame. In other words, the mechanization equations convert the IMU data to the Inertial Navigation System (INS) data. Concerning this conversion, error model of INS is developed using the perturbation of the mechanization equations and adding the IMU's sensor's error model to the perturbed mechanization equation. Based on this error model, a Kalman filter is constructed. Finally, current navigation data is calculated using IMU data with the help of the mechanization equations. GPS receiver supplies external measurement data to Kalman filter. Kalman filter estimates the error of INS using the error mathematical model and current navigation data is updated using Kalman filter error estimates.

Within the scope of this study, some real experimental tests are carried out using the software developed as a part of this study. The test results verify that feedback GPS/INS integration is more accurate and reliable than feed forward GPS/INS. In addition, some tests are carried out to observe the results when the GPS receiver's data lost. In these tests also, the feedback GPS/INS integration is observed to have better performance than the feed forward GPS/INS integration.

Keywords: Global Positioning System (GPS), Inertial Measurement Unit (IMU), Inertial Navigation System (INS), Sensor Integration, Kalman Filter, Feedback Loosely Coupled Integration, Feed Forward Loosely Coupled Integration.

ÖZ

KALMAN SÜZGECİ YARDIMI İLE KYS/ASS BİRLEŞTİRİLEREK BİR KARA ARACININ SEYRÜSEFER BİLGİSİNİN ELDE EDİLMESİ

Akçay, Mustafa Emre

Yüksek Lisans, Makina Mühendisliği Bölümü
Tez Yöneticisi: Yrd. Doç. Dr. E. İlhan Konukseven
Ortak Tez Yöneticisi: Prof. Dr. M. Kemal Özgören

Aralık 2008, 115 Sayfa

Ataletsel Ölçüm Birimi (AÖB) ve Küresel Yerbulum Sistemi (KYS) kara araçlarının seyrüsefer uygulamalarında oldukça sık kullanılan sensörlerdir. KYS konum ve/veya hız bilgisini dünyanın herhangi bir yerinde olan kullanıcıya verebilmektedir. Fakat KYS, hava koşullarından ve binalar, ağaçlar gibi çeşitli nesnelerin sinyallari engellemesinden etkilenmektedir. Bu sebebler de KYS'nin ölçüm hatalarını arttırmaktadır. Öte yandan AÖB Newton'un hareket yasalarına dayanarak çalışan bir sistemdir. Bu yüzden, diğer seyrüsefer sistemlerinde (örneğin radar, ultasonic algılayıcılar v.b.) olduğu gibi dışarıdan herhangi bir bozucu sinyal ile işlevselliğini kaybetmez. Bu özelliği hemen hemen tüm seyrüsefer sistemlerinde kullanılmasını zorunlu hala getirir. Fakat AÖB sisteminin bazı olumsuz yanları vardır, örneğin başlangıç yönelim hataları, nümerik hesaplardan dolayı meydana gelen hatalar ve algılayıcı hataları (sabit kayma hatası, boyutlandırma hatası, rasgele gürültüler, lineer olmayan etkiler v.b.). Bu sebeplerden dolayı, KYS ve AÖB sistemlerinin

birleştirilmesi yalnızca KYS veya yalnızca AÖB seyrüsefer bilgisinden çok daha hassas seyrüsefer bilgisi elde edilmesini sağlar.
Bu tez çalışmasında ileri beslemeli ve geri beslemeli gevşek bağlı AÖB ve KYS bütünleştirmesi gerçekleştirilmiştir. AÖB'nin atalet eksenine göre ölçtüğü ivme ve açısal hız verilerini istenen bir koordinat eksenine çeviren mekanizasyon denklemleri lokal coğrafi koordinat eksenine göre çıkarılmıştır. Diğer bir ifadeyle, bu denklemler AÖB yi Ataletsel Seyir Sistemine (ASS) dönüştürmektedir. Daha sonra, ASS'nin matematiksel hata modeli küçük sapmalar yönteminin mekanizasyon denklemlerine uygulanması ve AÖB algılıyıcılarının matematiksel hata modellerinin eklenmesiyle oluşturulmuştur. Bu matematiksel hata modeline dayanarak, Kalman filtresi oluşturulmuştur. Sonuç olarak, herhangi bir andaki seyrüsefer bilgisi mekanizasyon denklemlerinin AÖB tarafından ölçülen değerleri kullanarak hesaplanmasıyla bulunur, KYS alıcısı Kalman filtresine ölçüm bilgisi sağlar. Kalman filtresi de ASS'nin hatalarını matematiksel hata modeli sayesinde tahmin eder ve anlık seyrüsefer bilgisi tahmin edilen bu hata ile düzeltilir.

Tezin kapsamında içinde bazı gerçek testler tezin içinde geliştirilen yazılımı kullanarak gerçekleştirilmiştir. Sonuç olarak, geri beslemeli KYS/ASS bütünleştirmesi ileri beslemeli KYS/ASS bütünleştirmesine göre daha hassas ve güvenilir olduğunu göstermiştir. Buna ek olarak, KYS'nin ölçüm bilgisinin kaybolması durumunda ne olacağını araştırmak için de bazı testler yapılmıştır. Bu testlerde de, geri beslemeli KYS/ASS bütünleştirmesi, ileri beslemeli KYS/ASS sistemine göre daha iyi performans sağlandığı görülmüştür.

Anahtar Kelimeler : Küresel Yerbulum Sistemi (KYS; GPS), Ataletsel Ölçüm Birimi (AÖB; IMU), Ataletsel Seyir Sistemi (ASS; INS), Algılayıcı entegrasyonu, Kalman filtresi, Geri beslemeli gevşek bütünleştirme, İleri beslemeli gevşek bütünleştirme.

To My Family

ACKNOWLEDGMENT

I would like to thank my thesis supervisor Assist. Prof. Dr. E. İlhan Konukseven and co-supervisor Prof. Dr. M. Kemal Özgören for providing me this research opportunity, and guiding me through the study.

I would also like to thank to Özge Arslan and Orhan Ölçücüoğlu for their friendships.

Finally, I owe the greatest thanks to my dear family for their endless support throughout my education.

TABLE OF CONTENTS

LIST OF TABLES

LIST OF FIGURES

LIST OF SYMBOLS AND ABBREVIATIONS

Symbols

μ	Latitude
λ	Longitude
h	Height
R	Length of the semi-major axis of the Earth
r	Length of the semi-minor axis of the Earth
f	Flattening of the ellipsoid
e	Major eccentricity of the ellipsoid
Ω	Earth's rate
R_E	The transverse radius of curvature
R_N	The meridian radius of curvature
C	The meridian radius of curvature
Q	Kalman Filter noise covariance matrix
R	Kalman Filter measurement noise covariance matrix

Superscripts

(-)	Column Matrix
(→)	Vector
(^)	Matrix
(~)	Skew Symmetric Matrix
(-*1*)	Inverse
(*T*)	Transpose
(*gf*)	Geographic Frame

(*bf*)	Body Frame
(ecef)	Earth Centered Earth Fix Frame
(eci)	Earth Centered Inertial Frame

Subscripts

(*N*)	North
(*E*)	East
(*D*)	Down
(*gf*)	Geographic Frame
(*bf*)	Body Frame
(ecef)	Earth Centered Earth Fix Frame
(eci)	Earth Centered Inertial Frame

Abbreviations

IMU	Inertial Measurement Unit
GPS	Global Positioning System
INS	Inertial Navigation System
AÖB	Ataletsel Ölçüm Birimi
KYS	Küresel Yerbulum Sistemi
ASS	Ataletsel Seyir Sistemi
ECEF	Earth Centered Earth Fixed Frame
ECI	Earth Centered Inertial Frame
DGPS	Differential GPS
WGS84	World Geodesic System 1984

CHAPTER 1

INTRODUCTION

1.1 Navigation

In *The Global Positioning System and Inertial Navigation*, Farrell and Barth point to the fact that, the word navigation is used in two different senses in the autonomous vehicle literature:

1. To accurately determine position and velocity relative to a known reference
2. To plan and execute the maneuvers necessary to move between desired locations.

The first skill is the prerequisite of the second, in other words, the first feature is essential to accomplish the second one correctly [1]. The present study concentrates on the first definition of navigation.

This thesis exploits the fact that navigation is "the determination of the position, velocity, attitude and time of a moving vehicle relative to specified references" [2].

It is a well-known fact that navigation is among ancient skills. Since the beginning of the time, one of the most fundamental questions of human mind has been "Where am I?" Thus, mankind proceeds from this question to the next which was how to go on to reach a certain location. In the course of the journey, the navigator aims for an accurate route by correcting his errors [3]. In older times, the earliest mariners followed the coastlines; later on they realized that they could use the stars for orientation. For instance, the ancient Phoenicians employed the North Star as a compass in their navigation. Thus, they took the ultimate risk as explorers; to confront the open sea [2].

There are various forms of navigation. One of the simplest forms of navigation is following the instructions or directions. For instance, a person can lead another one with instructions for a particular destination. This method of navigation is based on

observation and identification of known attributes or fixed objects in our surroundings, hence travelling between them. In literature, the locations of these features are often referred as “way-points” [4].

Another form of navigation is executed by making use of a map. In this type, the navigator will find out his or her position by examining the geographical item such as roads, rivers, hills and valleys that are illustrated on the map. These features may be defined on the map by taking into consideration either a grid system or a reference frame such as Greenwich meridian and Equator [4]. As it will be presented in this study, the use of a suitable reference frame is vital in the process of navigation.

A further approach of navigation is to use the method of dead reckoning. This method can be explained as determining the present position in the light of the initial position information and the measurement of speed and direction. The process of dead reckoning is practiced by distinguishing the last known position and the time it was obtained. One must also have the knowledge of the average speed and heading since that time and the present time. Then, velocity components north and east can be calculated by utilizing the speed and the heading angle. Afterward, each velocity component is multiplied by the time which has elapsed since the last position was obtained [4]. In this way, the change in position is attained. Lastly, the position changes are added up with the initial position in order to reach to the present position.

A corresponding dead reckoning process may also be accomplished with the help of inertial sensors that are gyroscopes and accelerometers, that measures rotational and translational motion with respect to inertial reference frame. This phenomenon is known as inertial navigation [4].

1.2 Inertial Navigation

The operation of inertial navigation is governed by the laws of classical mechanics as formulated by Sir Isaac Newton. The laws tell us that a force acting on a body will generate a proportional acceleration for that body [4]. Therefore, once the

acceleration of the body can be measured, it would be possible to calculate the change in its velocity and position by carrying out consecutive mathematical integrations of the acceleration with regard to time. Acceleration can be measured by employing a device known as an accelerometer [4]. An inertial navigation system usually contains three accelerometers and three rate gyros and they are affixed with their sensitive axes joined at a 90 degree angles.

It is compulsory to note the alterations of accelerometer's sensitive axis' direction so as to navigate in keeping with the defined inertial reference frame. Rotational motion of the body regarding the inertial reference frame can be discerned by using gyroscopic sensors, which measure the angle turned by the vehicle or the angular rate of turn of the vehicle. Hence, they are used to determine the orientation of the accelerometers' sensitive axis throughout the navigation. In the light of this information, the accelerations can be resolved into the desired reference frame before the computation of position [4].

As a result, inertial navigation is the process in which the measurements supplied by gyroscopes and accelerometers are used to determine the position of the vehicle in which they are mounted. It is viable to identify the translational motion of the vehicle with respect to the inertial reference frame and in this way to calculate its position by means of fusing the two sets of measurements that are rotation and translation [4].

Inertial systems are entirely self-contained within the vehicle in contrast with other types of navigation system. To put it differently, inertial systems do not rely on the broadcasting of signals from the vehicle or receiving them from an external source. On the other hand, it should be underlined that inertial navigation systems depend on the availability of the precise knowledge of vehicle's initial position. In addition, inertial systems also suffer from some instances like inertial sensors' errors (i.e. accelerometer bias, gyroscopes drift) or some calculation errors [4].

Owing to these errors, some other navigation sensors are integrated with INS. To name a few: radar, altimeter, barometer, odometer and Global Positioning System (GPS) are such sensors that can be integrated with inertial navigation system. GPS in particular is a commonly used sensor to integrate with inertial navigation system due

to the factors that it is universal, precise and furthermore GPS receivers are easy to use.

GPS/INS integration is commonly executed by using a Kalman Filter [5-10]. However, there are also other techniques used for GPS/INS integration [11], [12].

In the study [13], tightly coupled GPS/INS integration is used. As discussed in Chapter 2, for tightly coupled GPS/INS integration, which satellites' pseudo and delta range are combined in one Kalman filter with INS error mathematical model, more complex and expansive GPS receivers are used. Also, mechanization of the INS is calculated in Earth Centered Earth Fixed Frame (ECEF). In this kind of mechanization, one has to deal with huge numbers which are greater than Earth radius. Therefore, extra memory and calculation time are needed for this purpose. Also, offline process in which data is collected using two computers at first and then GPS/INS integration is achieved using these collected data is developed. Thus, navigation path is computed after navigation data is completed.

In the literature, there are studies that do not use real experimental data, but instead employ simulation data. For instance, in [14], loosely coupled GPS/INS integration is developed for ballistic missiles. Loosely coupled GPS/INS integration is explained in Chapter 2. Yet, a brief explanation is that a loosely coupled GPS/INS integration contains two Kalman filters, one for calculation of positions and velocities from satellites' pseudo and delta range, and the other one for estimation of INS' error using the first Kalman filter output. In the same study, first, some ballistic missile data (that is x, y and z axis acceleration and gyroscopes measurement data) are generated using some application software like TÜBİTAK-SAGE FMCAD RSIM. Then, using fixed local geographical frame, mechanization is achieved. This kind of frame mechanization is proper for missiles because this frame is always fixed to the missile's target. On the other hand, it is not appropriate for land vehicle navigation in the fixed geographical frame is not easy as the geographical frame because of the planning. The planning is the second definition of navigation at the beginning of the text.

Loosely coupled GPS/INS integration is extensively used, because this approach provides GPS receivers' and GPS/INS integration's data independently. The two

systems are operated efficiently in cascade with the position and/or velocity estimates provided by the GPS receiver's data.

There are two main advantages of loosely coupled integration. These are algorithmic simplicity and redundancy. Here, redundancy is defined as the access number of separately received the GPS data, INS data and GPS/INS integration data. For example, in uncoupled and loosely coupled feed forward configurations all three data can be received separately. In the loosely coupled feedback configuration only GPS and GPS/INS integration data can be received separately whereas, in the tightly coupled configuration only the GPS/INS integration data can be received. Also, loosely coupled integration can be used with a simple and cheap GPS receiver.

1.3 Scope of the Thesis

In this thesis, a loosely coupled GPS/INS integration architecture is developed. Firstly, the theoretical background of GPS/INS integration is discussed then, Inertial Measurement Unit (IMU) mechanization equations are derived with respect to local level geographical frame. Later, using these equations, an error model of INS is established. Following this step, a Kalman filter is constructed using the linearized form of the mechanization equations. Next, using MATLAB Real Time Windows Target software, an application is developed to perform this GPS/INS integration unlike the studies [13] and [14]. In [14], GPS/INS integration is performed using the simulation data. On the other hand in [13], offline GPS/INS integration is developed that means first data is collected from IMU and GPS, after collection of the data the integration is carried out and the navigation data is achieved.

Finally, some tests are done in order to check the performance of the system. These tests are performed based on real time data collection and processing. Developed system is attached to a car and different paths are followed.

1.4 Thesis Outline

In Chapter 2, the theoretical background of inertial navigation system, global positioning system and the fundamentals of Kalman Filter are introduced. Moreover, in this chapter, IMU mechanization equations and Kalman filter mathematical model is explained. In addition, the foremost GPS/INS methods are also discussed.

In Chapter 3, the implementation of loosely coupled GPS/INS integration is given. Furthermore, MATLAB Real Time Windows Target implementation is introduced together with MATLAB Simulink diagrams.

In Chapter 4, the test results of GPS/INS integration are presented.

Chapter 5 consists of the conclusion in which a brief overview of the arguments made throughout the preceding chapters is given. This chapter also includes the main ideas for possible future work.

CHAPTER 2

THEORY

In this chapter of the present study, the theoretical background of INS, GPS, fundamentals of Kalman Filter and fusion or integration of GPS/INS systems are presented and discussed subsequently. Moreover, equations and other mathematical tools for Kalman Filter and IMU mechanization are given.

2.1 Inertial Navigation System

Inertial Navigation System is composed of inertial measurement sensors, namely three accelerometers and three rate gyroscopes and a computer which processes the data from the inertial sensors to generate location, velocity and orientation with respect to the desired reference frame.

In the following sections, basic information of accelerometers and gyroscopes are provided and the definition of IMU is given.

2.1.1 Accelerometers

To measure the acceleration components, accelerometers are used. There are two fundamental types of accelerometers; one is mechanical and the other type is known as solid state. In this section of the thesis, the working principles of a basic mechanical accelerometer are introduced. It must be noted that, in this thesis, an IMU which contains solid state accelerometers is used. In order to provide general background, an overview of the working principles of a basic mechanical accelerometer is presented.

The case of a basic mechanical accelerometer (Figure 2.1) is subjected to acceleration along its sensitive axis. As the casing of accelerometer moves, the proof mass tends to remains stationary due to its inertia. Hence, it appears to move in the direction opposite to the motion direction of the casing. However, its relative motion is restricted by a spring and a damper. Thus, the relative displacement of the proof mass becomes proportional to the net force in the spring in the steady state condition, i.e. after the transient behavior of the spring-mass-damper system disappears.

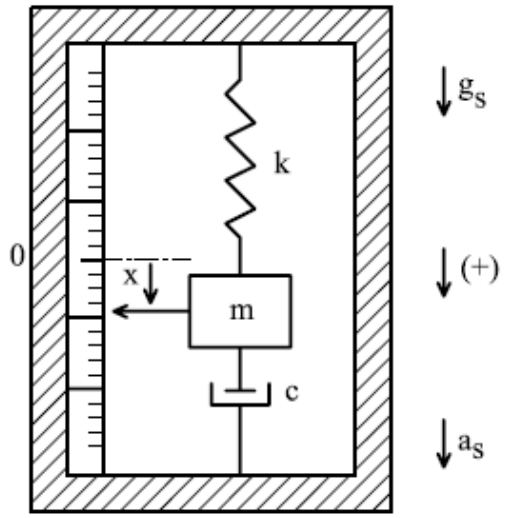

Figure 2.1 Basic Mechanical Accelerometer

The relevant differential equation and the steady state condition can be expressed as follows:

$$m\left(\ddot{x}+a_s\right)=\sum F=-kx-c\dot{x}+mg_s \tag{2.1}$$

$$m\ddot{x}+c\dot{x}+kx=-m\left(a_s-g_s\right) \tag{2.2}$$

$$kx_{ss}=-m\left(a_s-g_s\right) \tag{2.3}$$

$$\left(a_s-g_s\right)=-\omega_n^2 x_{ss} \quad ; \quad \omega_n^2=k/m \tag{2.4}$$

As noted above, assuming that the frequency content of (a_s-g_s) is much smaller than ω_n, the steady state displacement x_{ss} is proportional to (a_s-g_s). Therefore, it can be stated that the accelerometer measures the acceleration of the casing without the component of the gravity vector along the sensitive axis. In other words, the absolute acceleration of the body can be found by adding the measurement result to the gravitational acceleration.

More information about accelerometers can be found in references [4] and [15].

2.1.2 Gyroscopes

There are two types of gyroscopes according to the quantity measured. The first type measures the angle turned by the vehicle that carries the gyroscope. The second kind measures the angular rate of turn of the vehicle about the defined axis [4], [15].

Today, variety of different and accurate gyroscope architectures are developed. Some of them are Fiber Optic Gyros, Solid State gyros, Nuclear Magnetic Resonance Gyros, etc [4]. In this thesis, an IMU which contains solid state gyroscopes is used.

The basic principles of gyros can be explained through the mechanical gyros.

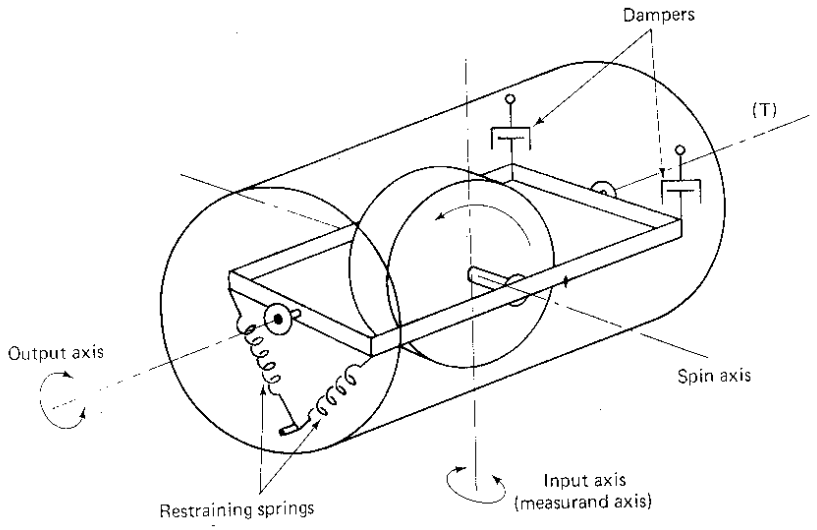

Figure 2.2 Basic Single Axis Mechanical Gyroscope [16]

The single axis mechanical gyroscope shown in Figure 2.2 consists of an inertia wheel that rotates at high angular velocity and a gimbal system. The inertia wheel maintains its orientation fixed in space unless a torque is applied through the input axis. If torque is applied by the turning vehicle, the inertia wheel rotates about the output axis. This rotation is refrained by springs and dampers. In the steady state, the turning rate of the vehicle becomes proportional to the deflection angle of the inertia wheel [3], [4], [15].

2.1.3 Inertial Measurement Unit

IMU is composed of three accelerometers and three rate gyroscopes. These three accelerometers and three rate gyroscopes establish an orthogonal coordinate frame with the purpose of measuring linear and angular motion as regards to inertial frame. Figure 2.3 shows a strap down IMU and Figure 2.4 shows a scheme of a gimbaled IMU, which will be defined later in this section [17].

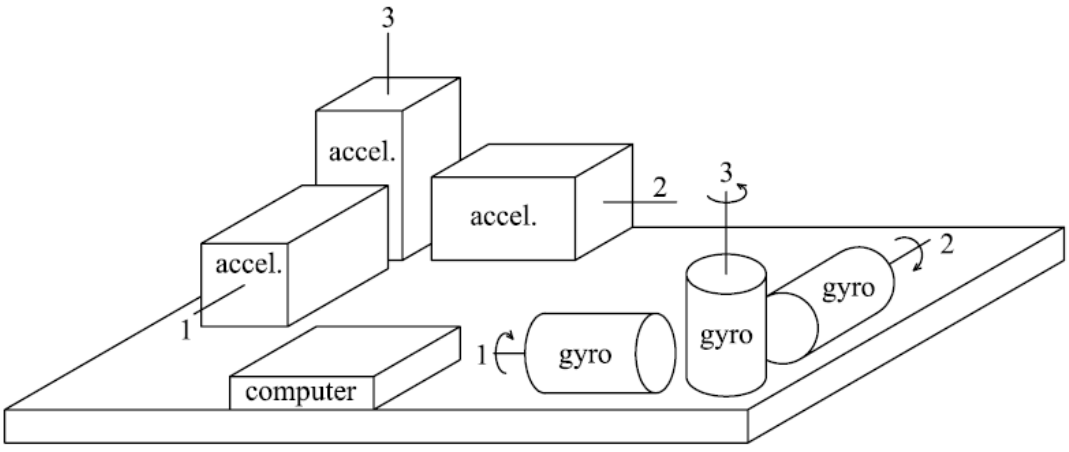

Figure 2.3 Scheme of a Strap Down IMU

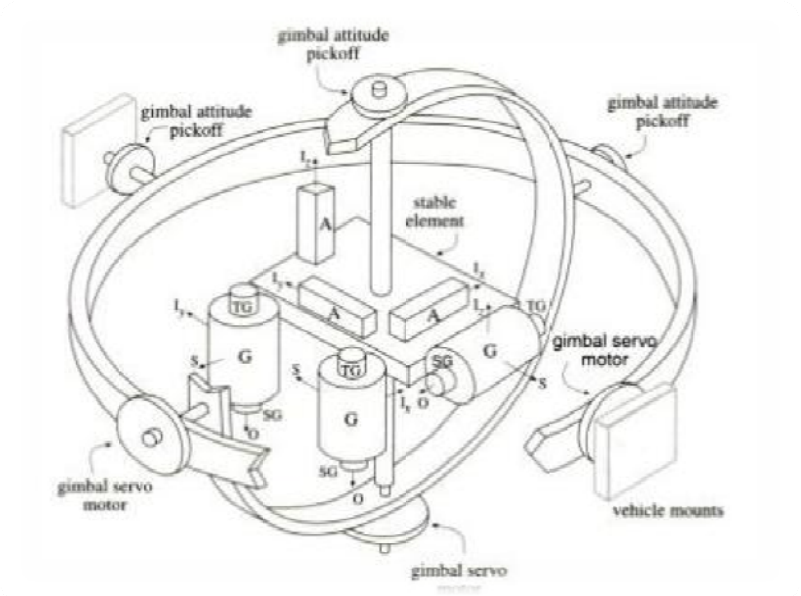

Figure 2.4 Scheme of a Gimbaled IMU [17]

IMU's implementation can take a range of forms. In earlier technology, inertial measurement unit was constituted with stable platform or gimbaled techniques. In such systems, the accelerometers are fastened on a stable platform, whose orientation is stabilized with respect to an inertial frame by means of feedback signals supplied by the gyroscopes. Thus, they are not mechanically affected by the rotational motion of the vehicle. Even today, in cases where very precise navigation data is required, stable platform IMU is still commonly used [4].

In most recent technology, gyroscopes and accelerometers are mounted firmly on the vehicle. This type of implementation which is called strap down IMU lessens the mechanical intricacy and hence, lower the cost. Moreover, the size of sensors is reduced and become much more reliable in comparison with the gimbaled IMU. As a result, inertial measurement unit can easily be used in any kind of system for navigation purposes like missiles, unmanned flight etc. However, there are some shortcomings of strap down IMUs. The major drawback is that there is much more computing complexity in strap down IMUs as opposed to gimbaled IMUs. Moreover, it is required for the sensors to be able to measure much higher rates of turn [4]. In this thesis, a strap down IMU is used.

2.2 Reference Frames

As mentioned above, IMUs measure linear and angular motion with respect to an inertial frame. For this reason, an inertial frame has to be defined. It is also necessary to define suitable coordinate frames so that the inertial measurements can be related to the Earth's reference directions (i.e. latitude, longitude etc.). The Earth's reference direction is important when the vehicle is moving closely near the Earth [17]. In this study, right handed and orthogonal reference frames are used. Definitions of frames which are used are given in the forthcoming five sections.

2.2.1 Inertial Frame

An inertial frame is defined as a frame such that the three rate gyros and the three accelerometers of an IMU fixed to that frame measure zero values. Although it is seen simple to define an inertial frame, it is very difficult to establish an inertial frame in our world due to its rotational motion around itself and around the sun. Therefore, in the geodetic literature, a quasi-inertial frame that is accelerating but not rotating around the Sun can be accepted as an inertial frame due to its practicality [17]. As can be seen in Figure 2.5, inertial frame's origin is Earth's mass center and z axis of this quasi-inertial frame coincides with polar axis of Earth. Besides, its x axis is pointing to the vernal equinox. This frame is called as Earth Centered Inertial Frame (ECI).

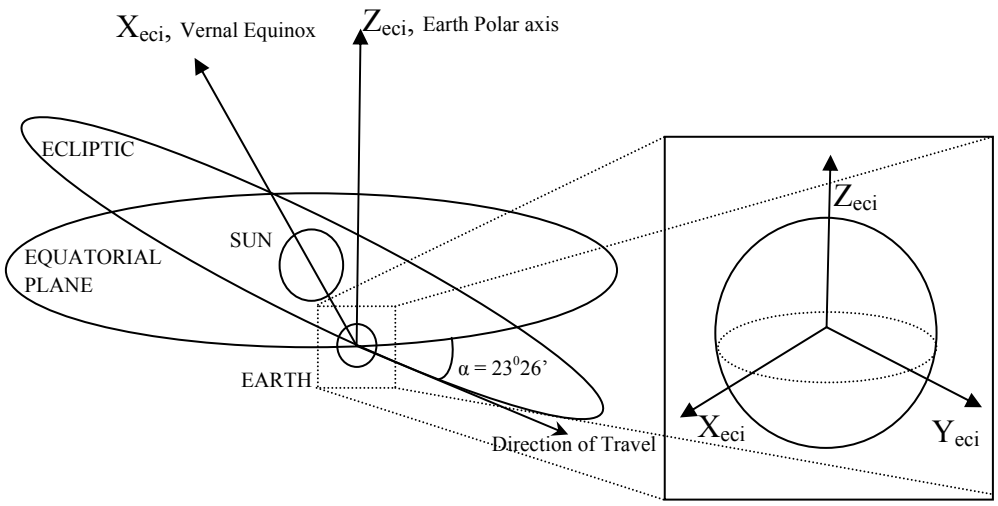

Figure 2.5 Earth Centered Inertial Reference Frame

2.2.2 Earth Centered Earth Fixed Frame

Earth Centered Earth Fixed Frame's (ECEF) origin is also at the Earth's mass center. When navigation starts, (i.e. t=0) both ECI and ECEF frames are coincident. As it can be seen from Figure 2.6, x axis of ECEF passes through the intersection of the plane of the Greenwich meridian and the Earth's equatorial plane. ECEF and ECI frames' z axis is always coincident. ECEF's axes are fixed with respect to Earth. Therefore, ECEF rotates with respect to ECI frame about z axis or polar axis.

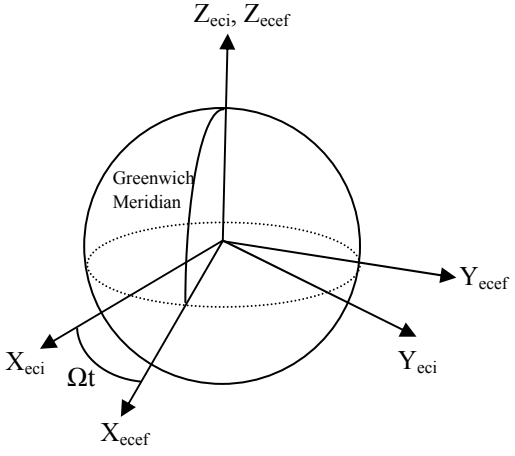

Figure 2.6 Earth Centered Earth Fixed Frame

2.2.3 Navigation Frame or Geographic Frame

Navigation frame is a local geographic frame whose origin is at the vehicle mass center. Its x axis' direction is towards the north pole of the Earth, y axis' direction is toward the East and z axis' direction is towards the Earth gravity center. In Figure 2.7 the navigation or geographical frame (GF) is demonstrated.

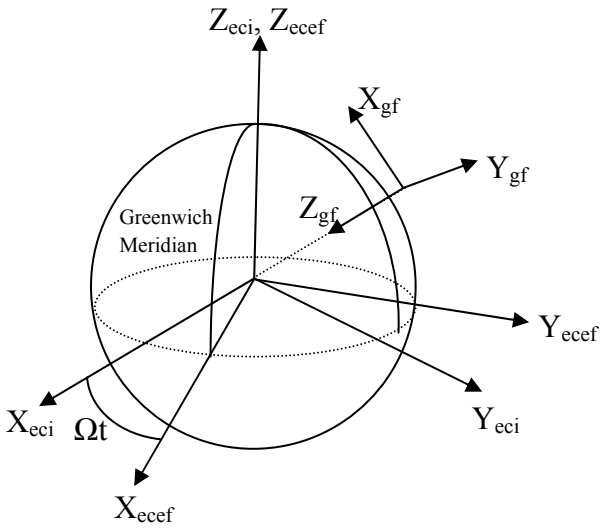

Figure 2.7 Geographical Frame

2.2.4 Body Frame

The body frame is also a Cartesian frame whose origin is at the vehicle mass center and fixed to the vehicle. Body frame's x axis describes a forward direction of motion. Its z axis points to the bottom of the vehicle from the mass center and the y axis can be found simply by using the right handed orthogonal frame property [1]. Figure 2.8 shows the body frame.

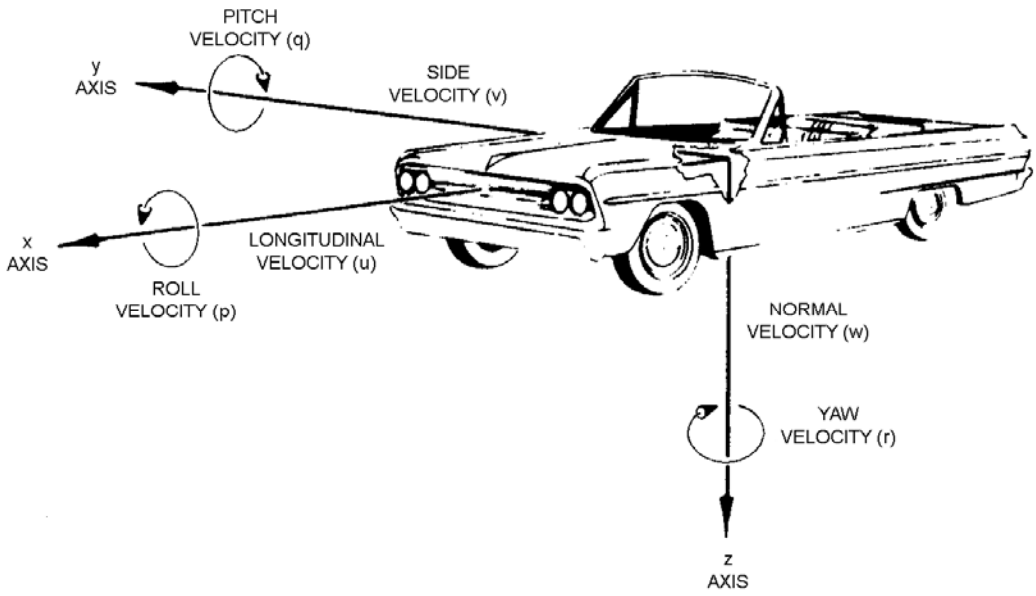

Figure 2.8 Body Frame

2.2.5 Sensor Frame

IMU's accelerometers and rate gyroscopes constitute an orthogonal frame, as mentioned earlier. Thus, the sensor frame of IMU is the frame shown in Figure 2.9. In this thesis, sensor frame and body frame are taken as coincident with each other.

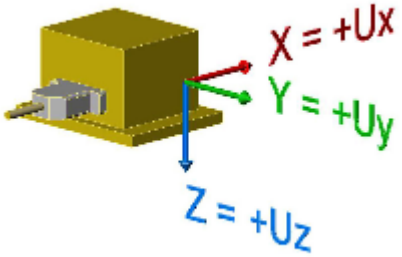

Figure 2.9 Sensor Frame

2.3 Mechanization Equations

Mechanization equations are differential equations whose solutions present the position, velocity and attitude information with respect to a particular frame by utilizing IMU output. It should be noted that IMU output comprises the acceleration and angular velocity of the vehicle with respect to the inertial frame. In this part, the mechanization equations are derived to generate position and attitude data with respect to the navigation or geographic frame.

The mechanization equations are derived by manipulating the equations shown in Appendix B and basic mathematical tools are given in Appendix A.

Let $\Im_a$ that is given in Appendix B be the ECI frame and $\Im_b$ be the ECEF, with points A and B being their origin, respectively. In this case, points A and B are coincident and this point is Earth mass center. Let this coincident points be O.

Using acceleration equation in Appendix B,

$$\vec{a}_{P/\Im_a(A)} = \vec{a}_{P/\Im_b(B)} + \vec{\alpha}_{b/a} \times \vec{r}_{P/B} + 2\vec{\omega}_{b/a} \times \vec{v}_{P/\Im_b(B)} + \vec{\omega}_{b/a} \times (\vec{\omega}_{b/a} \times \vec{r}_{P/B}) + \vec{a}_{B/\Im_a(A)} \quad (2.5)$$

In subscript notation, let inertial frame (ECI) be designated with "*eci*" and Earth centered Earth fixed frame (ECEF) be designated by "*ecef*". Hence,

$$\vec{a}_{P/eci} = \vec{a}_{P/ecef} + \vec{\alpha}_{ecef/eci} \times \vec{r}_{P/O} + 2\vec{\omega}_{ecef/eci} \times \vec{v}_{P/ecef} + \vec{\omega}_{ecef/eci} \times (\vec{\omega}_{ecef/eci} \times \vec{r}_{P/O}) + \vec{a}_{O/eci} \quad (2.6)$$

Here,

$$\vec{a}_{O/eci} = 0 \quad (2.7)$$

since point "O" is the common origin of the ECI and ECEF frames.

$\vec{\omega}_{ecef/eci}$ is the angular velocity vector of ECEF with respect to ECI. This value is constant, further information about this value can be found in Appendix C. In other words,

$$\vec{\alpha}_{ecef/eci} = 0 \quad (2.8)$$

Consequently, the acceleration equation of P point with respect to ECEF becomes

$$\vec{a}_{P/ecef} = \vec{a}_{P/eci} - 2\vec{\omega}_{ecef/eci} \times \vec{v}_{P/ecef} - \vec{\omega}_{ecef/eci} \times (\vec{\omega}_{ecef/eci} \times \vec{r}_{P/O}) \quad (2.9)$$

Let, $\vec{a}'_{P/ECI}$ be the acceleration sensed by the accelerometers. Due to the reasons explained in Section 2.11, $\vec{g}$ must be added to obtain the actual acceleration $\vec{a}_{P/ECI}$. That is,

$$\vec{a}_{P/ecef} = \vec{a}'_{P/eci} - 2\vec{\omega}_{ecef/eci} \times \vec{v}_{P/ecef} - \vec{\omega}_{ecef/eci} \times (\vec{\omega}_{ecef/eci} \times \vec{r}_{P/O}) + \vec{g} \quad (2.10)$$

or, with $D_{ecef} = \left.\frac{d}{dt}\right|_{ecef}$,

$$D_{ecef}\vec{v}_{P/ecef} = \vec{a}'_{P/eci} - 2\vec{\omega}_{ecef/eci} \times \vec{v}_{P/ecef} - \vec{\omega}_{ecef/eci} \times (\vec{\omega}_{ecef/eci} \times \vec{r}_{P/O}) + \vec{g}$$

(2.11)

Here, $\vec{\omega}_{ecef/if} \times (\vec{\omega}_{ecef/if} \times \vec{r}_{P/O})$ is the centripetal acceleration. Figure 2.10 shows this acceleration over the Earth surface.

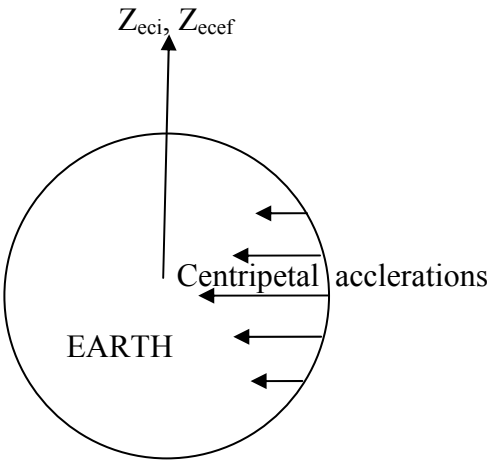

Figure 2.10 Centripetal Acceleration

As can be observed in Figure 2.10, centripetal acceleration direction is always pointing the polar axis of Earth. Therefore, in the literature, the combination of

gravity and centripetal acceleration is defined as a new gravity vector which is named as plump bob gravity.

$$\vec{g}_l = \vec{g} - \vec{\omega}_{ecef/eci} \times (\vec{\omega}_{ecef/eci} \times \vec{r}_{P/O}) \tag{2.12}$$

Then, Eq.2.8 becomes

$$D_{ecef}\vec{v}_{P/ecef} = \vec{a}'_{P/eci} - 2\vec{\omega}_{ecef/eci} \times \vec{v}_{P/ecef} + \vec{g}_l \tag{2.13}$$

Using the Transport Theorem, one can convert this equation into geographic frame or navigation frame. Let the geographic frame in subscript notation be designated as "*gf*".

$$D_{ecef}\vec{v}_{P/ecef} = D_{gf}\vec{v}_{P/ecef} + \vec{\omega}_{gf/ecef} \times \vec{v}_{P/ecef} \tag{2.14}$$

Then,

$$D_{gf}\vec{v}_{P/ecef} = D_{ecef}\vec{v}_{P/ecef} - \vec{\omega}_{gf/ecef} \times \vec{v}_{P/ecef} \tag{2.15}$$

Substituting Eq.2.13 into Eq.2.15 it is possible to obtain

$$D_{gf}\vec{v}_{P/ecef} = \vec{a}'_{P/eci} - 2\vec{\omega}_{ecef/eci} \times \vec{v}_{P/ecef} + \vec{g}_l - \vec{\omega}_{gf/ecef} \times \vec{v}_{P/ecef} \tag{2.16}$$

or

$$D_{gf}\vec{v}_{P/ecef} = \vec{a}'_{P/eci} - (2\vec{\omega}_{ecef/eci} + \vec{\omega}_{gf/ecef}) \times \vec{v}_{P/ecef} + \vec{g}_l \tag{2.17}$$

Here, as said before $\vec{a}'_{P/eci}$ is the IMU measurement with components in the body frame.

Thus, we need to convert these components into the geographic frame by employing component transformation. Let the body frame be denoted as "*bf*" in subscript notation.

Also, let

$$(2\vec{\omega}_{ecef/eci} + \vec{\omega}_{gf/ecef}) = \vec{\beta}_{gf/eci} \tag{2.18}$$

Then, matrix form of Eq.2.17 becomes

$$\left\{D_{gf}\vec{v}_{P/ecef}\right\}^{(gf)} = \hat{C}^{(gf,bf)}\overline{a}_{P/bf}^{'(bf)} - \tilde{\beta}_{gf/eci}^{(gf)}\overline{v}_{P/ecef}^{(gf)} + \overline{g}_{l}^{(gf)} \tag{2.19}$$

Where, from [4],

$$\overline{v}_{P/ecef}^{(gf)} = \begin{bmatrix} V_N \\ V_E \\ V_D \end{bmatrix} \tag{2.20}$$

$$\vec{\omega}_{ecef/eci} = \begin{bmatrix} \Omega\cos\mu & 0 & -\Omega\sin\mu \end{bmatrix}^T \tag{2.21}$$

$$\vec{\omega}_{gf/ecef} = \begin{bmatrix} \dot{\lambda}\cos\mu & -\dot{\mu} & -\dot{\lambda}\sin\mu \end{bmatrix}^T \tag{2.22}$$

and

$$\overline{a}_{P/bf}^{'(bf)} = \begin{bmatrix} a_x \\ a_y \\ a_z \end{bmatrix}$$

Here, μ is the latitude of geographical frame origin. λ is longitude of geographical frame origin and Ω is Earth's rotation rate. Additionally,

$$\tilde{\beta}_{gf/eci}^{(gf)} = \begin{bmatrix} b_{11} & b_{12} & b_{13} \\ b_{21} & b_{22} & b_{23} \\ b_{31} & b_{32} & b_{33} \end{bmatrix} \tag{2.23}$$

is the skew symmetric, corresponding to $\vec{\beta}_{gf/eci}$. More information can be found about skew symmetric matrices in Appendix A.

On the other hand, the transformation matrix form body frame to geographical frame can be written as

$$\hat{C}^{(gf,bf)} = \begin{bmatrix} c_{11} & c_{12} & c_{13} \\ c_{21} & c_{22} & c_{23} \\ c_{31} & c_{32} & c_{33} \end{bmatrix} \tag{2.24}$$

Thus, expanded form of Eq. 2.19 becomes

$$\begin{bmatrix} \dot{V}_N \\ \dot{V}_E \\ \dot{V}_D \end{bmatrix} = \begin{bmatrix} c_{11} & c_{12} & c_{13} \\ c_{21} & c_{22} & c_{23} \\ c_{31} & c_{32} & c_{33} \end{bmatrix} \begin{bmatrix} a_x \\ a_y \\ a_z \end{bmatrix} - \begin{bmatrix} b_{11} & b_{12} & b_{13} \\ b_{21} & b_{22} & b_{23} \\ b_{31} & b_{32} & b_{33} \end{bmatrix} \begin{bmatrix} V_N \\ V_E \\ V_D \end{bmatrix} + \begin{bmatrix} g_x \\ g_y \\ g_z \end{bmatrix} \tag{2.25}$$

Position equation with respect to ECEF is

$$D_{ecef}\vec{r}_{P/ecef} = \vec{v}_{P/ecef} \tag{2.26}$$

In matrix form,

$$\left\{D_{ecef}\vec{r}_{P/ecef}\right\}^{(ecef)} = \hat{C}^{(ecef,gf)}\overline{v}^{(gf)}_{P/ecef} \tag{2.27}$$

Using spherical coordinate as can be seen in Figure 2.11,

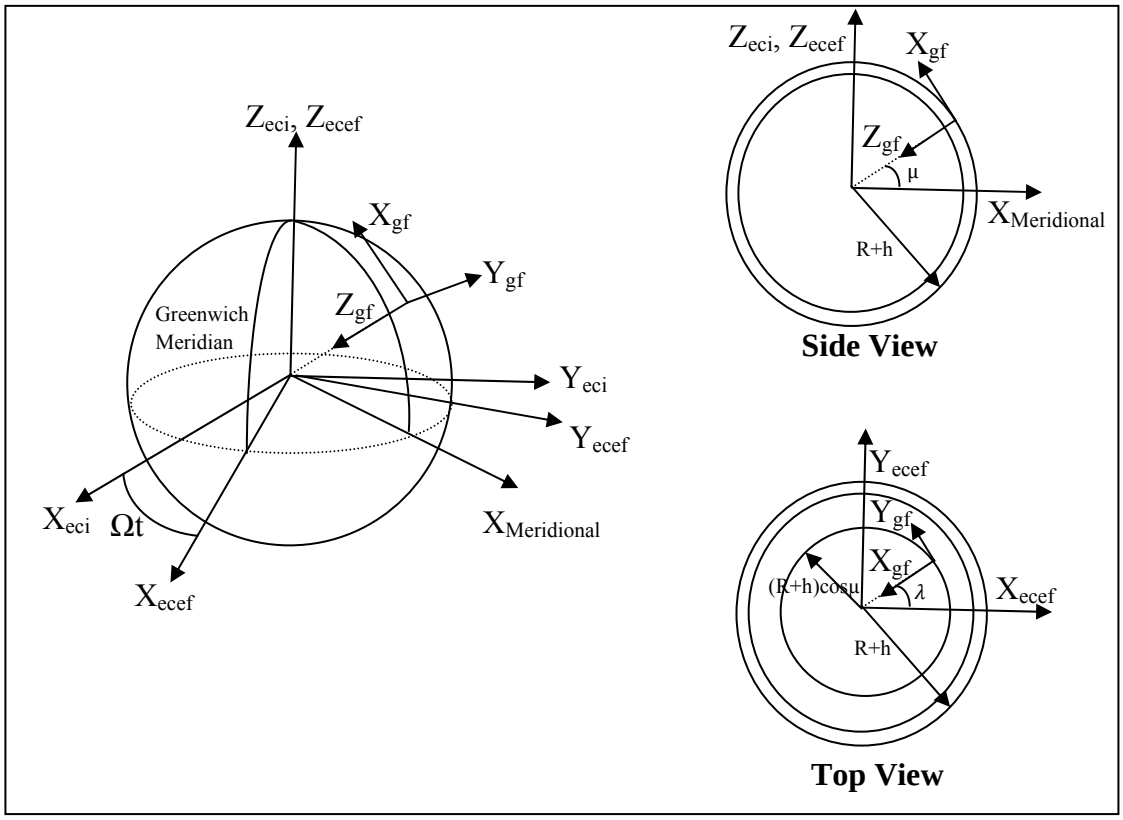

Figure 2.11 Spherical Coordinate Representation of Geographical Frame Origin

$$\dot{\mu} = \frac{V_N}{R+h} \tag{2.28}$$

$$\dot{\lambda} = \frac{V_E}{(R+h)\cos\mu} \tag{2.29}$$

$$\dot{h} = -V_D \tag{2.30}$$

Up to this point, the shape of Earth is assumed to be spherical. However, the Earth flattens slightly at the poles and bulges a bit at the Equator. An ellipsoid obtained by rotating an ellipse about its shorter axis is the most approximate geometrical figure used in geodesy to indicate the shape of the Earth. According to World Geodesic System (WGS84), the constants such as length of the semi-major axis, length of the semi-minor axis, the flattening of the ellipsoid and Earth's rate are determined. Table 2.1 presents these constants [4].

Name of Constant	**Symbol of Constant**		**Value of Constant**	**Unit of Constant**
Length of the semi-major axis	R		6378137	m
Length of the semi-minor axis	r	$r = R(1-f)$	6356752.3142	m
Flattening of the ellipsoid	f	$f = \frac{R-r}{R}$	1/298.257223563	-
Major eccentricity of the ellipsoid	e	$e = [f(2-f)]^{1/2}$	0.0818191908426	-
Earth's rate	Ω		7.292115×10^{-5}	rad/s

Table 2.1 Constants of the Earth in WGS 84

Figure 2.12 illustrates the Earth's ellipsoid shape.

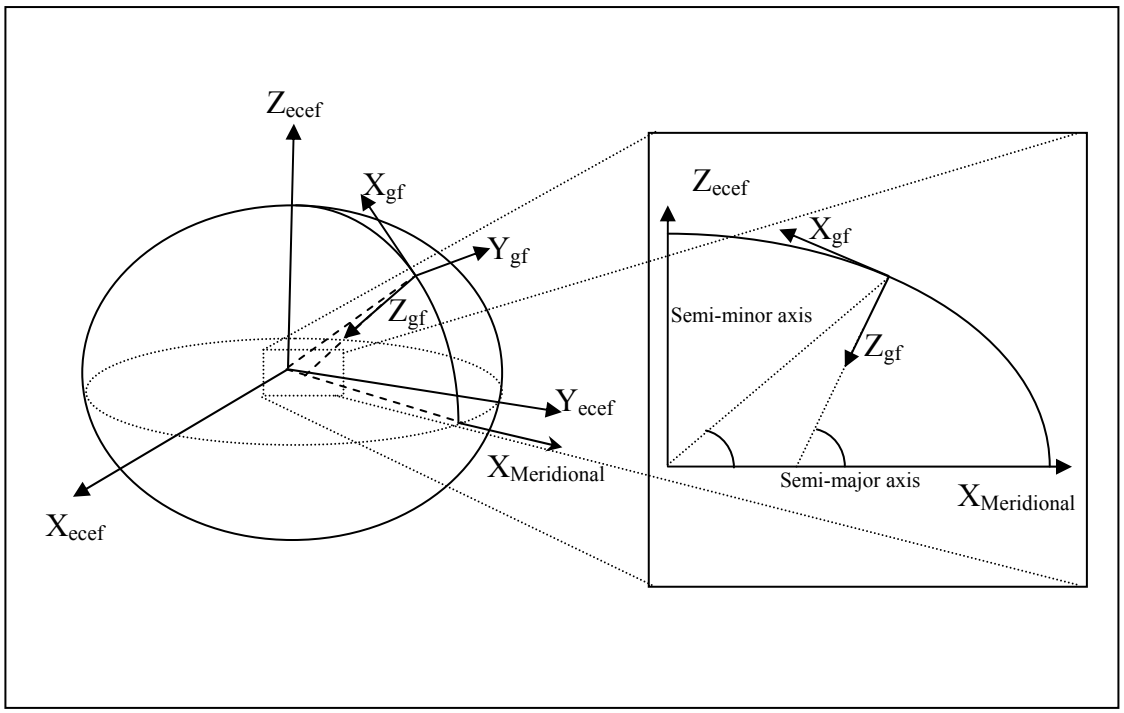

Figure 2.12 Ellipsoid Shape of the Earth

In the light of this information, Eq.2.28 and Eq.2.29, are modified as follows[4].

$$\dot{\mu} = \frac{V_N}{R_N + h} \tag{2.31}$$

$$\dot{\lambda} = \frac{V_E}{\left(R_E + h\right)\cos\mu} \tag{2.32}$$

where R_E and R_N are the transverse radius of curvature and the meridian radius of curvature respectively and can be expressed as follows,

$$R_N = \frac{R\left(1-e^2\right)}{\left(1-e^2\sin^2\mu\right)^{3/2}} \tag{2.33}$$

$$R_E = \frac{R}{\left(1-e^2\sin^2\mu\right)^{1/2}} \tag{2.34}$$

Propagation of attitude with time can be found using the following equation [4]

$$\dot{\hat{C}}^{(gf,bf)} = \hat{C}^{(gf,bf)}\tilde{\omega}_{bf/gf}^{(bf)} \tag{2.35}$$

where,

$$\bar{\omega}_{bf/gf}^{(bf)} = \bar{\omega}_{bf/eci}^{(bf)} - \hat{C}^{(bf,gf)}\left[\bar{\omega}_{ecef/eci}^{(gf)} + \bar{\omega}_{gf/ecef}^{(gf)}\right] \tag{2.36}$$

Here, $\bar{\omega}_{bf/eci}^{(bf)}$ is the measurement coming from IMU's x, y and z axis. $\bar{\omega}_{ecef/eci}^{(gf)}$ and $\bar{\omega}_{gf/ecef}^{(gf)}$ are given by Eq.2.21 and Eq.2.22, respectively.

$\hat{C}^{(gf,bf)}$ is an orthogonal matrix. Therefore, $\hat{C}^{(gf,bf)}$ orthogonalisation should be checked and corrected in computation of $\hat{C}^{(gf,bf)}$. For this purpose, method explained in [4] is used.

In this respect, *i*th and *j*th rows of $\hat{C}^{(gf,bf)}$ becomes $\hat{C}_i$ and $\hat{C}_j$. Therefore, their dot product should be zero. Yet, one can find the error using below equation.

$$\Delta_{ij} = \hat{C}_i \hat{C}_j^T \tag{2.37}$$

Here, Δ_{ij} is an angle error defined about an axis perpendicular to $\hat{C}_i$ and $\hat{C}_j$, or orthogonality error between two rows. The orthogonality errors can be eliminated by the following equations:

$$\begin{aligned} \hat{C}_i^* &= \hat{C}_i - \frac{1}{2}\Delta_{ij}\hat{C}_j \\ \hat{C}_j^* &= \hat{C}_j - \frac{1}{2}\Delta_{ij}\hat{C}_i \end{aligned} \tag{2.38}$$

Here superscript * indicates the corrected value. Same process for *i*th row to *i*th should be made. Following equations are used for this purpose [4]. Eq.2.39 is used for finding the normalization error in the *i*th row and Eq.2.40 is used for correction of this error.

$$\Delta_{ii} = 1 - \hat{C}_i \hat{C}_i^T$$

(2.39)

$$\hat{C}_i^* = \hat{C}_i - \frac{1}{2}\Delta_{ii}\hat{C}_i \tag{2.40}$$

2.3.1 Gravity Model

The exact knowledge of the gravity vector is crucial for high accuracy application [4]. In this work, a low cost IMU is used. Therefore, the precise knowledge of gravity vector is not required. Hence, Somigliana's formula, is used [4].

$$g(0) = 9.780318\left(1 + 5.3024x10^{-3}\sin^2(\mu) - 5.9x10^{-6}\sin^2(2\mu)\right)\left[\frac{m}{s^2}\right] \tag{2.41}$$

This formula represents gravity at sea level. The variation of gravity with altitude can be defined as follows [4].

$$g(h) = \frac{g(0)}{\left(1 + \frac{h}{R_0}\right)^2} \tag{2.42}$$

Here, $g(0)$ is the Somigliana's formula, which is given in the Eq.2.41.

This equation is in scalar form. In Section 2.3 the gravity vector is introduced. The gravity vector can be defined as follows when expressed in navigation or geographical frame [4].

$$\bar{g}^{(gf)} = \begin{bmatrix} \dfrac{-\Omega(R_0+h)}{2}\sin(2\mu) \\ 0 \\ g(h) - \dfrac{-\Omega(R_0+h)}{2}\left(1+\cos(2\mu)\right) \end{bmatrix} \tag{2.43}$$

2.4 Global Positioning System

Global Positioning System (GPS) is "a worldwide, accurate, continuous coverage satellite based radio navigation system" [1].

Space, control and user segments are the major segments of GPS, Figure 2.13 illustrates these segments. Each segment is briefly discussed in the following subtitles.

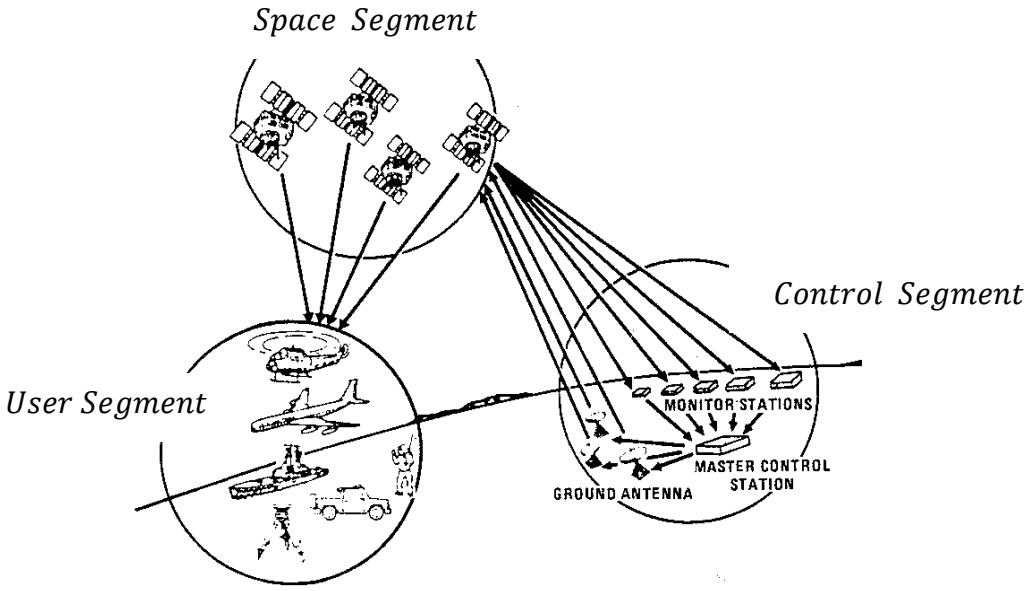

Figure 2.13 GPS Segments [18]

2.4.1 Space Segment

GPS satellites produce the Space segment. There are 24 GPS satellites that orbit around the Earth in six different orbital planes. The duration of orbiting is approximately one sidereal day. The concept of sidereal day is explained in Appendix C. The orbits are roughly circular with radii of approximately 20,200 km and inclination angles relative to the equator of 55^0. Additionally, these six orbits are equally spaced around the equator with 60^0 separations. In the Figure 2.14, GPS satellites are shown. Owing to this consolidation, one can see at least four satellites at anytime and anywhere on the Earth [24].

Figure 2.14 GPS Space Segment [19]

2.4.2 Control Segment

The control segment consists of one master control station, six monitor stations and four ground antennas located around the world. There are also backup stations in this system. In the case of failure of any station, these backup stations become online right away [24].

The control segment's chief task is the correction of GPS satellites atomic clock and orbital correction [24] Figure 2.13.

2.4.3 User Segment

The user segment of GPS is composed of antennas and receiver processor. These antennas receive the satellite transmissions and processors decode them in order to provide the user with positioning, velocity and precise timing information. The unlimited number of users can make use of the GPS space segment. Yet, in the case that the path between the receiver and a satellite is blocked, the satellite signal then will not be received [24] Figure 2.13.

2.4.4 GPS Navigation Signals

Each GPS satellite constantly transmits a Navigation Message at 50 bit/s giving the time-of-week, GPS week number and satellite health information. All these are broadcasted in the first part of the message. Then, in the second part of the message an ephemeris is transmitted, followed by the transmission of an almanac. The messages are sent in frames and it takes 30 seconds to transmit 1500 bits of each frame. Every satellite broadcasts its navigation message with at least two different kinds of spread spectrum codes: the Coarse / Acquisition (C/A) code and the Precise (P) code. The Coarse / Acquisition (C/A) code is freely available to the public, yet the Precise (P) code is in general encrypted and reserved for military applications [24].

2.4.5 GPS Position Determination

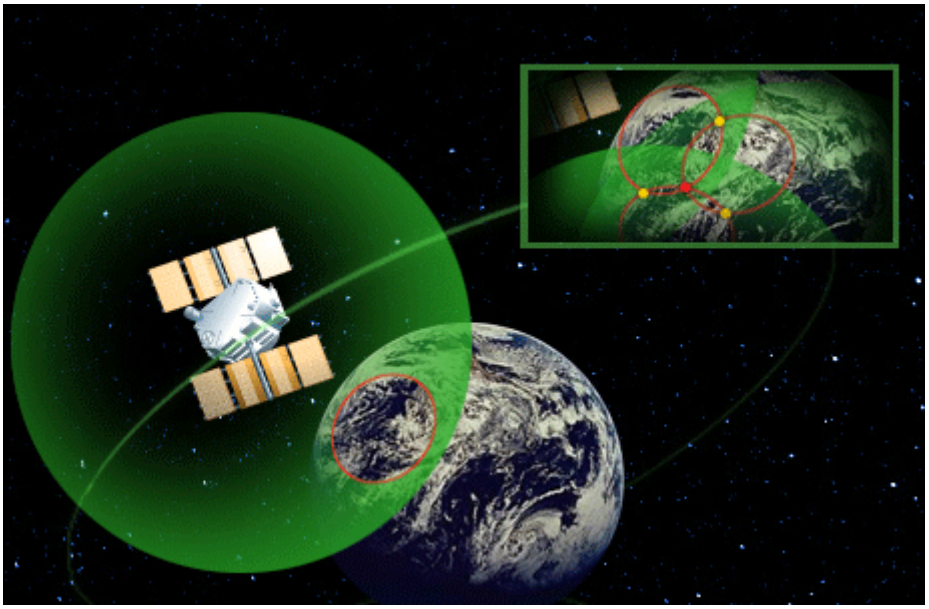

Figure 2.15 GPS Position Determination Geometry [20]

Using four sphere triangulation techniques, GPS receivers find its location. Figure 2.15 shows a basic GPS position determination geometry. The distance from the GPS receiver to the satellite is called pseudo range. A sphere can be defined using this value The GPS satellites are well separated that, Earth, which is assumed as one sphere, and one satellite's pseudo range intersection is a circle, two satellites' pseudo ranges and Earth intersect at two points and three satellite' pseudo range and Earth intersect at one point. Thus, GPS receiver should take at least three satellites' signal. According to [24], for a more accurate height data, the number of satellites should be increased to four.

2.4.6 Differential GPS (DGPS)

Differential GPS is a technique for reducing the error [21]. This technique requires a reference station whose location is exactly known and a DGPS radio beacon antenna. Here, the reference station collects signal from GPS satellites and utilizing position determination technique that is used generally by GPS receivers, calculates its

location. It must be underlined that the location of the reference station is exactly known with respect to the Earth. Therefore, employing this information and calculated location data, reference station can calculate the GPS error. After this step, using radio beacon antenna, reference station sends a correction signal. Accordingly, another GPS receiver takes this correction signal and corrects its calculated location. Figure 2.16 illustrates DGPS technique. More information can be found in [21].

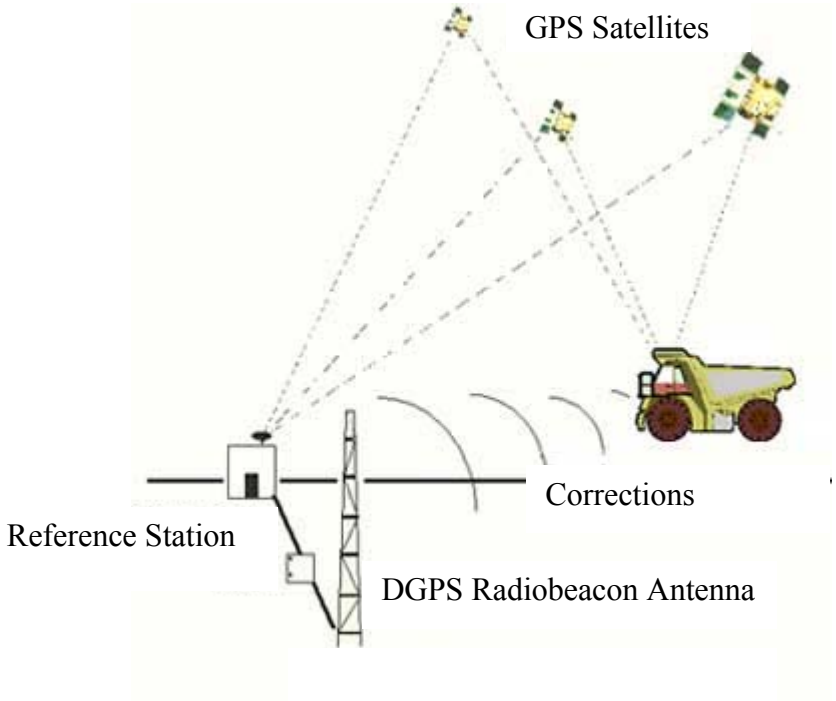

Figure 2.16 DGPS Scheme [21]

2.5 Kalman Filter

The Kalman Filter is an estimator for state of a linear system. In other words, it is used in order to estimate the instantaneous state of a linear dynamic system perturbed by inputs with white noise using measurements linearly related to the dynamic system which are also perturbed by white noise. This state estimator is statistically optimal in the sense of minimizing a quadratic function of the estimation error [22].

Before giving the mathematical background of the Kalman Filter, a brief information about stochastic systems is given.

2.5.1 Stochastic Systems

Systems that involve random processes are called stochastic systems. The mathematical form of a linear stochastic system is as follows

$$\begin{aligned} \dot{x}(t) &= A(t)x(t) + B(t)u(t) + G(t)w(t) \\ z(t) &= C(t)x(t) + D(t)u(t) + v(t) \end{aligned} \tag{2.44}$$

where $x(t)$ is $n\times 1$ state vector, $z(t)$ is $l\times 1$ measurement vector, $u(t)$ is $r\times 1$ deterministic input vector, $A(t)$ is $n\times n$ time varying dynamic coefficient matrix, $B(t)$ is $n\times r$ time varying state derivative coupling matrix, $C(t)$ is $l\times n$ time varying measurement sensitivity matrix, $D(t)$ is $l\times r$ time varying output coupling matrix, $G(t)$ is $n\times r$ time varying process noise coupling matrix, $w(t)$ is $r\times 1$ zero mean uncorrelated plant noise process, $v(t)$ is $l\times 1$ zero mean uncorrelated measurement noise process.

The expected values and the correlations of the random noises are as given below.

$$E\left\langle w(t)\right\rangle = 0$$

$$E\left\langle v(t)\right\rangle = 0$$

$$E\left\langle w(t_1)w^T(t_2)\right\rangle = Q(t_1)\delta(t_2 - t_1)$$

$$E\left\langle v(t_1)v^T(t_2)\right\rangle = R(t_1)\delta(t_2 - t_1)$$

$$E\left\langle v(t_1)v^T(t_2)\right\rangle = M(t_1)\delta(t_2 - t_1)$$

The symbols Q, R and M represent $r \times r$, $l \times l$ and $r \times l$ matrices, respectively. δ is Dirac delta function.

The discrete form of the stochastic system is

$$\begin{aligned} x_k &= \phi_{k-1}x_{k-1} + \Gamma_{k-1}u_{k-1} + G_{k-1}w_{k-1} \\ z_k &= C_k x_k + D_k u_k + v_k \end{aligned} \tag{2.45}$$

Here,

$$\phi_{k-1} = e^{A((k-1)T-kT)}$$

$$\Gamma_{k-1} = \int_{kT}^{(k-1)T} e^{A((k-1)T-kT)}B(s)ds$$

$$G_{k-1} = \int_{kT}^{(k-1)T} e^{A((k-1)T-kT)}G(s)ds$$

Also, $u(t) = u_{k-1}$ and $w(t) = w_{k-1}$ for $(k-1)T \le t \le kT$.

More information can be found in reference [22].

2.5.2 Discrete Kalman Filter

The discrete Kalman Filter is a recursive filter. That means the computer does not keep all the past values in its memory to estimate the current value of the states. For this reason, the discrete Kalman Filter is suitable for computer implementation. The algorithm of the discrete Kalman filter is given as flow chart in Figure 2.17.

In Figure 2.17, $\hat{x}_k^-$ is the predictive value of the state vector. P_k^- is the predictive error covariance matrix and $\hat{x}_k$ is the estimated value of the state vector. P_k is the estimated error covariance matrix.

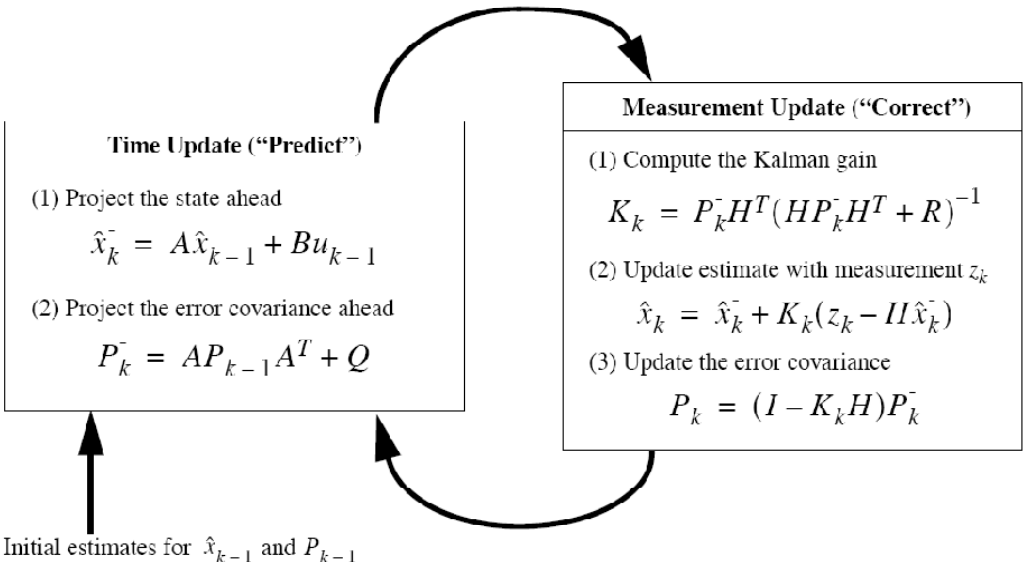

Figure 2.17 Discrete Kalman Filter Loop

2.5.3 Linear Form of the Mechanization Equations

As mentioned before, the mechanization equations are the differential equations whose solutions present the position, velocity and attitude information with respect to a particular frame by utilizing IMU output. Since there are some errors in computation of the mechanization equations like gyroscopes' drift, accelerometer bias etc., these errors can be estimated using the Kalman Filter. On the other hand, Kalman Filter's mathematical model must be linear. Therefore, the mechanization equations can be linearized using perturbation technique.

The mechanization equations can be written compactly as

$$\dot{x} = f(x,u) \tag{2.46}$$

where

$$x = \begin{bmatrix} \phi & \theta & \psi & V_N & V_E & V_D & \mu & \lambda & h \end{bmatrix}^T$$

$$u = \begin{bmatrix} \omega_x & \omega_y & \omega_z & a_x & a_y & a_z \end{bmatrix}^T$$

Here, roll, pitch, yaw angles, North, East, down velocities and latitude, longitude and height are the components of x. Drifts of x, y and z axis gyroscopes and biases of x, y and z axis accelerometers are the components of u.

The perturbed mechanization equation becomes

$$\delta \dot{x} = A\delta x + B\delta u \tag{2.47}$$

where

$$\delta x = \begin{bmatrix} \delta\phi & \delta\theta & \delta\psi & \delta V_N & \delta V_E & \delta V_D & \delta\mu & \delta\lambda & \delta h \end{bmatrix}^T$$

$$\delta u = \begin{bmatrix} \delta\omega_x & \delta\omega_y & \delta\omega_z & \delta a_x & \delta a_y & \delta a_z \end{bmatrix}^T$$

and

$$A = \left.\frac{\partial f(x,u)}{\partial x}\right|_{x,u}, \quad B = \left.\frac{\partial f(x,u)}{\partial u}\right|_{x,u}$$

The details of A and B matrices are given in reference 4.

$$B = \begin{bmatrix} \hat{C}^{(gf,bf)} & 0 \\ 0 & -\hat{C}^{(gf,bf)} \end{bmatrix}$$

$$A = \begin{bmatrix}
0 & -\Omega\sin\mu - \frac{V_E}{R}\tan\mu & \frac{V_N}{R} & 0 & \frac{1}{R} & 0 & -\Omega\sin\mu & 0 & -\frac{V_E}{R^2} \\
\Omega\sin\mu + \frac{V_E}{R}\tan\mu & 0 & \Omega\cos\mu + \frac{V_E}{R} & -\frac{1}{R} & 0 & 0 & 0 & 0 & \frac{V_N}{R^2} \\
-\frac{V_N}{R} & -\Omega\cos\mu - \frac{V_E}{R} & 0 & 0 & -\frac{\tan\mu}{R} & 0 & -\Omega\cos\mu + \frac{V_E}{R\cos^2\mu} & 0 & \frac{V_E}{R^2}\tan\mu \\
0 & -a_D & a_E & \frac{V_D}{R} & -2\Omega\sin\mu - \frac{2V_E}{R}\tan\mu & \frac{V_N}{R} & -2V_E\Omega\cos\mu - \frac{V_E^2}{R\cos^2\mu} & 0 & \frac{1}{R^2}\left(V_E^2\tan\mu - V_N V_D\right) \\
a_D & 0 & -a_N & \left(2\Omega\sin\mu + \frac{V_E}{R}\tan\mu\right) & \frac{1}{R}\left(V_N\tan\mu + V_D\right) & 2\Omega\cos\mu + \frac{V_E}{R} & \left(2\Omega\left(V_N\cos\mu - V_D\sin\mu\right) + \frac{V_N V_E}{R\cos^2\mu}\right) & 0 & -\frac{V_E}{R^2}\left(V_N\tan\mu + V_D\right) \\
-a_E & a_N & 0 & -\frac{2V_N}{R} & -2\Omega\cos\mu - \frac{2V_E}{R} & 0 & 2\Omega V_E\sin\mu & 0 & \frac{1}{R^2}\left(V_N^2 + V_E^2\right) \\
0 & 0 & 0 & \frac{1}{R} & 0 & 0 & 0 & 0 & -\frac{V_N}{R^2} \\
0 & 0 & 0 & 0 & \frac{1}{R\cos\mu} & 0 & \frac{V_E\tan\mu}{R\cos\mu} & 0 & -\frac{V_E}{R^2\cos\mu} \\
0 & 0 & 0 & 0 & 0 & -1 & 0 & 0 & 0
\end{bmatrix}$$

2.5.4 Error Model of IMU

According to ref. [4], δu consists of fixed bias and drifts term, the g dependent bias coefficient, the anisoelastic coefficient etc. and white noise.

Therefore, one can decompose δu as

$$\delta u = \delta c + w \tag{2.48}$$

where δc is constant and w is the white noise in the sensors [23].

$$w = \begin{bmatrix} w_{dx} & w_{dy} & w_{dz} & w_{ax} & w_{ay} & w_{az} \end{bmatrix}^T \tag{2.49}$$

w consists of white noise terms associated with gyro x, gyro y, gyro z, accelerometer x, accelerometer y and accelerometer z.

So, Eq.2.41 becomes

$$\begin{bmatrix} \delta\omega_x \\ \delta\omega_y \\ \delta\omega_z \\ \delta a_x \\ \delta a_y \\ \delta a_z \end{bmatrix} = \begin{bmatrix} d_x \\ d_y \\ d_z \\ b_x \\ b_y \\ b_z \end{bmatrix} + \begin{bmatrix} w_{dx} \\ w_{dy} \\ w_{dz} \\ w_{ax} \\ w_{ay} \\ w_{az} \end{bmatrix} \tag{2.50}$$

Where, $\delta c = \begin{bmatrix} d_x & d_y & d_z & b_x & b_y & b_z \end{bmatrix}^T$ comprises the drift terms of the rate gyros and the bias terms of the accelerometers.

According to ref. [23], δc is assumed to not change with time. Actually, this assumption is made because the mathematical model of δc is very complex.

In other words,

$$\delta\dot{c} = \begin{bmatrix} \dot{d}_x \\ \dot{d}_y \\ \dot{d}_z \\ \dot{b}_x \\ \dot{b}_y \\ \dot{b}_z \end{bmatrix} = 0 \tag{2.51}$$

2.5.5 Kalman Filter for State and Parameter Estimation

The Kalman Filter can be extended by combining Eq.2.47 and Eq.2.51 as follows so that it can be used to estimate both δx and δc.

$$\begin{bmatrix} \delta\dot{x} \\ \delta\dot{c} \end{bmatrix} = \begin{bmatrix} A & B \\ 0 & 0 \end{bmatrix} \begin{bmatrix} \delta x \\ \delta c \end{bmatrix} + \begin{bmatrix} B \\ 0 \end{bmatrix} w \tag{2. 52}$$

2.5.6 Kalman Filter Measurement Model

GPS receivers supply latitude, longitude and height information and also North, East and down velocities. This information is used for the Kalman Filter measurement. In this present work, all information (i.e. latitude, longitude, height and North, East, down velocities) is used for the Kalman Filter measurement.

According to the Kalman Filter System model, the augmented state vector is

$$\begin{bmatrix} \delta x \\ \delta c \end{bmatrix} = \begin{bmatrix} \delta\phi & \delta\theta & \delta\psi & \delta V_N & \delta V_E & \delta V_D & \dots \\ \delta\mu & \delta\lambda & \delta h & dx & dy & dz & bx & by & bz \end{bmatrix}^T \tag{2.53}$$

On the other hand, the GPS receiver provides μ, λ, h, V_N, V_E, V_D. Therefore, the Kalman Filter measurement model becomes

$$z = \begin{bmatrix} 0 & 0 & 0 & 0 & 0 & 0 & 1 & 0 & 0 & 0 & 0 & 0 & 0 & 0 & 0 \\ 0 & 0 & 0 & 0 & 0 & 0 & 0 & 1 & 0 & 0 & 0 & 0 & 0 & 0 & 0 \\ 0 & 0 & 0 & 0 & 0 & 0 & 0 & 0 & 1 & 0 & 0 & 0 & 0 & 0 & 0 \\ 0 & 0 & 0 & 1 & 0 & 0 & 0 & 0 & 0 & 0 & 0 & 0 & 0 & 0 & 0 \\ 0 & 0 & 0 & 0 & 1 & 0 & 0 & 0 & 0 & 0 & 0 & 0 & 0 & 0 & 0 \\ 0 & 0 & 0 & 0 & 0 & 1 & 0 & 0 & 0 & 0 & 0 & 0 & 0 & 0 & 0 \end{bmatrix} \begin{bmatrix} \delta x \\ \delta c \end{bmatrix} \tag{2.54}$$

2.6 GPS/INS Integration

INS has some errors due to gyroscopes' drift and accelerometer's bias. In addition to this, it suffers from some calculation errors caused by numerical methods. Therefore, these errors must be reduced by means of some other assisting sensors like magnetic compass, barometer, altimeter, GPS etc.

In this work, GPS and INS integration is dealt with. Three different types of GPS/INS integration can be distinguished. These are uncoupled, loosely coupled and tightly coupled systems.

2.6.1 Uncoupled GPS/INS Integration

This is the most basic method of GPS/INS integration. In this approach, GPS and INS are working autonomously. That means there is no data feedback from either instrument (i.e. GPS or INS) to the other for the purpose of improving its performance. Figure 2.18 shows uncoupled GPS/INS integration method. In the Figure 2.18, ρ indicates the estimated distances from the GPS receiver to the satellites, called pseudo ranges, P and V designate the position and velocity, respectively.

In the uncoupled GPS/INS integration model, by using GPS receiver's position and velocity estimates, the INS error is reset. In this way, the INS errors are bounded. Yet, uncoupled GPS/INS integration does not provide performance enhancement because INS and GPS run separately. In other words, there is no data feedback from one sensor to the other [4].

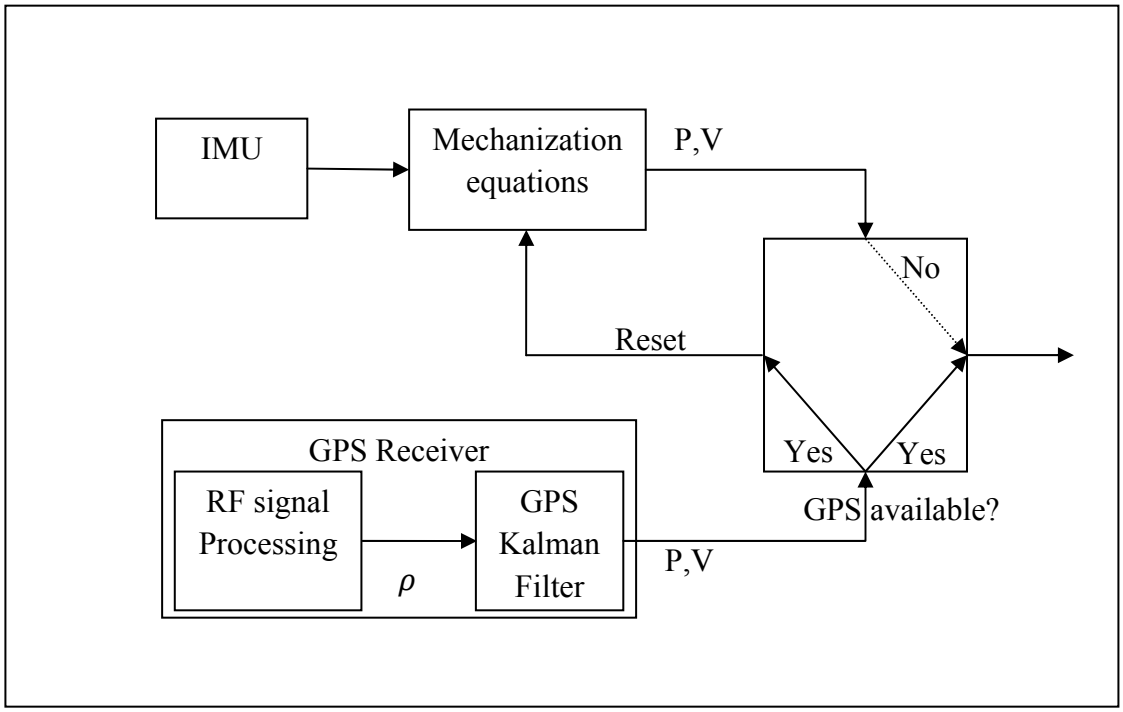

Figure 2.18 Uncoupled GPS/INS Integration

2.6.2 Loosely Coupled GPS/INS Integration

This approach allows the GPS to function independently, as a separate device but at the same time it simultaneously brings in measurement updates to the inertial system. That means in loosely coupled GPS/INS integration, GPS data is used for Kalman Filter measurement data. In addition to that, Kalman Filter improves the INS's performance by estimating the errors of mechanization equations. Thus, the two systems are operated efficiently in cascade with the position and/or velocity estimates provided by the GPS [4]. A simplified diagram of a loosely coupled GPS/INS integration is given in Figure 2.19. Similar to Figure 2.18, ρ indicates the

estimated distances from the GPS receiver to the satellites, called pseudo ranges, P and V designate the position and velocity, respectively.

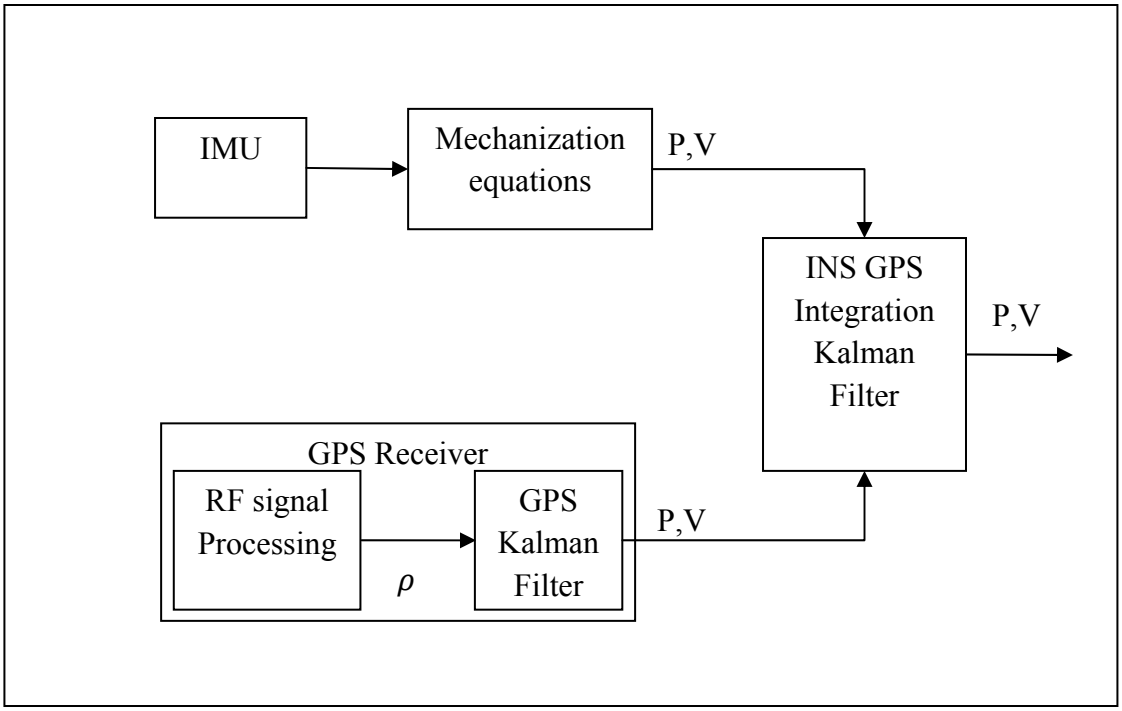

Figure 2.19 Loosely Coupled GPS/INS Integration Diagram

There are two main advantages of loosely coupled integration. These are simplicity and redundancy. Here, simplicity means the loosely coupled GPS/INS integration can be implemented with any kind of GPS receivers and IMUs. Redundancy means the loosely coupled GPS/INS integration provides GPS and integrated data at the same time.

2.6.3 Tightly Coupled GPS/INS Integration

Figure 2.20 shows a simplified representation of a tightly coupled GPS/INS integration. This method is also known as centralized or direct integration model. In this methodology, Kalman Filter equations become more complex than loosely coupled one. Thus, pseudo range and mechanization equations' output are accepted by Kalman Filter. These pseudo ranges are used in the calculation of estimates of the errors in the INS. Then, the corrected INS navigation solution becomes the integrated

navigation solution [4]. In addition to that, in the tightly coupled GPS/INS integration, GPS and IMU are treated as a single system and the output is only the integrated data. Therefore, system is tighter than the loosely coupled GPS/INS integration.

Compared to the loosely coupled system, the tightly coupled system performs better in terms of both accuracy and system robustness. Yet, in tightly coupled system, GPS receiver provides pseudo ranges to the user. Thus, every GPS receiver cannot be used in the tightly coupled system.

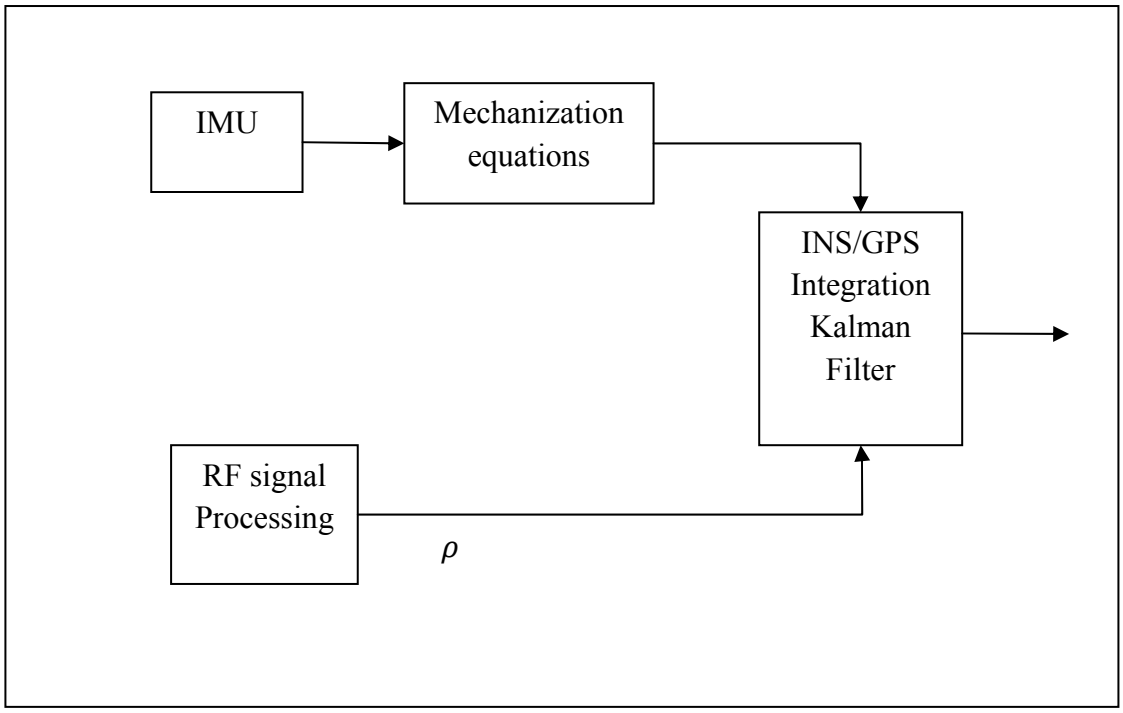

Figure 2.20 Tightly Coupled GPS/INS Integration Diagram

2.6.4 Feedback Loosely Coupled GPS/INS Integration

In this approach, the Kalman Filter error states estimations are fed back to the mechanization equations simultaneously. The solutions of the mechanization equations are obtained by performing discrete integral calculations. Therefore, in the discrete integral calculations, the state variables of the previous step are updated using the Kalman Filter estimations of the error states. Thus, the outputs of the mechanization equations are prevented from containing cumulative IMU errors.

Figure 2.21 illustrates the feedback loosely coupled GPS/INS integration methodology.

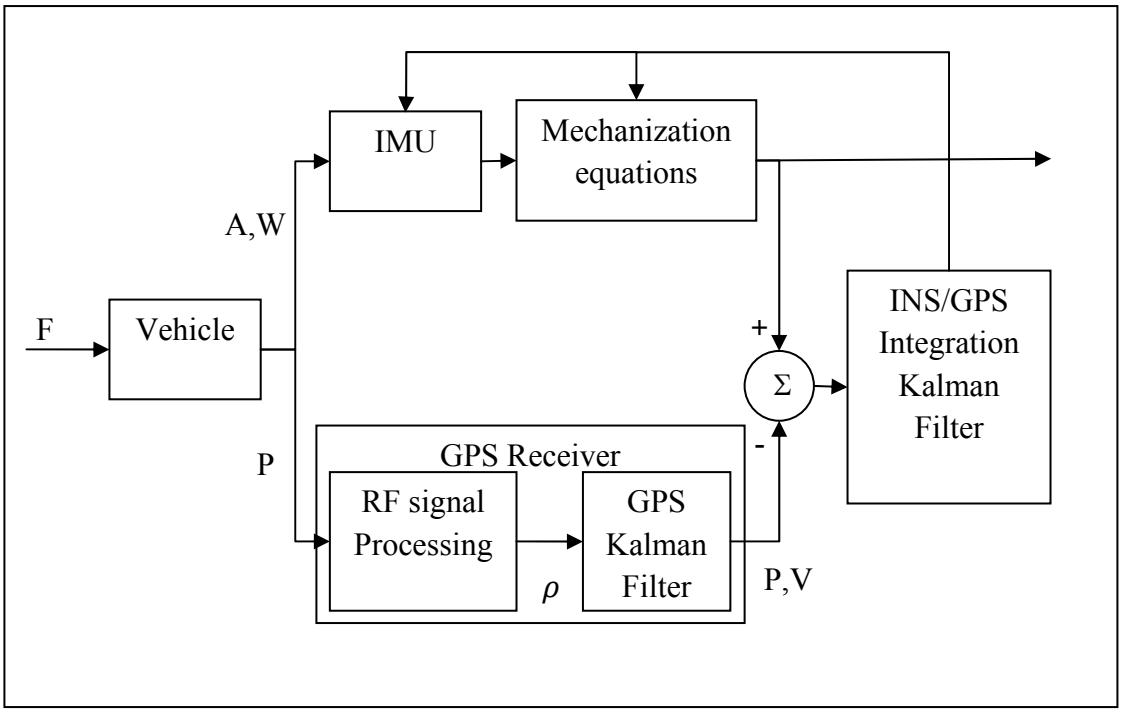

Figure 2.21 Feedback Loosely Coupled GPS/INS Integration Diagram

2.6.5 Feed Forward Loosely Coupled GPS/INS Integration

In this approach, the Kalman Filter estimations of the error states are fed forward. In other words, the Kalman Filter estimations of the error states are subtracted directly from the mechanization equations' outputs. Thus, the integration process of the mechanization equations is not interrupted as done in the feedback method. Therefore, the feed forward method is simpler to implement as compared to the feedback method but naturally it is less accurate, because the estimated corrections tend to grow in time due to the fact that the mechanization equations are kept being integrated without any interruption. Figure 2.22 shows the feed forward loosely coupled GPS/INS integration methodology.

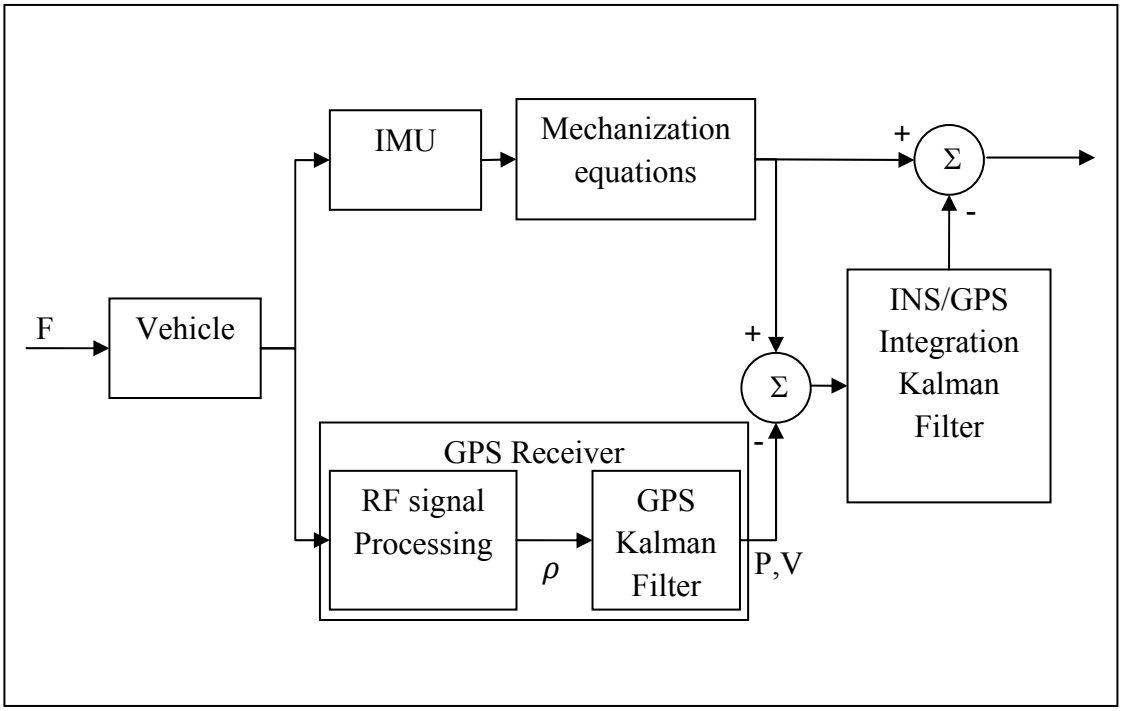

Figure 2.22 Feed Forward Loosely Coupled GPS/INS Integration

In the current study, both feed forward and feedback loosely coupled GPS/INS system are studied and implemented. In Chapter 3, the implementations are explained in more detailed.

CHAPTER 3

TEST SETUP AND MATLAB PROGRAM

3.1 Test Setup

In the current study, GARMIN 10 GPS receiver and CROSSBOW IMU 440 CA 200 are used.

3.1.1 GARMIN 10 GPS Receiver

Figure 3.1 Garmin GPS 10

In this study, Bluetooth Garmin 10 GPS receiver is used. It is capable of sending NMEA 0183 sentences, which is a data specification for communication between marine electronic devices such as sonar, GPS etc.

In Appendix E, the NMEA 0183 sentences are shown.

3.1.2 CROSSBOW IMU 440 CA 200

Figure 3.2 Crossbow IMU 440 CA 200

Crossbow IMU 440 CA 200 model IMU is utilized in this thesis. It is used at 100 Hz data receiving frequency and communication between computer and IMU is achieved via a standard serial port. Basic specifications of Crossbow IMU are given in Appendix D.

3.2 IMU Initialization

As mentioned in the preceding chapter, the INS mechanization is realized by using differential equations. Thus, accurate values of the initial conditions of IMU are required. In literature, there are a wide range of methods for initialization. For further information, see ref [4]. In this study, however, the effect of the initial alignment errors on the estimated location of the vehicle is tried to be eliminated by using GPS assistance.

3.2.1 Position and Velocity Initialization

In this study, the position initialization is achieved by making use of the GPS outputs. After mounting the IMU to the vehicle, data are collected from the GPS for approximately five minutes when the vehicle is stationary. Then, the average value of these data is calculated. As a result, the initial position values for the IMU are attained. The initial velocity values are zero because when the navigation begins the vehicle is at rest.

3.2.2 Navigation Frame Alignment

IMU's z axis alignment is done by looking at the z axis' accelerometer. This accelerometer value should be the absolute value of the gravity vector. IMU's x axis can be aligned with the true North by the Google Earth program [25]. In this process, IMU's x axis is approximately aligned, by taking some reference point of the true North like a tree etc. and by spotting that point using the Google Earth program.

3.3 Kalman Filter System Noise Covariance Matrix (Q) Analysis

IMU data is collected for three hours in order to find the noise covariance matrix. For this purpose, IMU is situated in a stationary position and 1080000 numbers of data is collected at 100 Hz. Later, the standard deviation of these data is calculated.

Assuming zero cross-correlations, the Kalman Filter noise covariance matrix is conjectured to be

$$Q = \begin{bmatrix} \sigma^2_{\omega_x} & 0 & 0 & 0 & 0 & 0 \\ 0 & \sigma^2_{\omega_y} & 0 & 0 & 0 & 0 \\ 0 & 0 & \sigma^2_{\omega_z} & 0 & 0 & 0 \\ 0 & 0 & 0 & \sigma^2_{a_x} & 0 & 0 \\ 0 & 0 & 0 & 0 & \sigma^2_{a_y} & 0 \\ 0 & 0 & 0 & 0 & 0 & \sigma^2_{a_z} \end{bmatrix}$$

where

$\sigma_{\omega_x}, \sigma_{\omega_y}, \sigma_{\omega_z}, \sigma_{a_x}, \sigma_{a_y}, \sigma_{a_z}$ are the standard deviations of the x, y, z axis' gyroscopes data and the x, y , z axis' accelerometer data.

The calculated numerical values for the elements of Q are given below.

$$Q = \begin{bmatrix} 3x10^{-6} & 0 & 0 & 0 & 0 & 0 \\ 0 & 1x10^{-5} & 0 & 0 & 0 & 0 \\ 0 & 0 & 1.2x10^{-5} & 0 & 0 & 0 \\ 0 & 0 & 0 & 0.3x10^{-5} & 0 & 0 \\ 0 & 0 & 0 & 0 & 0.7x10^{-5} & 0 \\ 0 & 0 & 0 & 0 & 0 & 0.9x10^{-5} \end{bmatrix}$$

3.4 Kalman Filter Measurement Noise Covariance Matrix (R) Analysis

In this case, similar to the process described above, about eight hours of GPS data is collected for finding the noise covariance matrix. The GPS receiver, in this course of action, is also kept at a standstill position. 28800 numbers of data at 1 Hz are collected. Later, standard deviations are calculated.

The Kalman Filter noise covariance matrix is also conjectured to be diagonal. That is,

$$R = \begin{bmatrix} \sigma_{\mu}^2 & 0 & 0 & 0 & 0 & 0 \\ 0 & \sigma_{\lambda}^2 & 0 & 0 & 0 & 0 \\ 0 & 0 & \sigma_{h}^2 & 0 & 0 & 0 \\ 0 & 0 & 0 & \sigma_{V_N}^2 & 0 & 0 \\ 0 & 0 & 0 & 0 & \sigma_{V_E}^2 & 0 \\ 0 & 0 & 0 & 0 & 0 & \sigma_{V_D}^2 \end{bmatrix}$$

The calculated numerical values for the elements of R are given below.

$$R = \begin{bmatrix} 1x10^{-6} & 0 & 0 & 0 & 0 & 0 \\ 0 & 1x10^{-6} & 0 & 0 & 0 & 0 \\ 0 & 0 & 225 & 0 & 0 & 0 \\ 0 & 0 & 0 & 1x10^{-1} & 0 & 0 \\ 0 & 0 & 0 & 0 & 1x10^{-1} & 0 \\ 0 & 0 & 0 & 0 & 0 & 1x10^{-1} \end{bmatrix}$$

3.5 MATLAB Program

In this thesis, the implementation of the loosely coupled GPS/INS integration method is made by using MATLAB program. In the following section, MATLAB Simulink Real Time Windows Target is introduced and then MATLAB Simulink Block diagrams are given.

Figure 3.3 and 3.4 show the implementation architectures.

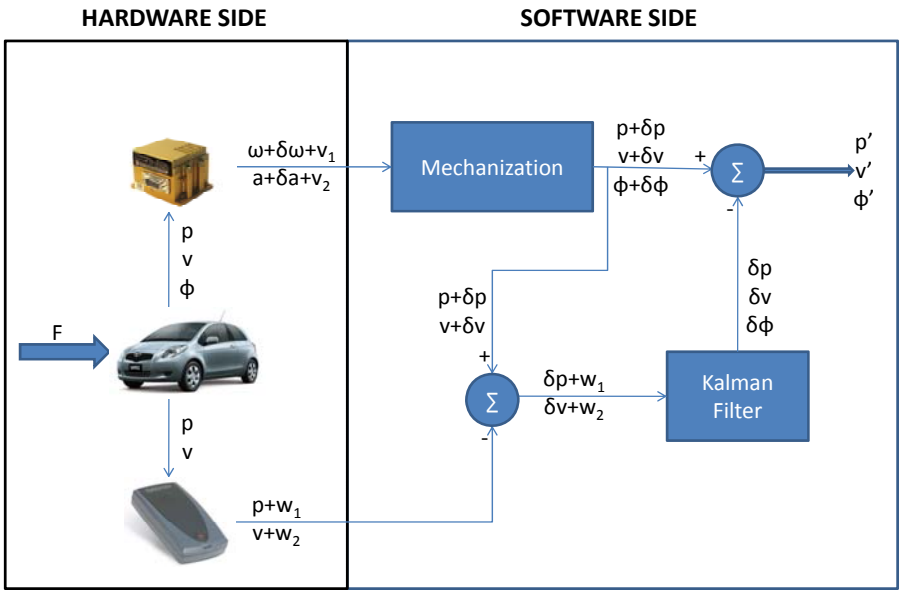

Figure 3.3 Feed Forward Loosely Coupled GPS/INS Integration

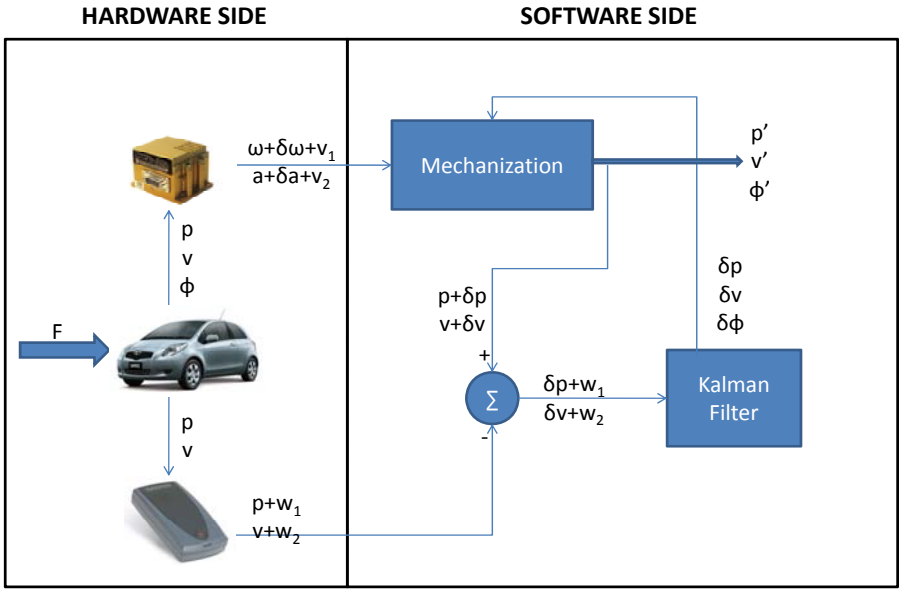

Figure 3.4 Feedback Loosely Coupled GPS/INS Integration

3.5.1 MATLAB Simulink Real Time Windows Target

The Real-Time Workshop (RTW) is a program that creates C language code for Simulink. This program, generates C code for employing Simulink block diagram models. These automatically generated C code programs can be operated in real time in real-time hardware including microcontrollers or digital signal processors.

The real-time kernel is the heart of the Real-Time Windows Target. This unit interfaces with the Microsoft Windows operating system. The Real-time kernel facilitates the assignment of the highest priority of execution. In this way, a real-time executable that is created by the Real-Time Workshop is prioritized within Windows operating system.

The Real-Time Windows Target, on the other hand, is a software program that authorizes you to run C code constructed by Real-Time Workshop on a PC in real time. In this case, the PC is turned into the host for MATLAB, Simulink, and the Real-Time Workshop.

As soon as C code is generated and compiled, PC is then used as a target for running the generated code. Signal processing, real-time control, and hardware-in-the-loop simulation are the most common usages of the Real-Time Windows Target.

Within a Windows NT operating system, the generated code runs efficiently by using standard I/O boards. The course of Real-Time Windows Target proceeds as follows: Firstly, while the program on the PC is running in real time, Real-Time Windows Target takes over a sample of data from one or more input channels. Next, it immediately processes these received data and then sends it back by the use of an output channel of an I/O board. In doing this, the Real-Time Windows Target utilizes the real-time capabilities of a kernel.

3.5.2 MATLAB Simulink Diagrams

In this subtitle, Simulink block diagrams are shown.

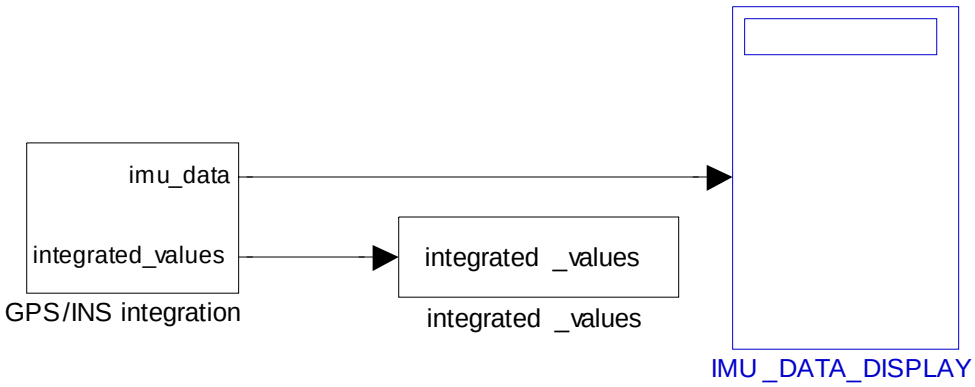

Figure 3.5 MATLAB Simulink Diagram of GPS/INS Integration

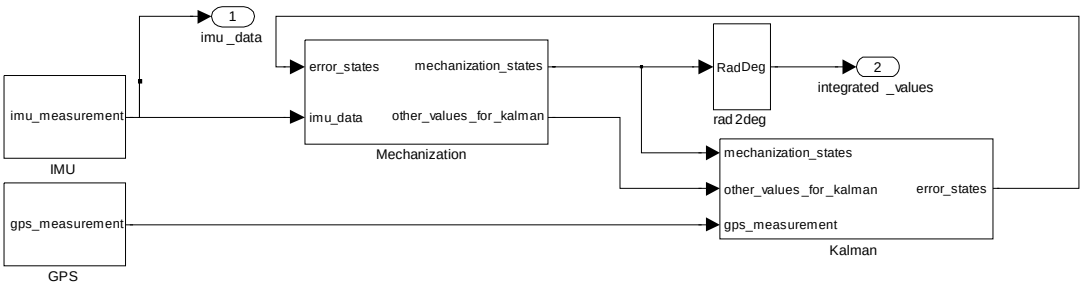

Figure 3.6 Subsystem of GPS/INS Integration Block

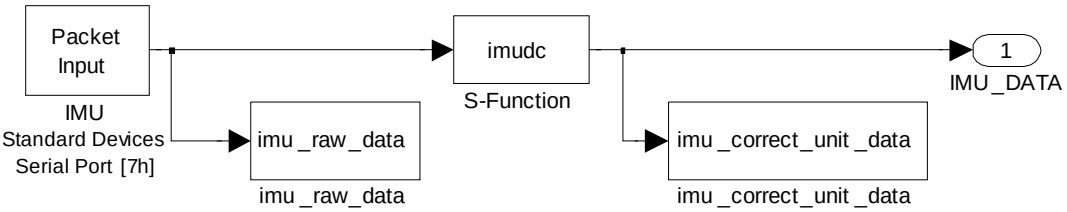

Figure 3.7 Subsystem of IMU Block

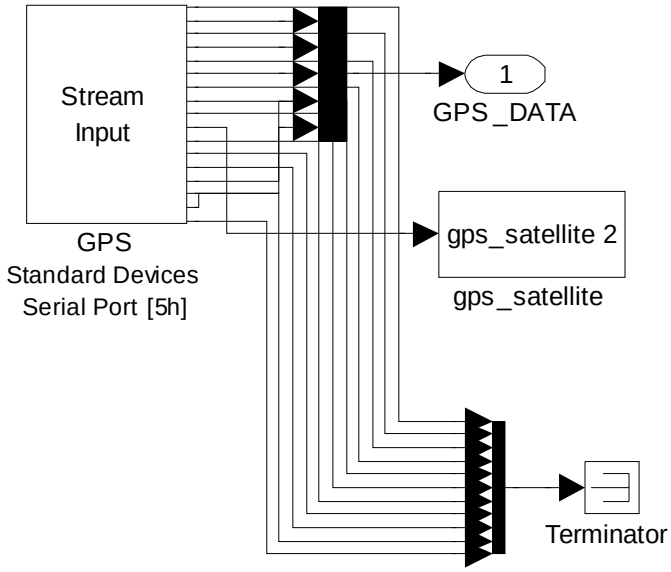

Figure 3.8 Subsystem of GPS Block

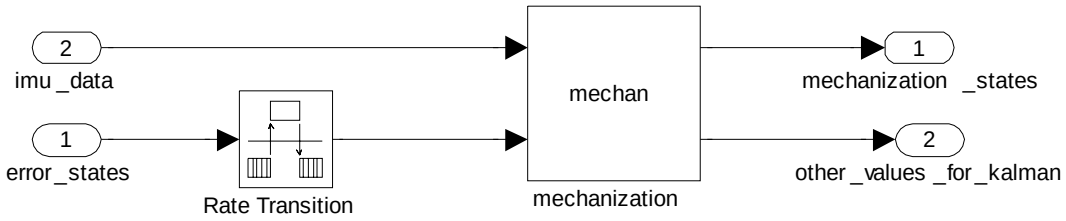

Figure 3.9 Subsystem of Mechanization Block

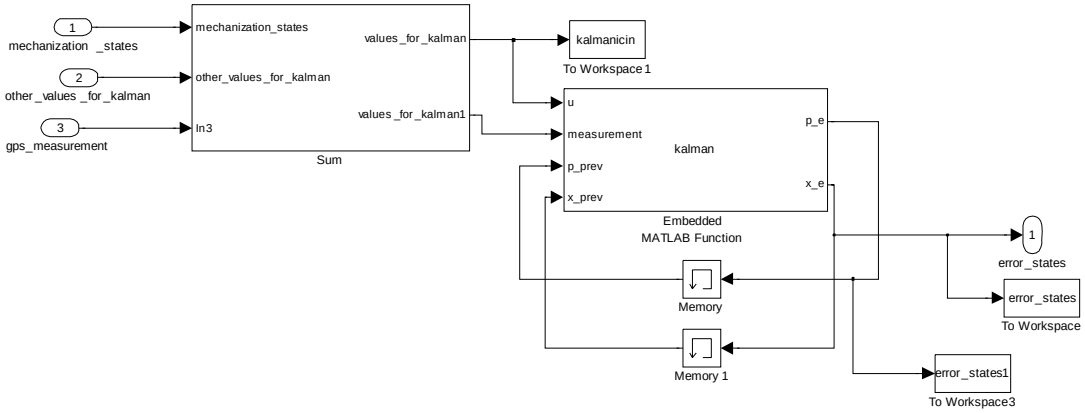

Figure 3.10 Subsystem of Kalman Block

CHAPTER 4

EXPERIMENTAL RESULTS

In this chapter, the test results of the GPS/INS integration described in this thesis are given.

The results can be divided into two main categories. The first category consists of the results of the feed forward GPS/INS integration. The second category consists of the results of the feedback GPS/INS integration. These two categories are separated further into two sub categories, which are associated with locating a stationary point and following a specified path.

Later, an additional test is made to study the effects of different initial positions and initial orientations. Furthermore, it is also studied what happens when the GPS data is lost for a while during the process.

4.1 Feed Forward GPS/INS Integration Results

For feed forward GPS/INS integration, first, the test results for a stationary point are given. Then, the test results for path following are presented. As mentioned in Section 2.6.5, the outputs of feed forward GPS/INS integration reach almost correct value when the Kalman Filter corrections are added to the outputs of the mechanization equations. On the other hand, the estimated corrections tend to grow due to the fact that the mechanization equations are kept being integrated without any interruption.

4.1.1 Results of Feed Forward GPS/INS Integration Obtained for a Stationary Position

The velocity with respect to the geographical frame must be zero for a stationary point. Besides, the estimated position of the vehicle must be constant.

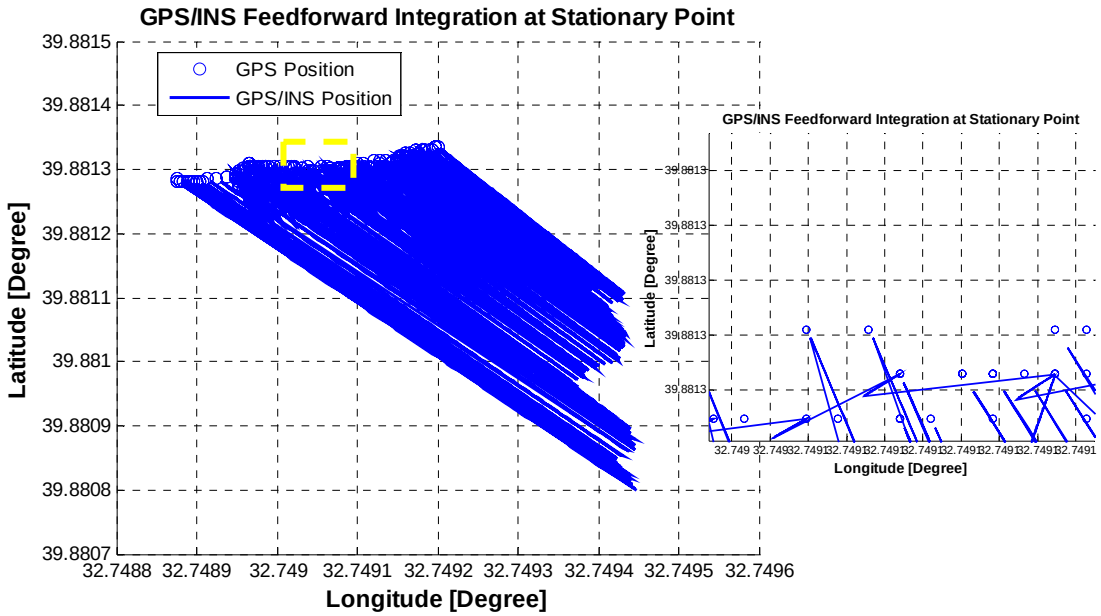

Figure 4.1 Feed Forward GPS/INS Integration Solutions for Latitude and Longitude at Stationary Point

In Figure 4.1, the latitude and longitude values provided by the feed forward GPS/INS integration are shown at the same time. As mentioned before, for feed forward loosely GPS/INS integration, when the Kalman Filter estimations of error states are used, the mechanization equations outputs become almost actual values. Otherwise, the mechanization equations outputs will become worse. In the figure, the upper bound is the GPS only output and the lower bound is the INS only output. In the zoomed figure, the integrated values can be seen.

INS only outputs grow away from the actual position due to the alignment errors, computational errors and instrumentation errors (e.g., bias, scale factor, random noise, nonlinearity etc.).

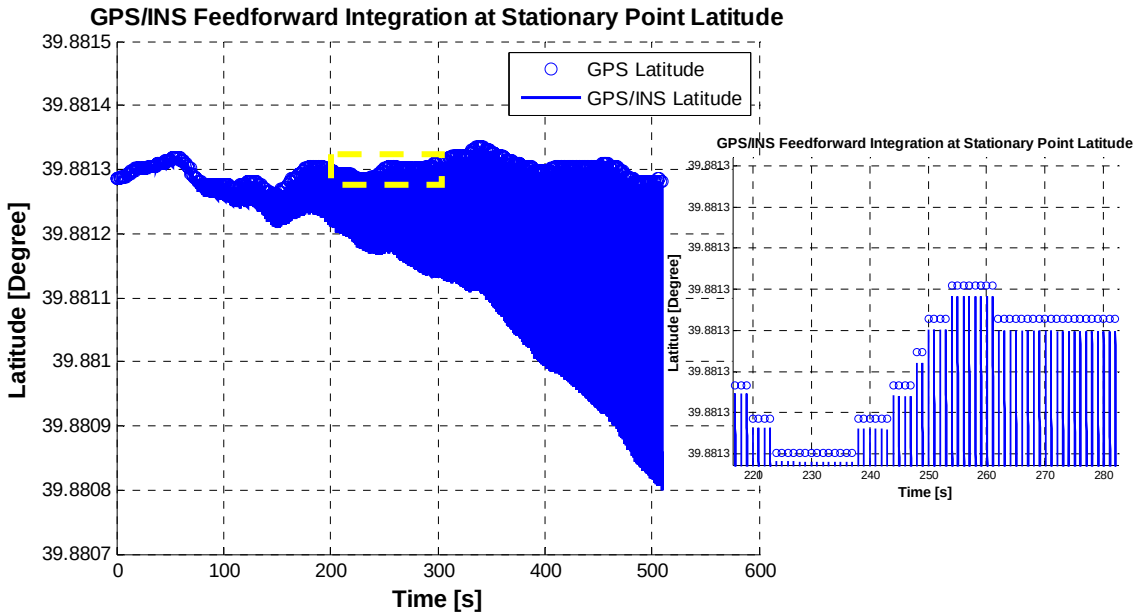

Figure 4.2 Latitude Solution of Feed Forward GPS/INS Integration at Stationary Point

The latitude solution of the GPS/INS integration is given in Figure 4.2. As can be seen from figure, the latitude error is growing for the loosely coupled feed forward GPS/INS integration. Only when the Kalman Filter output is added, the latitude becomes close to the actual value.

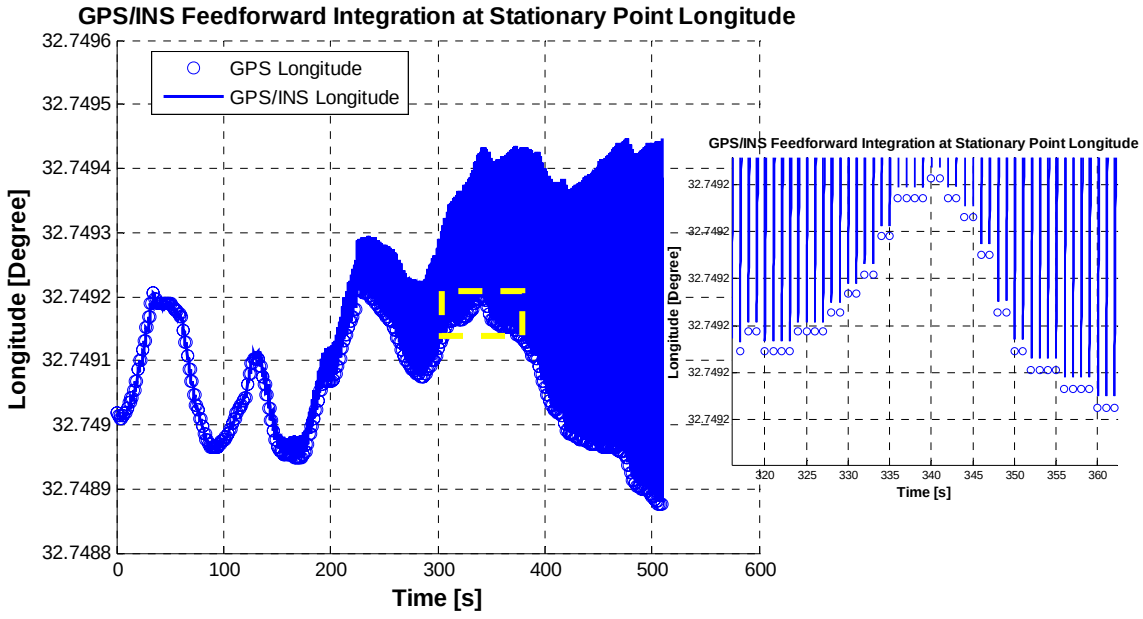

Figure 4.3 Longitude Solution of Feed Forward GPS/INS Integration at Stationary Point

The longitude solution is similar to the latitude solution. Owing to the reasons discussed above, this result is also anticipated.

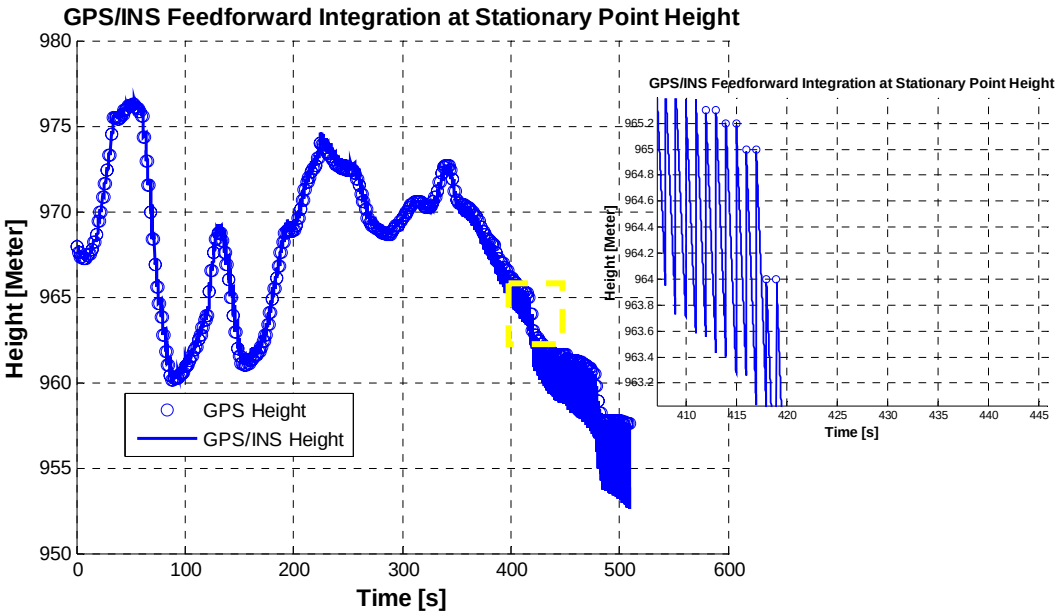

Figure 4.4 Height Solution of Feed Forward GPS/INS Integration at Stationary Point

The height solution is similar to the latitude and longitude solutions. Only when the Kalman Filter output is added, the height reaches an almost actual value.

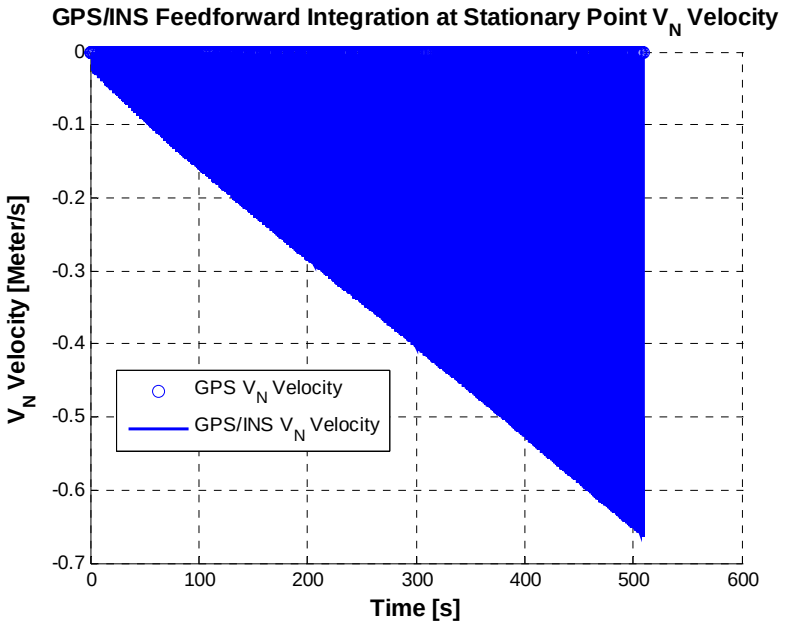

Figure 4.5 North Velocity Solution of Feed Forward GPS/INS Integration at Stationary Point

The Figure 4.5 shows the North velocity solution. Actually due to the same reasons discussed in Section 2.6.5, the mechanization equations output grow away from the actual values. Yet, when the Kalman Filter estimations of error states are used, the mechanization equations outputs become close to the actual value. Like the position solution, the upper bound is the GPS only solution and the lower bound is the INS only solution. About 510 seconds later at the stationary point, -0.67 m/s error occurs in the INS only solution.

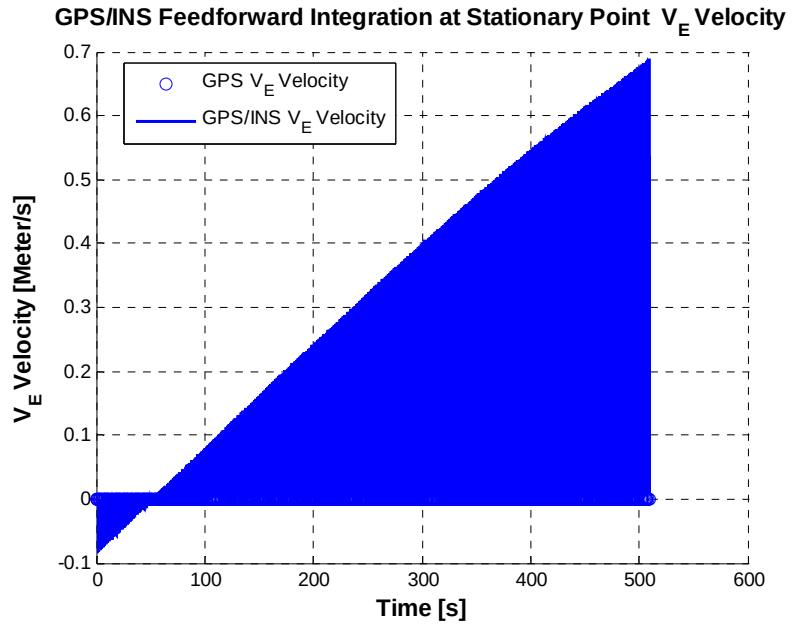

Figure 4.6 East Velocity Solution of Feed Forward GPS/INS Integration at Stationary Point

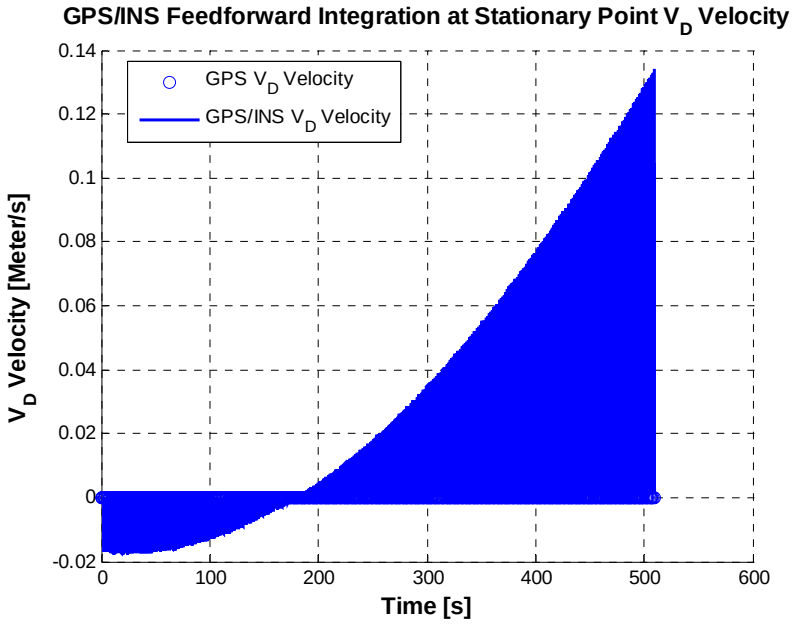

Figure 4.7 Down Velocity Solution of Feed Forward GPS/INS Integration at Stationary Point

The solutions for the East and Down velocities are similar to the North velocity solution. Owing to the reasons discussed above, these results are also expected.

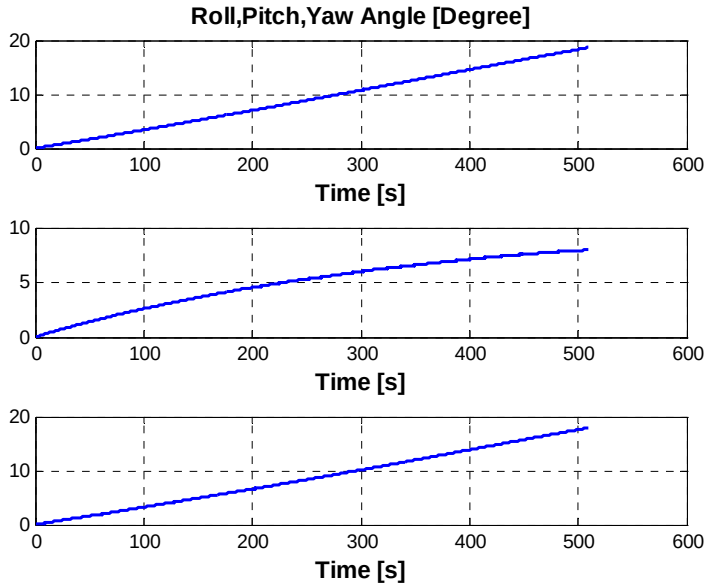

Figure 4.8 Roll, Pitch and Yaw Angle Solution of Feed Forward GPS/INS Integration at Stationary Point

The body frame x, y and z axis angular position with respect to the geographical frame is shown in Figure 4.8. They must be almost zero. Yet, they are increasing in the feed forward loosely coupled GPS/INS integration. Because in the loosely coupled feed forward GPS/INS integration, the outputs of the Kalman Filter are added after the mechanization equations are computed. Therefore, the Kalman Filter estimations of orientation errors do not correct the roll, pitch and yaw angles.

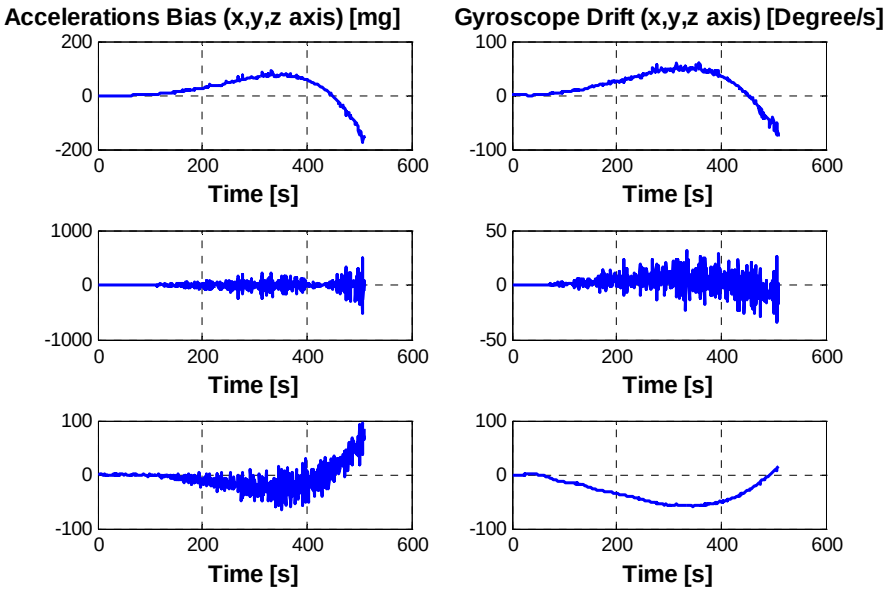

Figure 4.9 Gyro Drifts and Accelerometer Biases Estimation of Feed Forward GPS/INS Integration at Stationary Point

The biases of accelerometer and drifts of rate gyroscopes are similar to solutions of the roll, pitch and yaw angle.

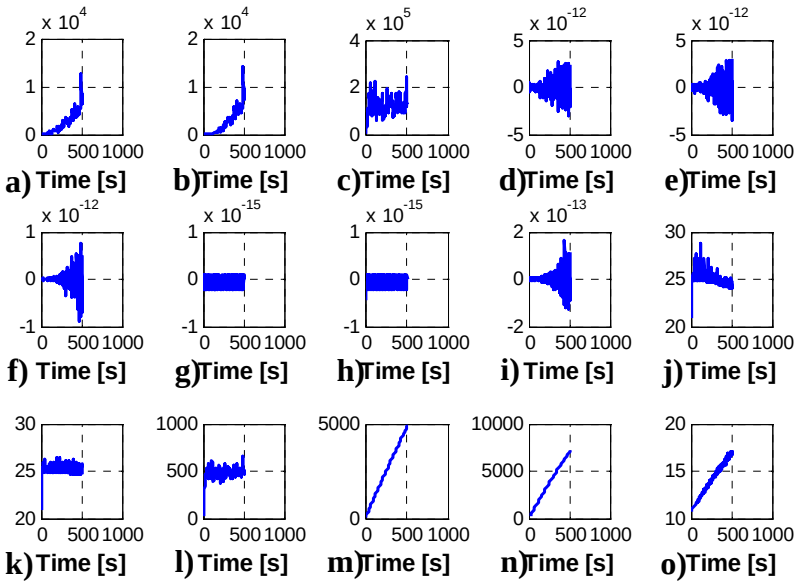

Figure 4.10 P Matrix Convergence Test of Feed Forward GPS/INS Integration at Stationary Point

P matrix is the error covariance matrix of the Kalman Filter. In Figure 4.10, convergence test results of P matrix are shown. Actually, values of convergence test results should be zero. Yet, as it can be seen from figure, they are not zero. Due to reasons discussed in Section 2.6.5, the estimated corrections tend to grow due to the fact that the mechanization equations are kept being integrated without any interruption.

4.1.2 Results of Feed Forward GPS/INS Integration Obtained While Following a Path

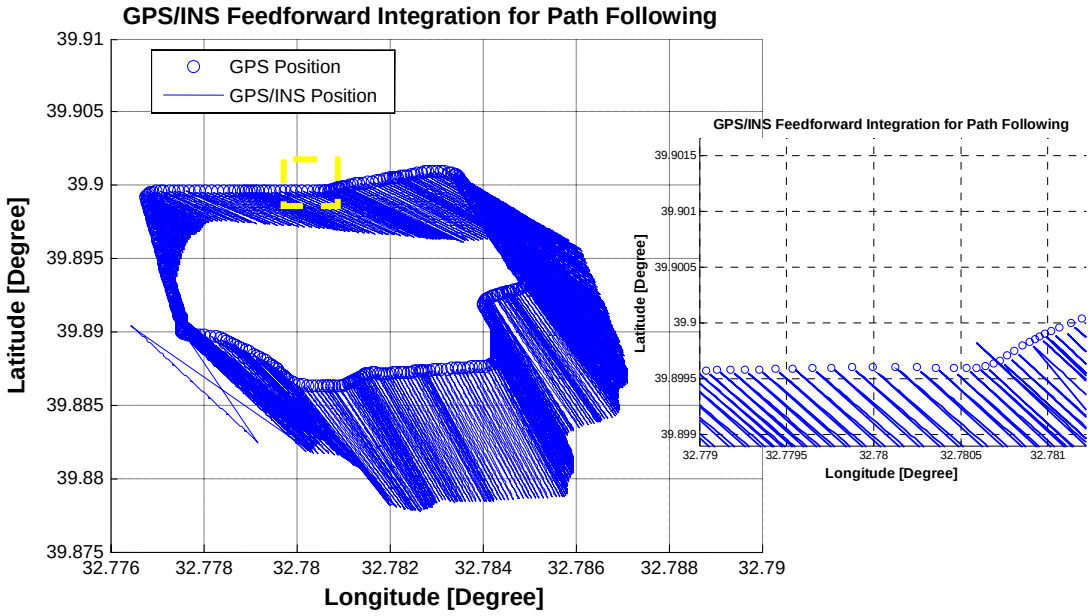

Figure 4.11 Feed Forward GPS/INS Integration Solution of Latitude and Longitude for Path Following

In Figure 4.11, the latitude and longitude values provided by the feed forward GPS/INS integration are shown in the same time. Like the stationary case, for the feed forward loosely GPS/INS integration, when the Kalman Filter estimations of error states are used, the mechanization equations outputs become almost actual. Otherwise, the mechanization equations outputs become worse. In the figure, the

upper bound is the GPS only output and the lower bound is the INS only output. In the zoomed figure, the integrated values can be seen.

The outputs of INS grow away from the actual values due to the alignment errors, computational errors and instrumentation errors (e.g., bias, scale factor, random noise, nonlinearity etc.).

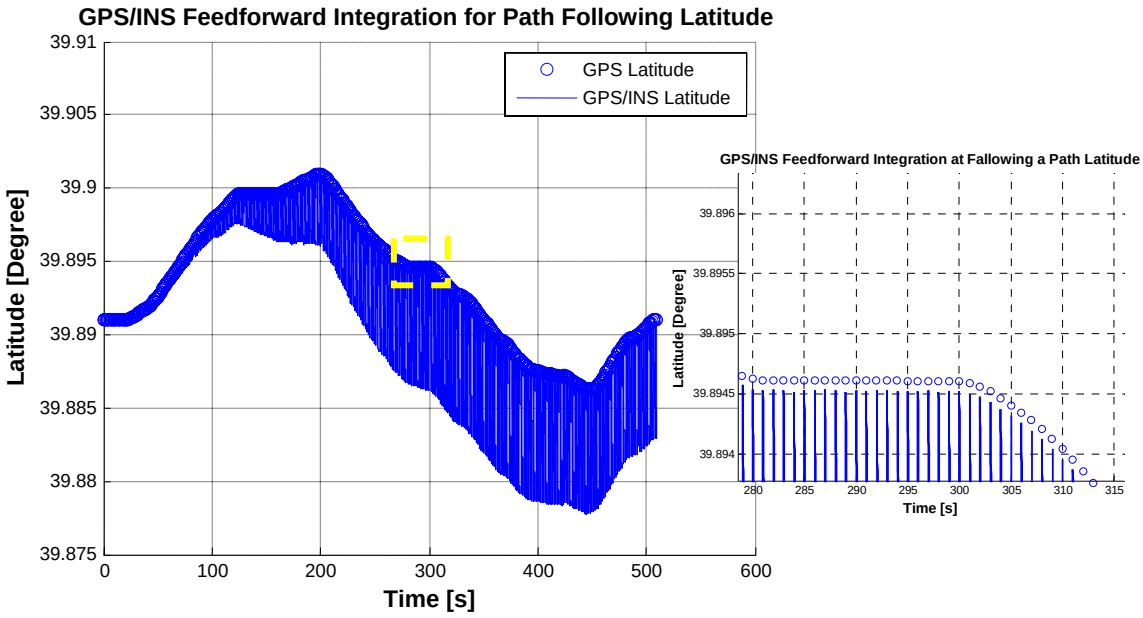

Figure 4.12 Latitude Solution of Feed Forward GPS/INS Integration for Path Following

The latitude solution of the GPS/INS integration is given in Figure 4.12. As can be seen from the figure, the latitude error is growing for the loosely coupled feed forward GPS/INS integration. Only when the Kalman Filter output is added, the latitude becomes close to the actual value. The upper bound is the GPS only output and the lower bound is the INS only output. In the zoomed figure, the GPS/INS integrated values can be seen.

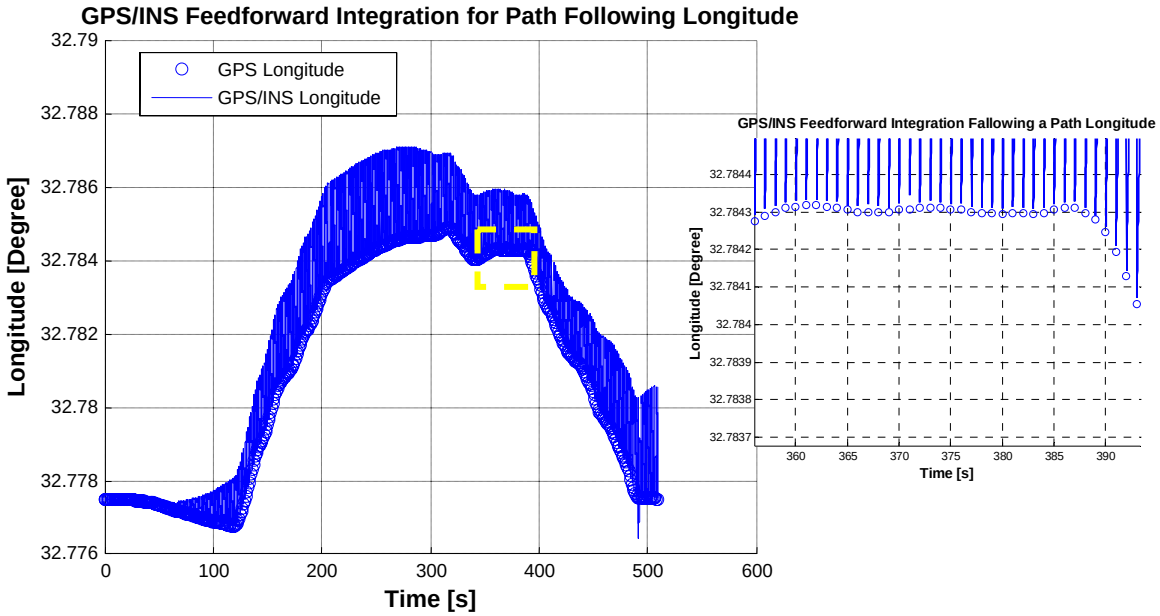

Figure 4.13 Longitude Solution of Feed Forward GPS/INS Integration for Path Following

The longitude solution is similar to the latitude solution. Owing to the reasons discussed above, these results are also expected. The upper bound is the GPS only output and the lower bound is the INS only output. In the zoomed figure, the integrated values can be seen.

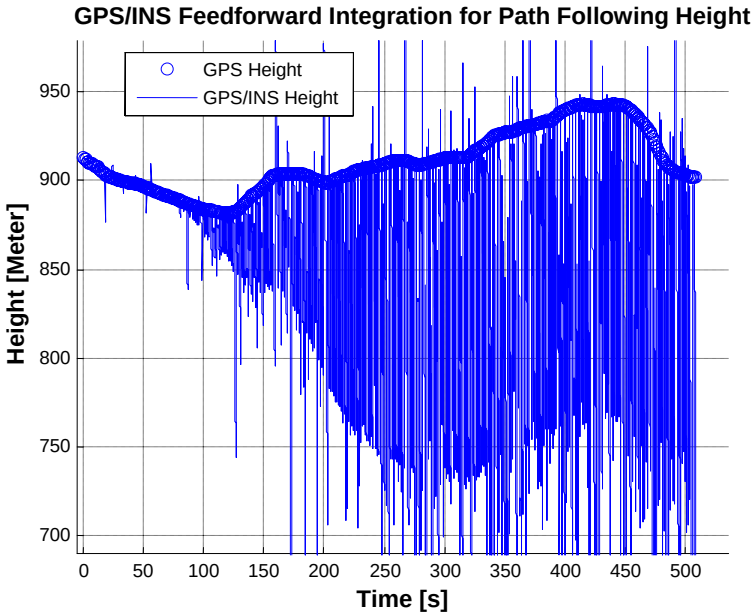

Figure 4.14 Height Solution of Feed Forward GPS/INS Integration for Path Following

The height solution is similar to the latitude and longitude solutions. Only when the Kalman Filter output is added, the height reaches an almost actual value.

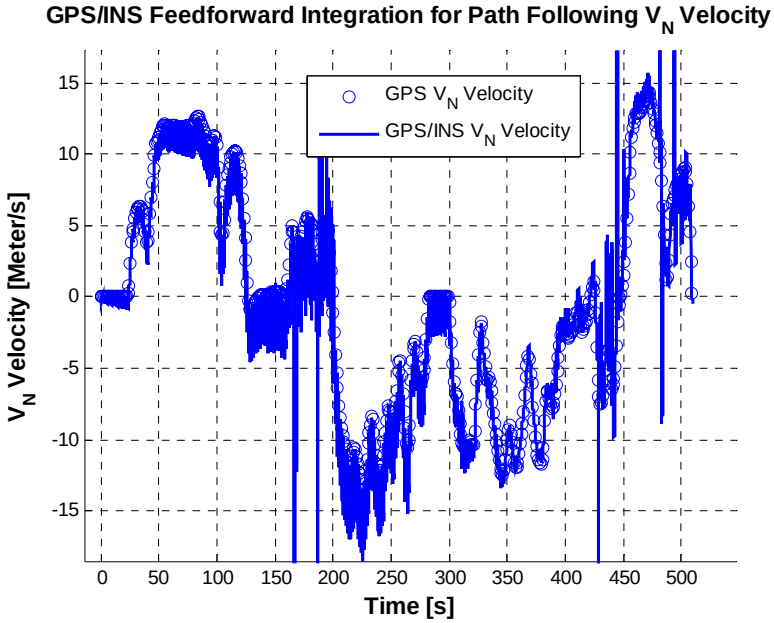

Figure 4.15 North Velocity Solution of Feed Forward GPS/INS Integration for Path Following

The Figure 4.15 shows the North velocity solution. Actually due to same reasons discussed in Section 2.6.5, the mechanization equations output errors grow. Yet, when the Kalman Filter estimations of error states are used, the outputs of the mechanization equations outputs become close to the actual values. Like the position solution, the upper bound is the GPS only solution and the lower bound is the INS only solution.

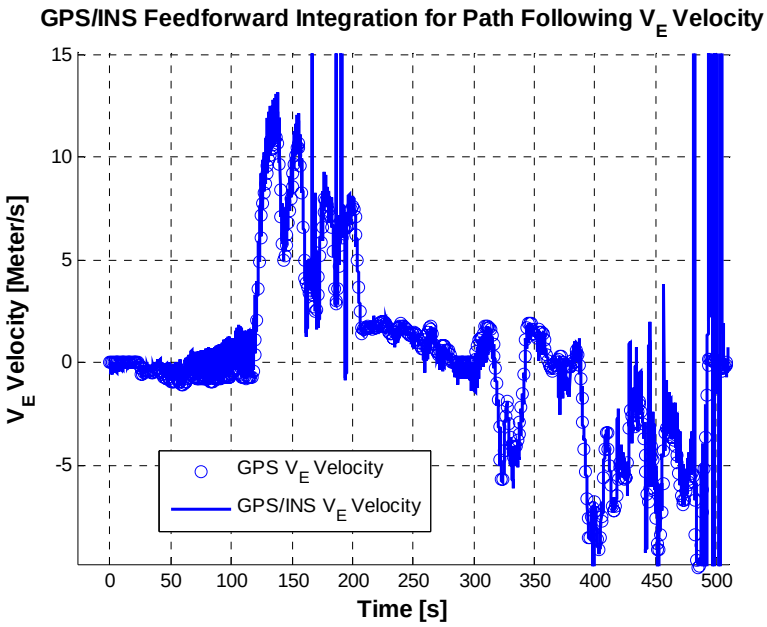

Figure 4.16 East Velocity Solution of Feed Forward GPS/INS Integration for Path Following

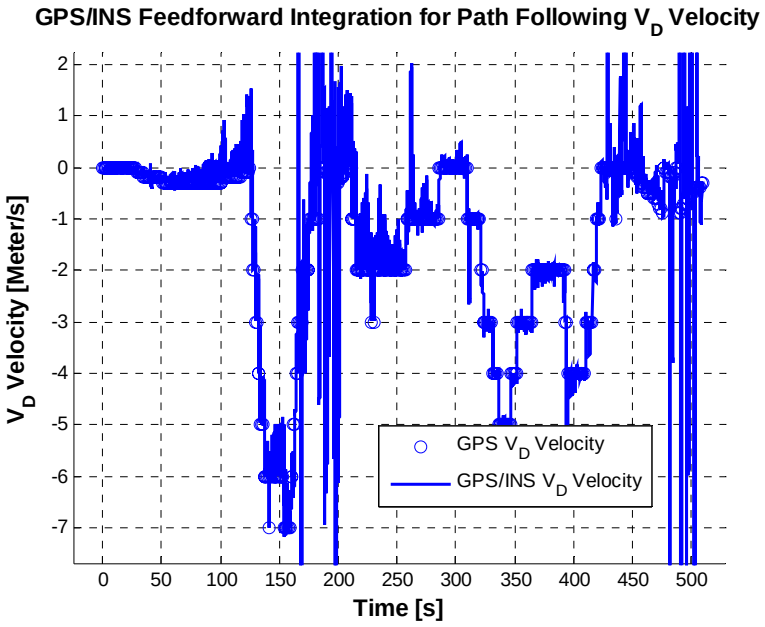

Figure 4.17 Down Velocity Solution of Feed Forward GPS/INS Integration for Path Following

The solutions for the East and down velocities are similar to the North velocity solution. Owing to the reasons discussed above, these results are also expected.

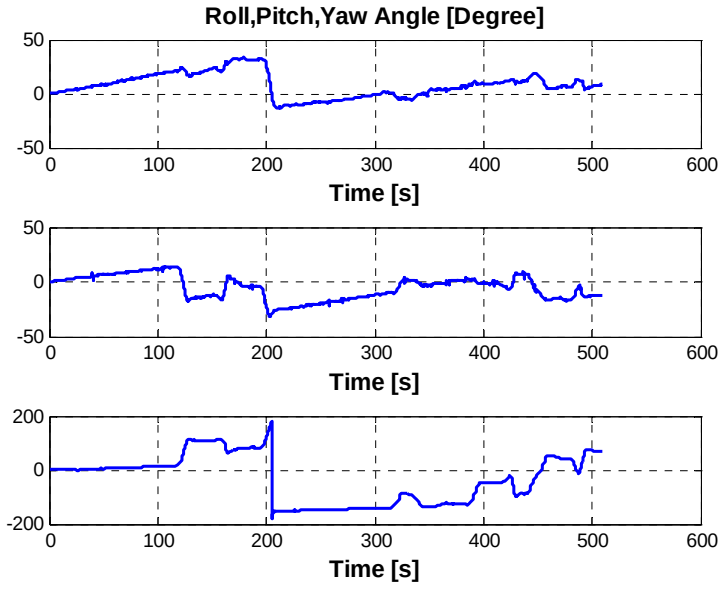

Figure 4.18 Roll, Pitch and Yaw Angle solution of feed forward GPS/INS integration for Path Following

The body frame x, y and z axis angular position with respect to the geographical frame is shown in Figure 4.18. In the loosely coupled feed forward GPS/INS integration, the outputs of the Kalman Filter are added after the mechanization equations are computed. Therefore, the Kalman Filter estimations of orientation errors do not correct the roll, pitch and yaw angles.

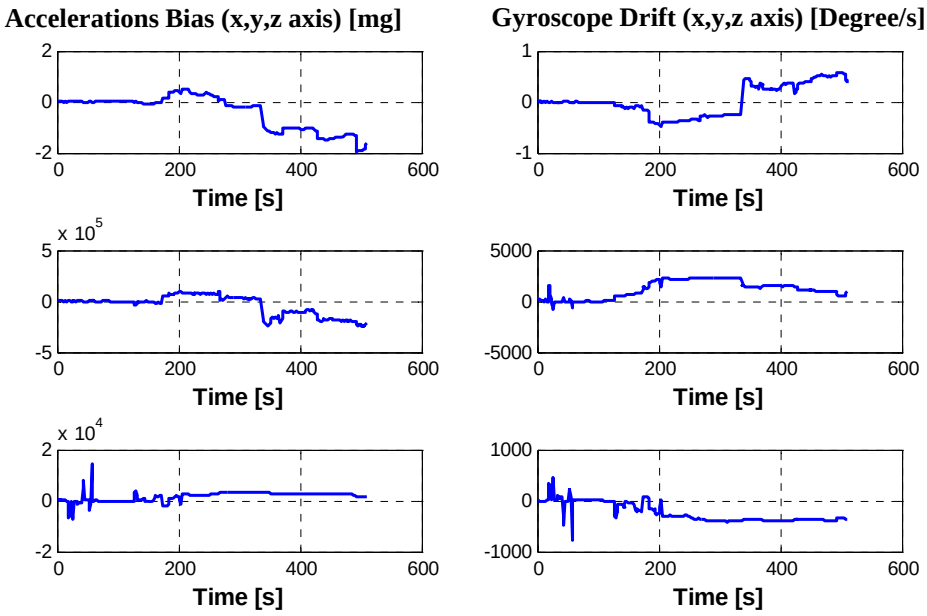

Figure 4.19 Gyro Drifts and Accelerometer Bias Estimation of Feed Forward GPS/INS Integration for Path Following

The biases of accelerometer and drifts of rate gyroscopes are similar to solutions of the roll, pitch and yaw angle.

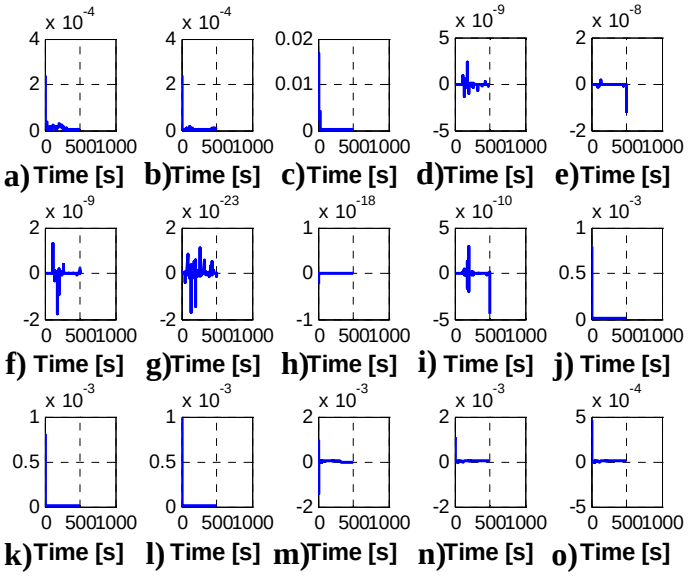

Figure 4.20 P Matrix Convergence Test of Feed Forward GPS/INS integration for Path Following

In Figure 4.20, convergence test results of P matrix are shown. Actually, values of convergence test results should be zero. Yet, as it can be seen from figure, they are not zero. Due to the same reasons at stationary point feed forward GPS/INS integration.

4.2 Feedback GPS/INS Integration Results

For feedback GPS/INS integration, first, the test results for a stationary point are given. Then, the test results for path following are presented. As mentioned in Section 2.6.4, the Kalman Filter estimations of error states are fed back to the mechanization equations simultaneously. The solutions of the mechanization equations are obtained by performing discrete integral calculations. Therefore, in the discrete integral calculations, the state variables of the previous step are updated using the Kalman Filter estimations of the error states. Thus, the outputs of the mechanization equations are prevented from containing cumulative IMU errors.

4.2.1 Results of Feedback GPS/INS Integration Obtained for a Stationary Position

At the stationary position, the velocity with respect to the geographical frame must be zero. In addition, it is required that the estimated position of the vehicle must be constant.

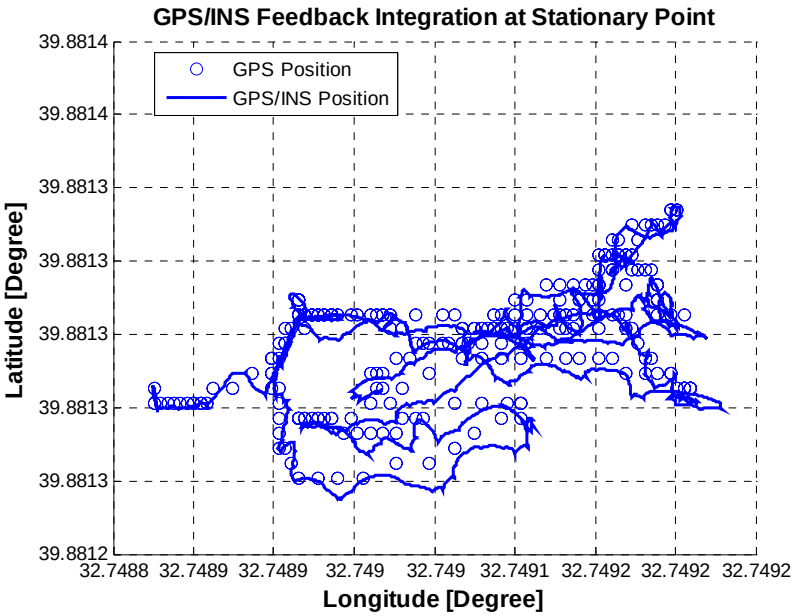

Figure 4.21 Feedback GPS/INS Integration Solutions of Latitude and Longitude at Stationary Point

In Figure 4.21, the latitude and longitude values provided by the feedback GPS/INS integration are shown at the same time. If Figure 4.21 is compared with Figure 4.1, it can be observed that the solution of feedback GPS/INS integration is much more accurate than the solution of feed forward GPS/INS integration.

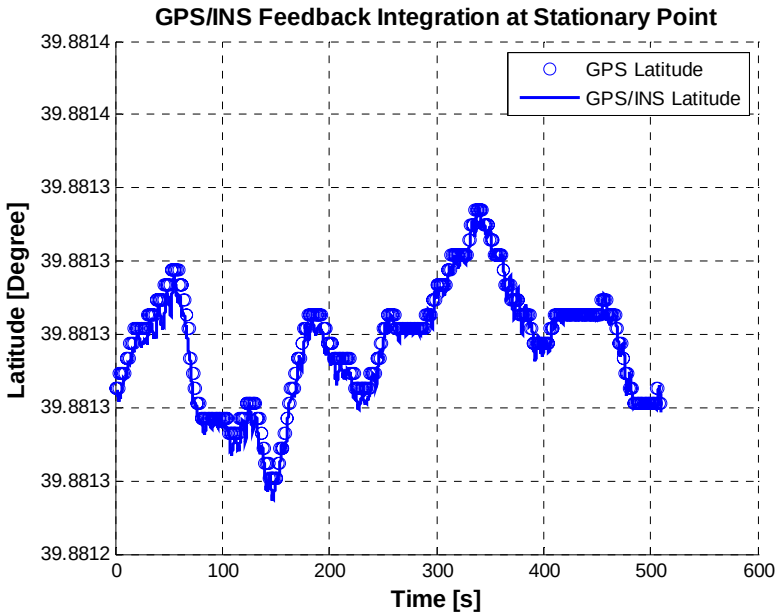

Figure 4.22 Latitude Solution of Feedback GPS/INS Integration at Stationary Point

The latitude solution of the GPS/INS integration is given in Figure 4.22. As can be seen from Figure, the latitude solution of feedback GPS/INS integration is bounded unlike feed forward GPS/INS integration. In feed forward GPS/INS integration, error of the latitude is always growing (Figure 4.2).

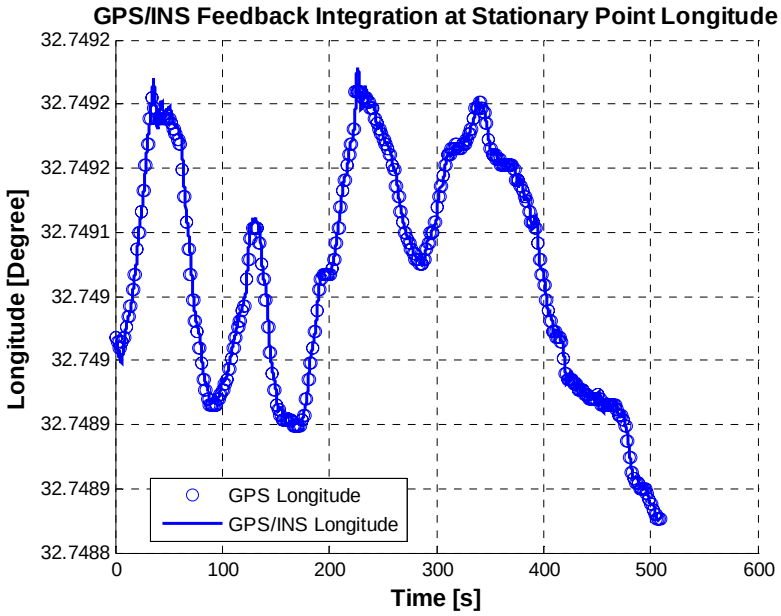

Figure 4.23 Longitude Solution of Feedback GPS/INS Integration at Stationary Point

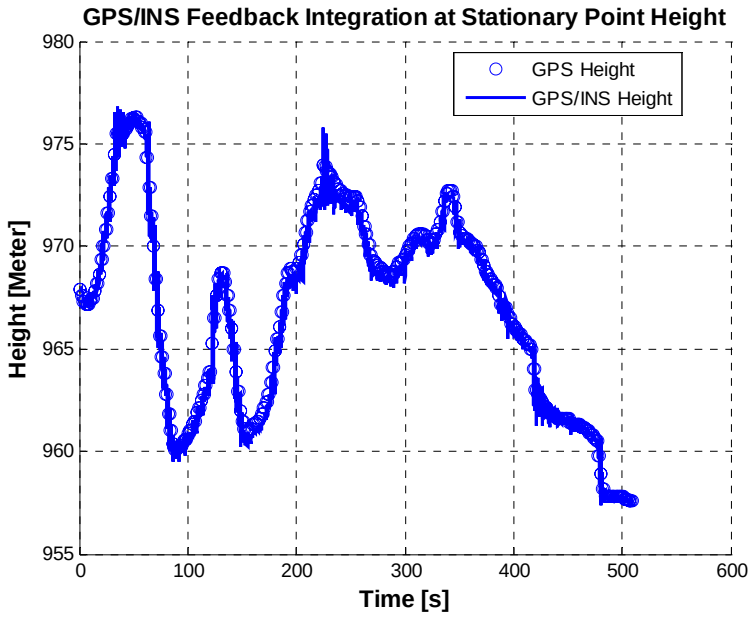

Figure 4.24 Height Solution of Feedback GPS/INS Integration at Stationary Point

The longitude and height solutions are similar to the latitude solution. Owing to the reasons discussed above, these results are also expected.

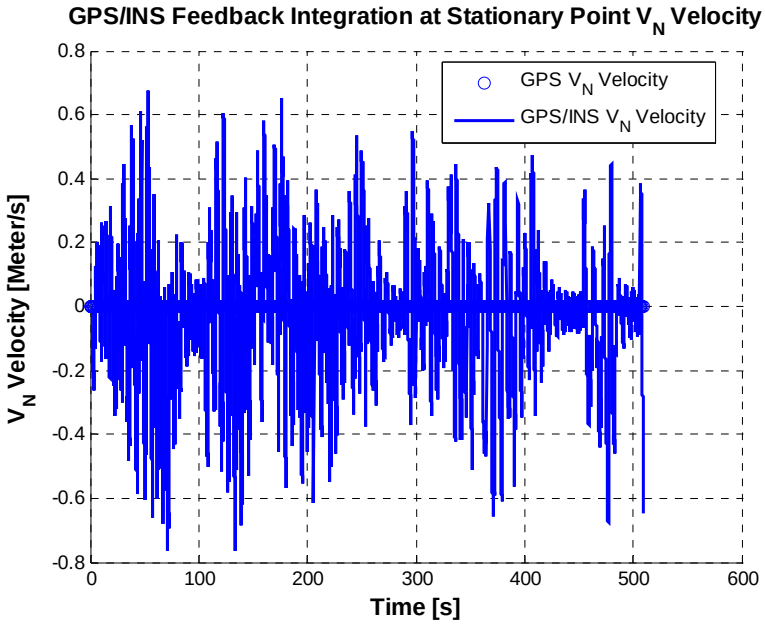

Figure 4.25 North Velocity Solution of Feedback GPS/INS Integration at Stationary Point

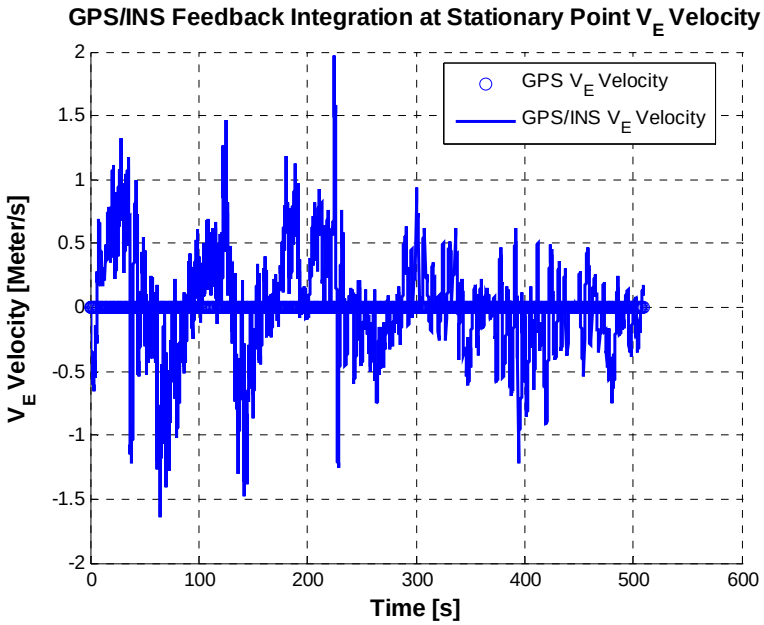

Figure 4.26 East Velocity Solution Of Feedback GPS/INS Integration at Stationary Point

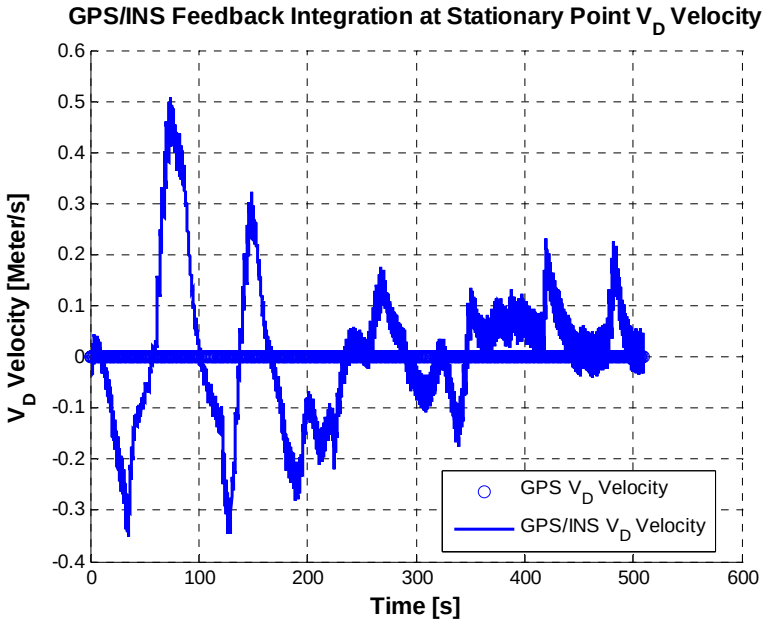

Figure 4.27 Down Velocity Solution Feedback GPS/INS Integration at Stationary Point

The North, East and Down velocities of feedback GPS/INS integration are shown in Figures 4.25, 4.26. and 4.27. It can be noted that from figures unlike feed forward case the values are bounded, as expected.

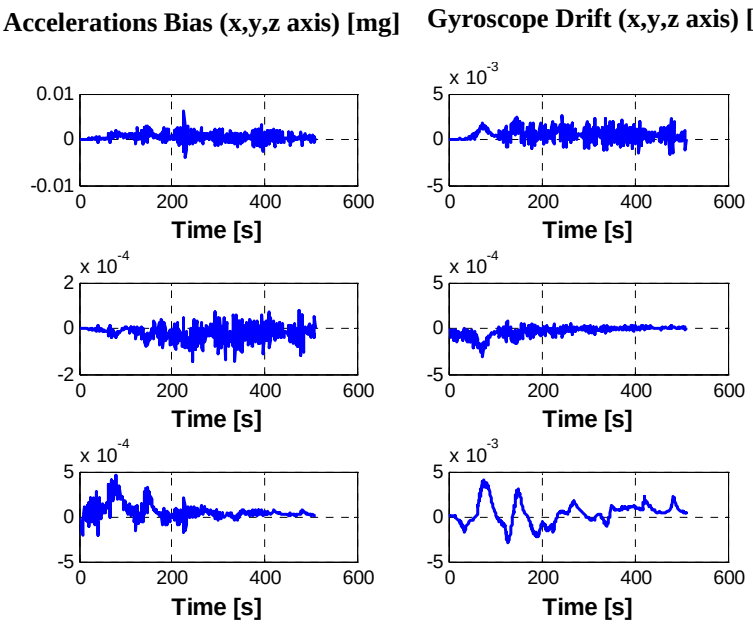

Figure 4.28 Gyro Drifts and Accelerometer Bias Estimation of Feedback GPS/INS Integration at Stationary Point

The biases and drifts of accelerometers and rate gyroscopes are shown in Figure 4.28. Actually, compared to feed forward case, they are small values and they are in an acceptable range which is defined in reference [4].

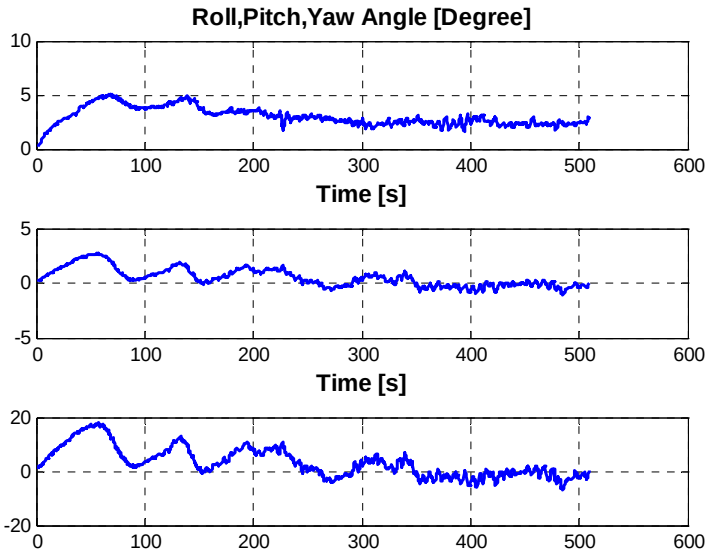

Figure 4.29 Roll, Pitch and Yaw Angles of Feedback GPS/INS Integration at Stationary Point

In Figure 4.29, the roll, pitch and yaw angles error are smaller than feed forward case. Actually, they are close to zero value compared to feed forward case.

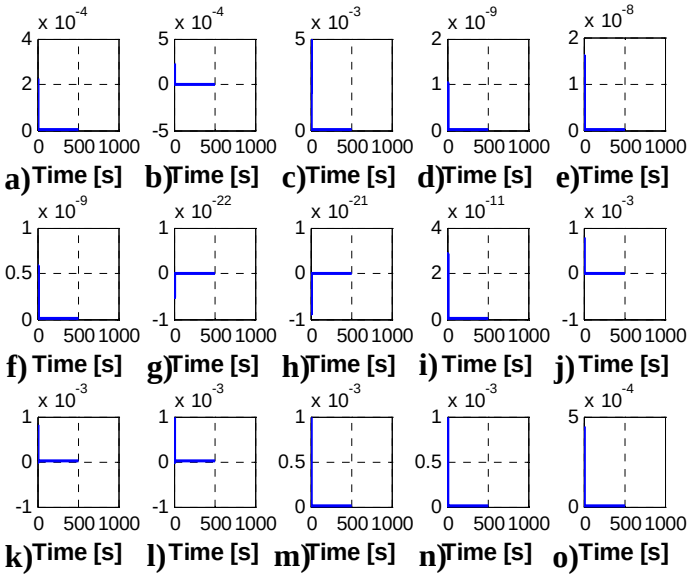

Figure 4.30 P Matrix Convergence Test of Feedback GPS/INS Integration at Stationary Point

In Figure 4.30, convergence test results of P matrix are shown. In feed forward case they are not exactly zero, but in feedback case they converge to zero value.

4.2.2 Results of Feedback GPS/INS Integration Obtained While Following a Path

The Google Earth picture of the path which is followed is shown in Figure 4.31.

Figure 4.31 Google Earth Picture of Feedback GPS/INS Integration [25]

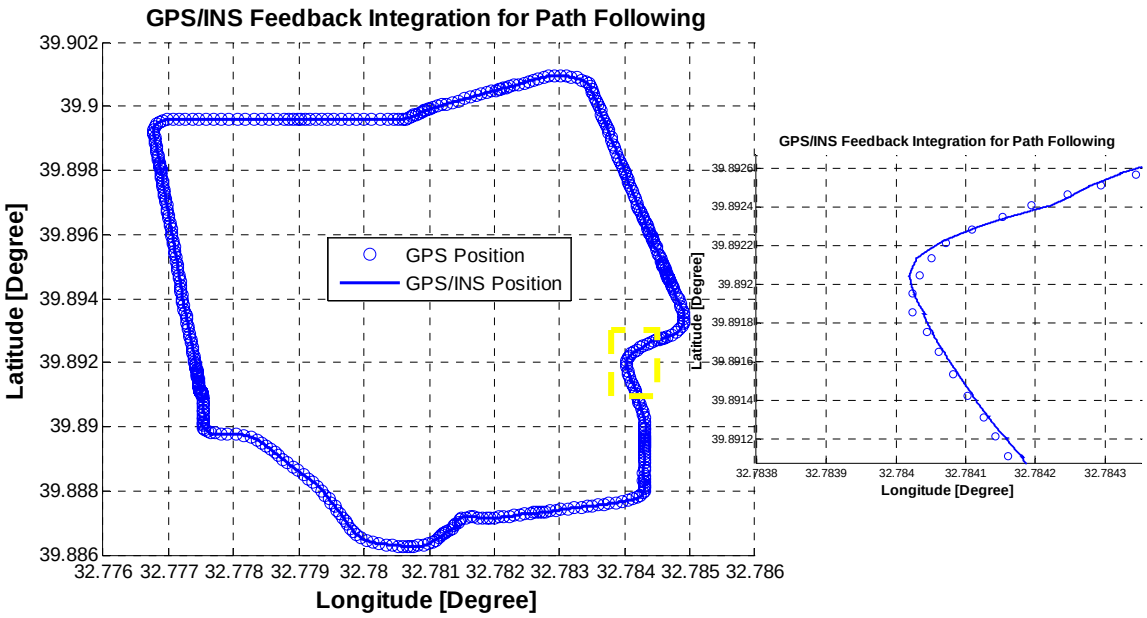

Figure 4.32 Feedback GPS/INS Integration Solutions of Latitude and Longitude for Path Following

In Figure 4.32, the latitude and longitude values provided by the feedback GPS/INS integration are shown at the same time. If Figure 4.32 is compared with Figure 4.11. It can be observed that the solution of feedback GPS/INS integration is more accurate than the solution of feed forward GPS/INS integration.

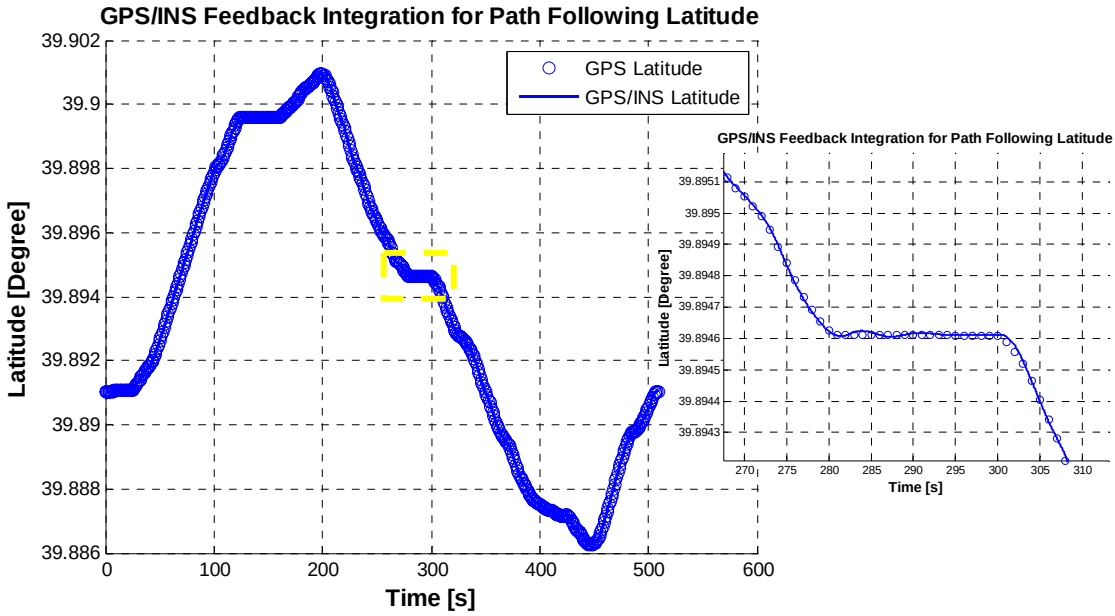

Figure 4.33 Latitude Solution of Feedback GPS/INS Integration for Path Following

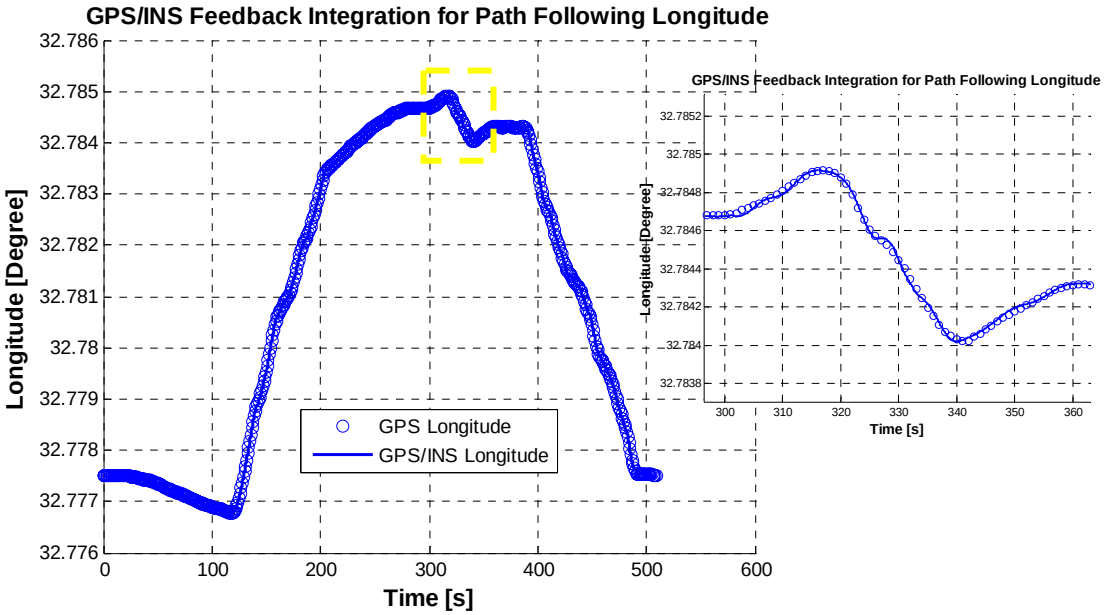

Figure 4.34 Longitude Solution of Feedback GPS/INS Integration for Path Following

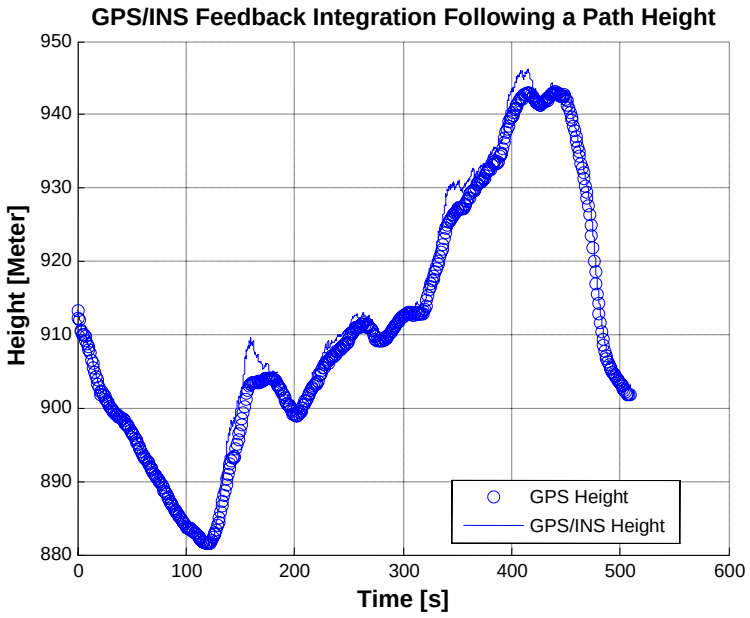

Figure 4.35 Height Solution of Feedback GPS/INS Integration for Path Following

In the Figures 4.33, 4.34 and 4.35, like the feedback GPS/INS integration at the stationary point, the errors of feedback GPS/INS integration following a path are not grown and they are smoother than the feed forward case.

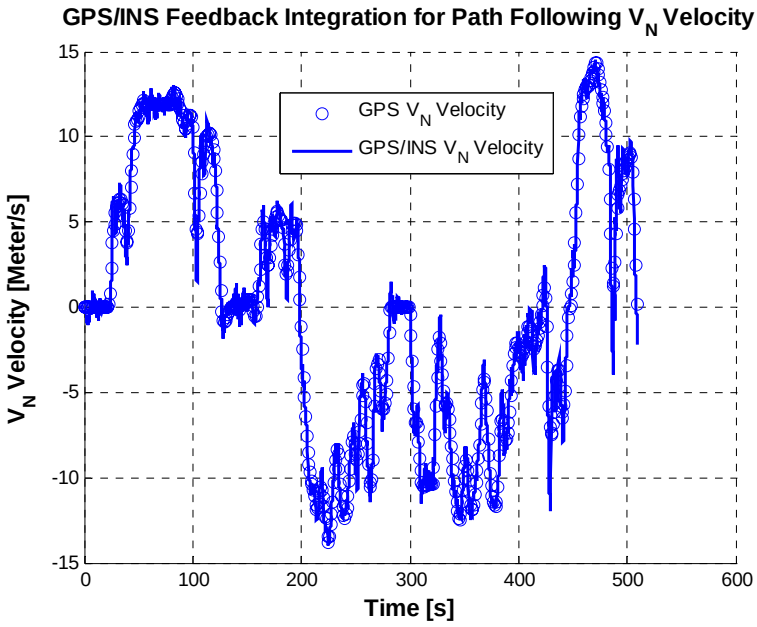

Figure 4.36 North Velocity Solution of Feedback GPS/INS Integration for Path Following

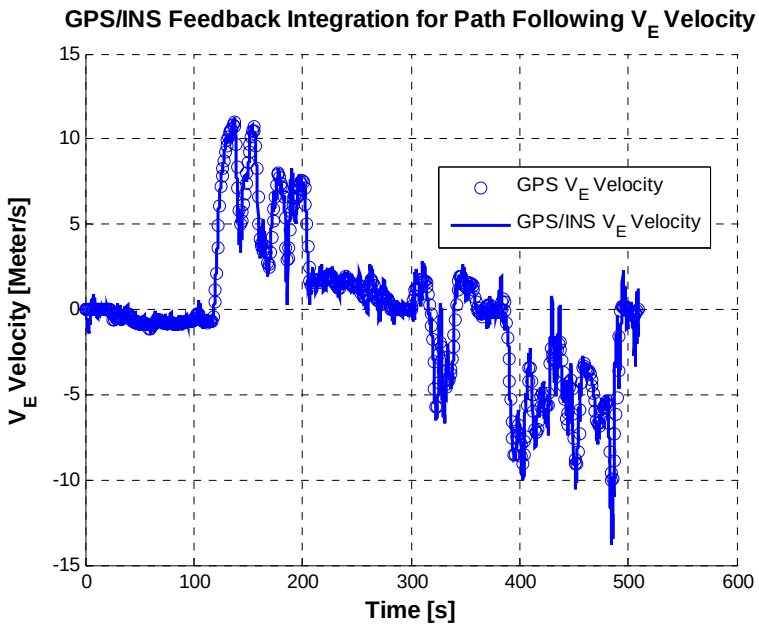

Figure 4.37 East Velocity Solution of Feedback GPS/INS Integration for Path Following

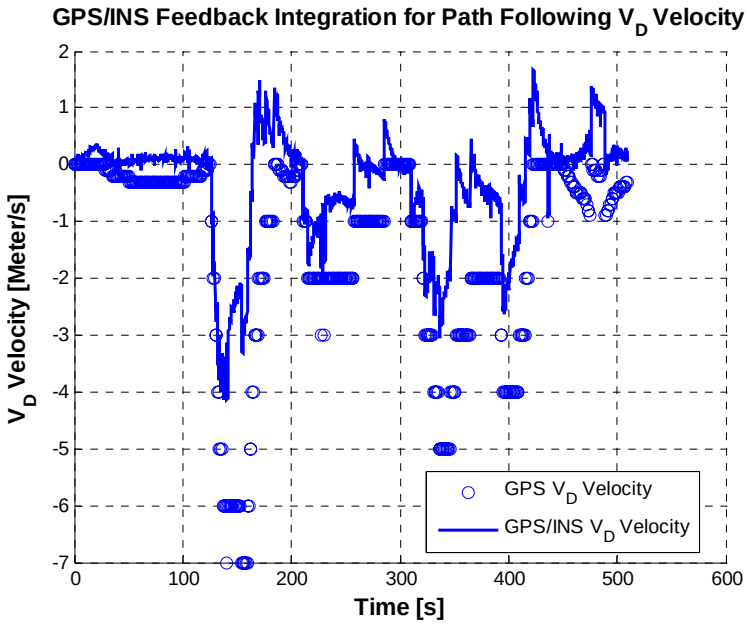

Figure 4.38 Down Velocity Solution of Feedback GPS/INS Integration for Path Following

In Figures 4.36, 4.37 and 4.38, Latitude, Longitude, height and North, East and down velocities are plotted. Like stationary feedback case, errors are small and equal to almost exact values.

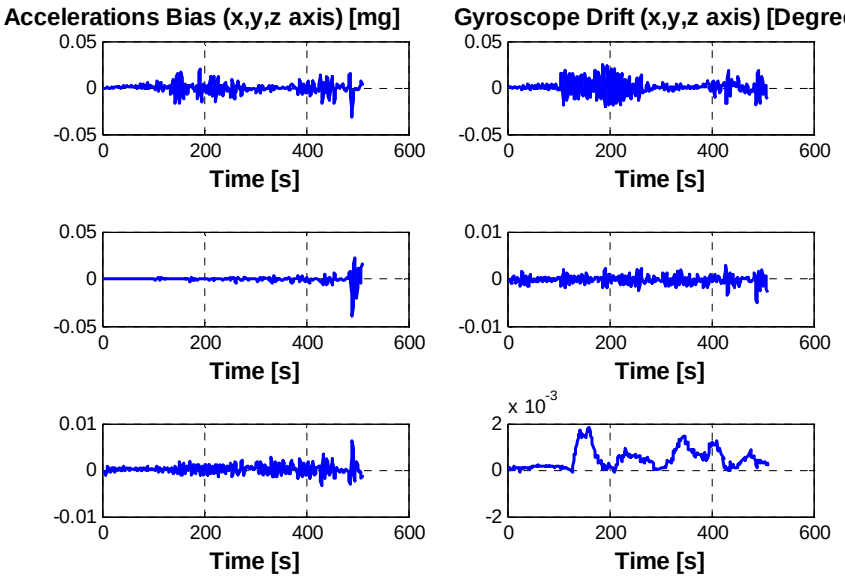

Figure 4.39 Gyro Drifts and Accelerometer Biases Estimation of Feedback GPS/INS Integration for Path Following

The biases and drifts of accelerometers and rate gyroscopes are shown in Figure 4.39. Actually, compared to feed forward case, they are small values and they are acceptable range from data in reference [4].

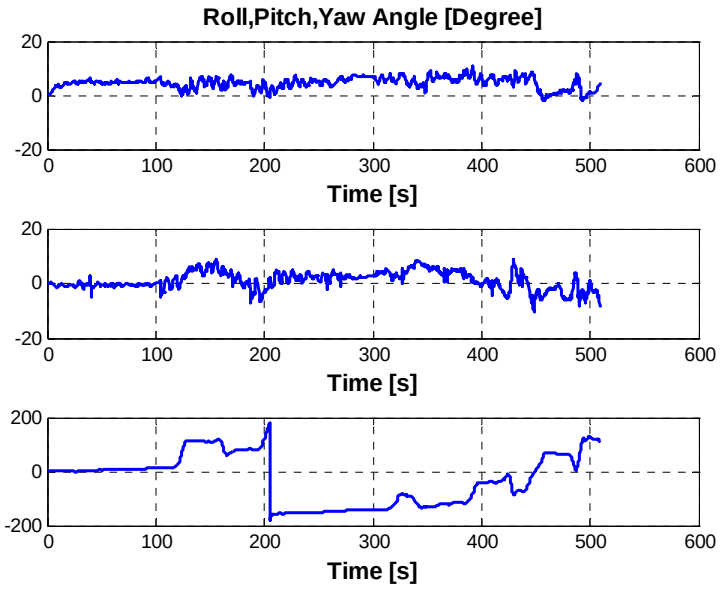

Figure 4.40 Roll, Pitch and Yaw Angles of Feedback GPS/INS Integration for Path Following

In Figure 4.40, the roll, pitch and yaw angles error are smaller than feed forward case. Actually, they are acceptable because roll and pitch angle of the vehicle does not exceed 40 degrees. But in feed forward case they exceed 40 degrees.

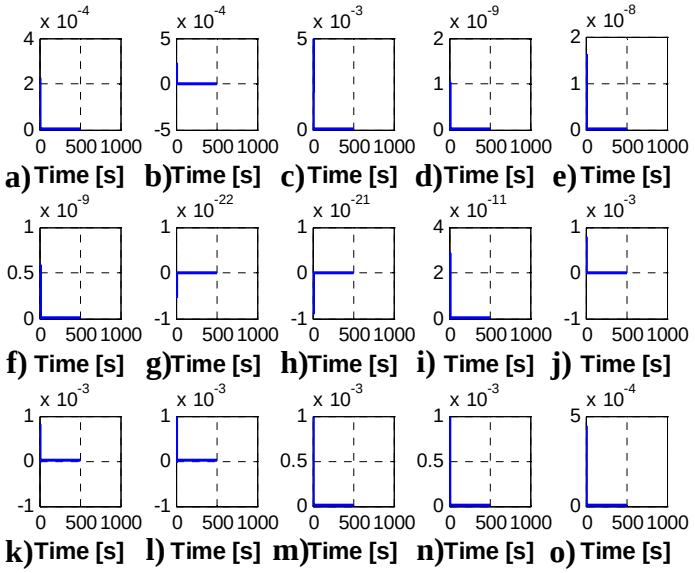

Figure 4.41 P Matrix Convergence Test of Feedback GPS/INS Integration for Path Following

In Figure 4.41, convergence test results of P matrix are shown. In feed forward case they are not exactly zero, but in feedback case they converge to zero value.

4.3 Absolute Error of Feedback, Feed Forward Cases at Stationary Point

The actual location is known at stationary point using Google Earth program. Thus, the absolute error of feed forward and feedback GPS/INS integration can be calculated.

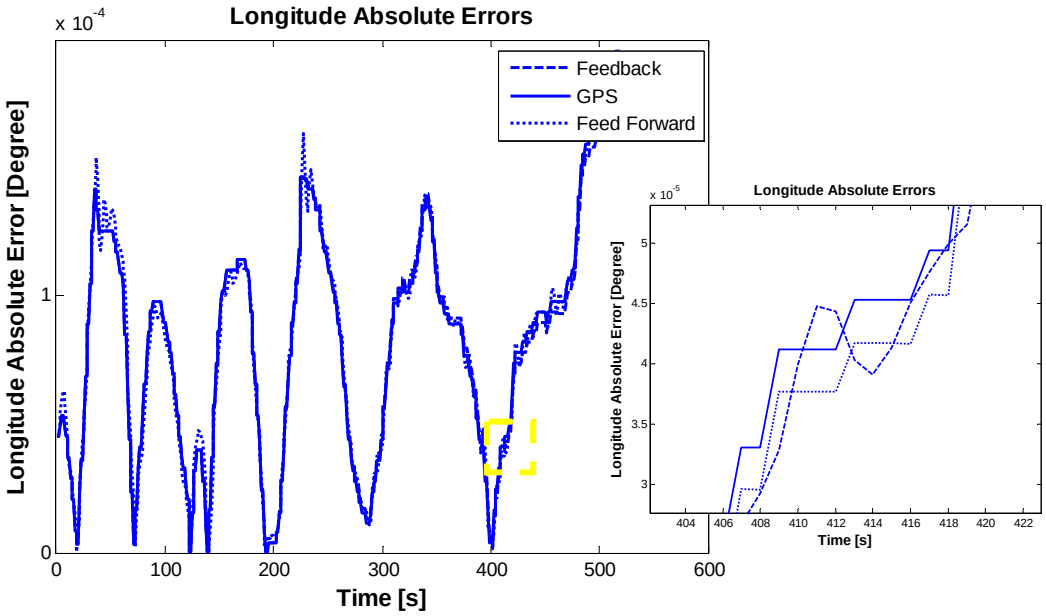

Figure 4.42 Absolute Errors of Feed Forward, Feedback GPS/INS Integration and the GPS

In Figure 4.42, the absolute errors of feed forward, feedback GPS/INS integration and GPS only solutions are shown. Only the Kalman Filter correction points are given for feed forward case. Also, RMS values of these errors are calculated. Calculated values are 1.6052e-006 for feedback GPS/INS integration, 1.6259e-006 for feed forward GPS/INS integration and 1.6475e-006 for GPS only solution.

Actually, the RMS is a measure of accuracy, so small value is desired. Thus, feedback GPS/INS integration is the most accurate integration.

4.4 The Affect of Initial Position and Initial Orientation

In this section, initial position and initial orientation effects are studied. Only feedback GPS/INS integration while following a path is given. 0.2 degree errors are given initially to the system for Latitude, Longitude and 70 meters error is given for height. In addition, about 50 degrees and 10 degrees errors are given for roll angle.

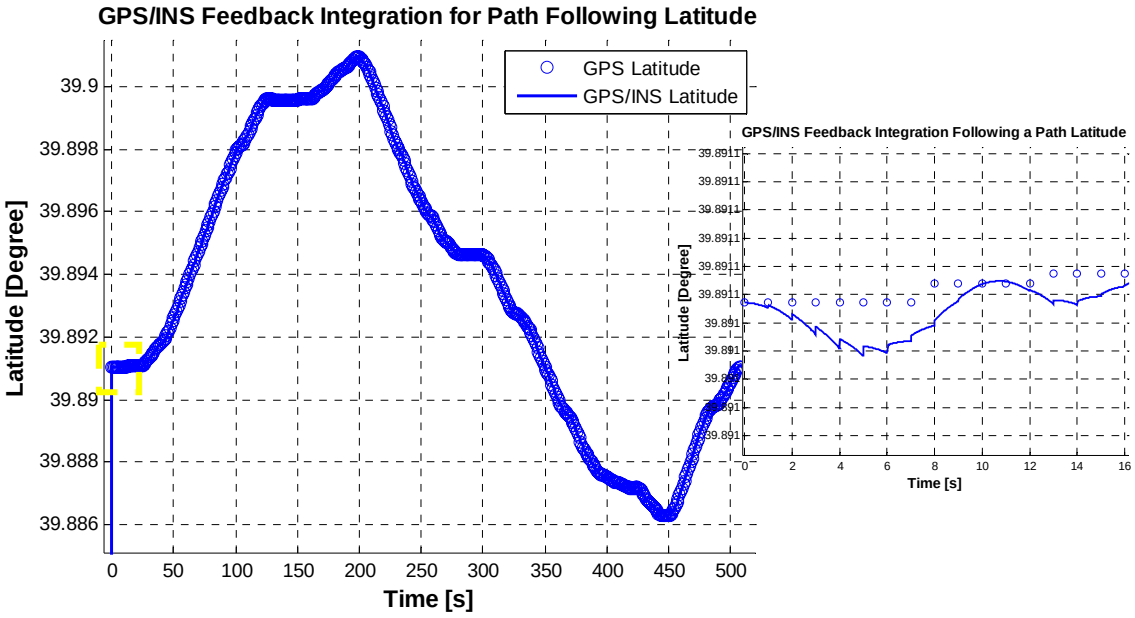

Figure 4.43 Latitude Solution of Feedback GPS/INS Integration for Initial Errors

As it can be seen from Figure 4.43 the initial error of Latitude converges almost zero value after few seconds later. Actually, GPS receiver provides the latitude data. Thus, the Kalman Filter corrects the latitude error using the Latitude data of GPS receiver.

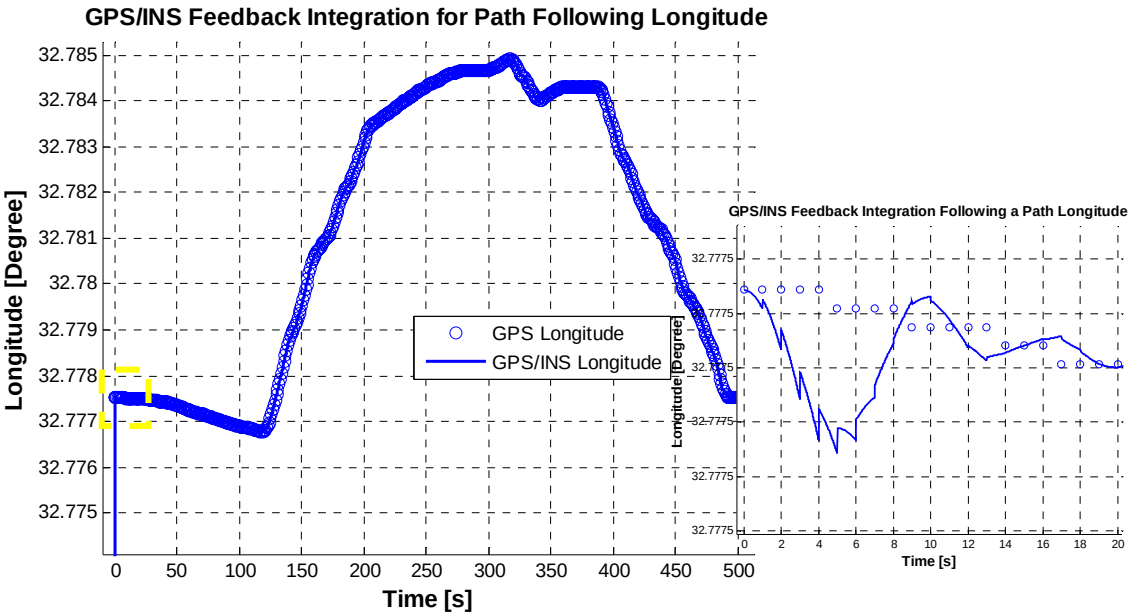

Figure 4.44 Longitude Solution of Feedback GPS/INS Integration for Initial Errors

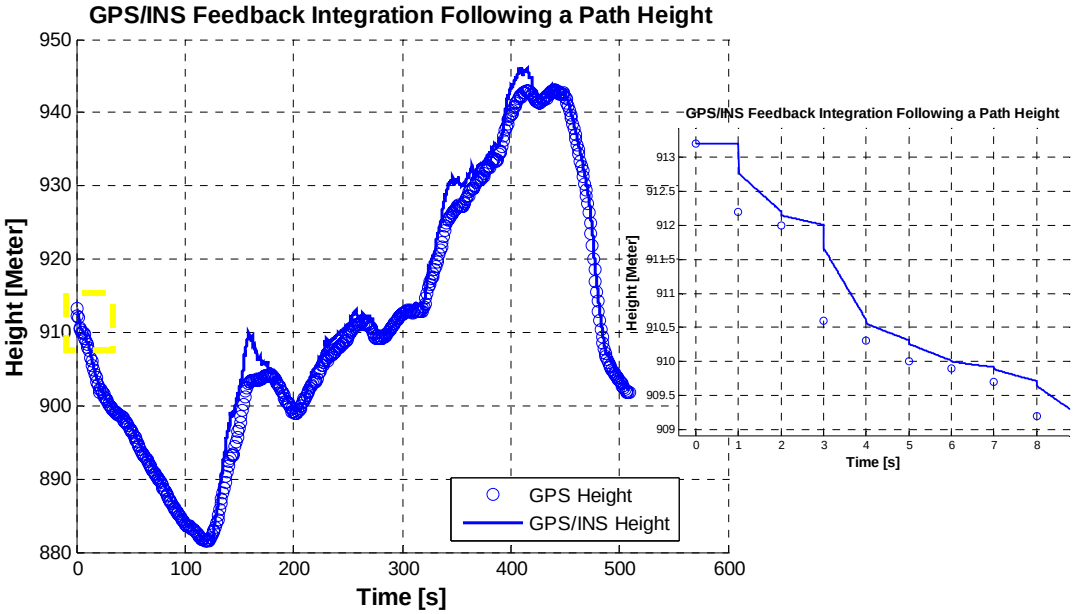

Figure 4.45 Height Solution of Feedback GPS/INS Integration for Initial Errors

The Longitude and height are given in Figures 4.44 and 4.45. The solutions of Longitude and height are similar to the latitude. Owing to the reasons discussed above, these results are also expected.

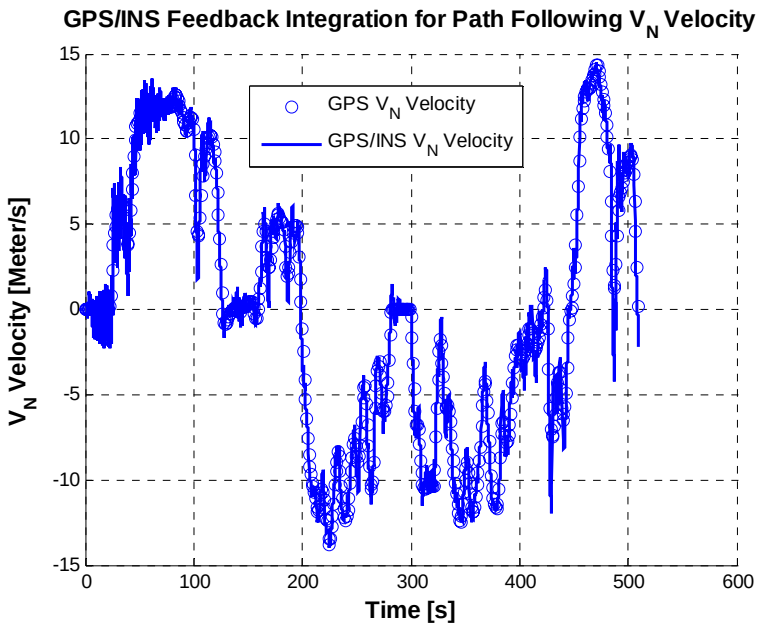

Figure 4.46 North Velocity Solution of Feedback GPS/INS Integration for Initial Errors

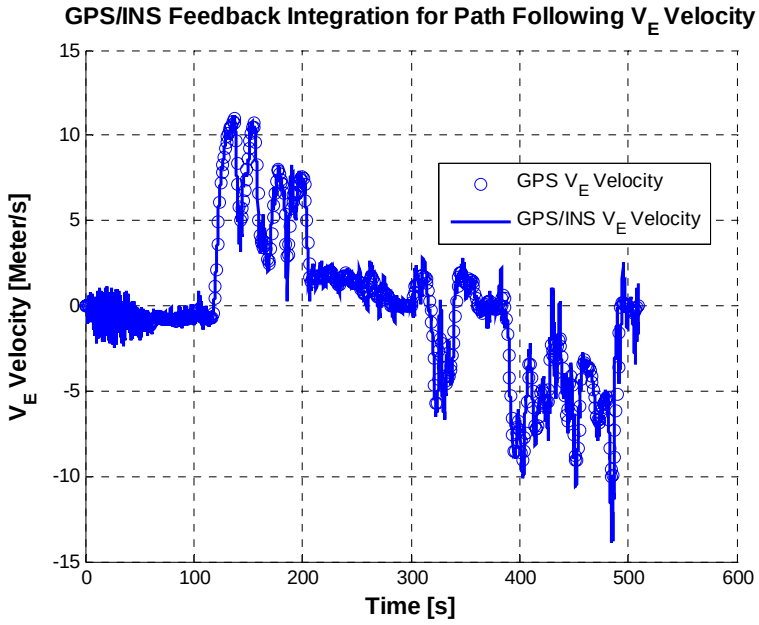

Figure 4.47 East Velocity Solution of Feedback GPS/INS Integration for Initial Errors

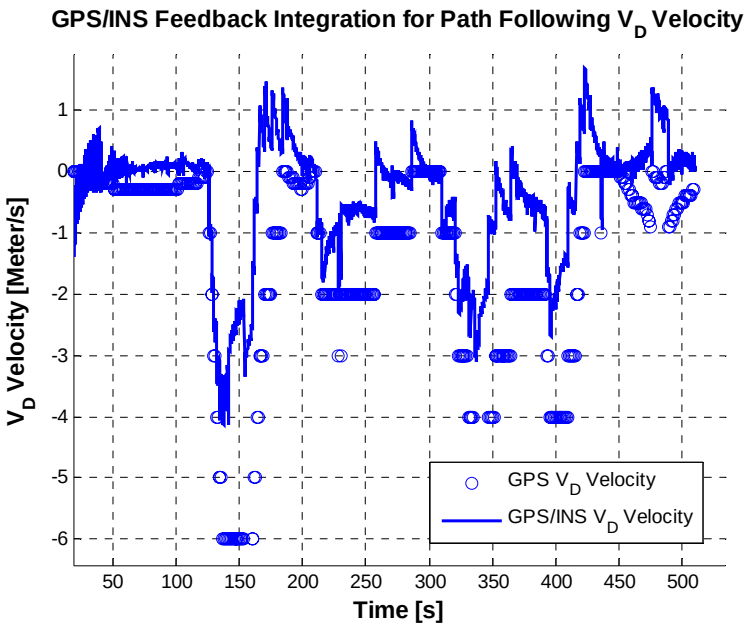

Figure 4.48 Down Velocity Solution of Feedback GPS/INS Integration for Initial Errors

Because of the initial errors of orientation, the values of North, East and down velocities are different from the previous feedback GPS/INS integration velocity values. But, they are close to the actual value.

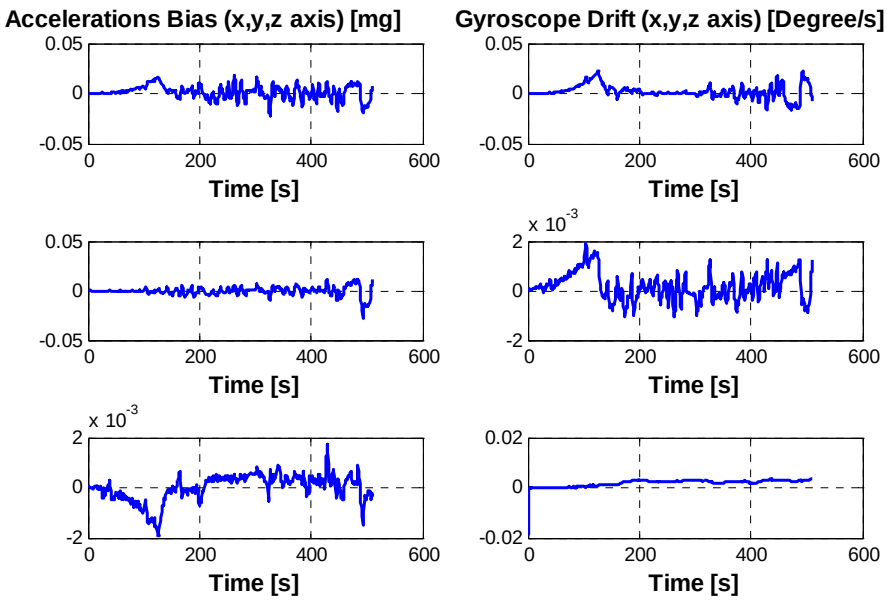

Figure 4.49 Gyro Drifts and Accelerometer Biases Solution of Feedback GPS/INS Integration for Initial Errors

The biases and drifts of accelerometers and rate gyroscopes are shown in Figure 4.49. Essentially, the values of gyros drifts and accelerometers biases are different from the values of the previous feedback GPS/INS integration due to the error of initial orientation. For instance, drift of gyro y is about 10^{-3} without initial error but it is about $2x10^{-3}$ with initial error.

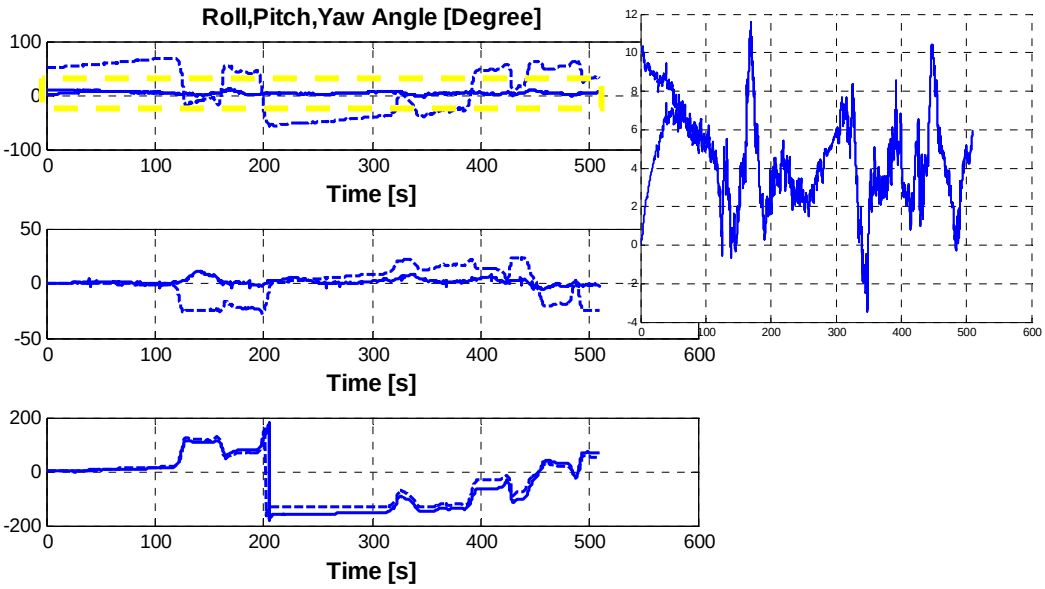

Figure 4.50 Roll, Pitch and Yaw Angles Solution of Feedback GPS/INS Integration for Initial Errors

In Figure 4.50, 10 degrees and 50 degrees errors are given initially. The solution of 50 degrees initial error is drawn using the dash lines. Also, the zoomed figure shows for 10 degrees initial roll error and 0 degree initial roll angle. Actually, the Kalman Filter corrects the 10 degrees initial error. Yet, it does not correct the 50 degrees initial error because, Kalman filter runs out of linear range; it does not estimate the error values.

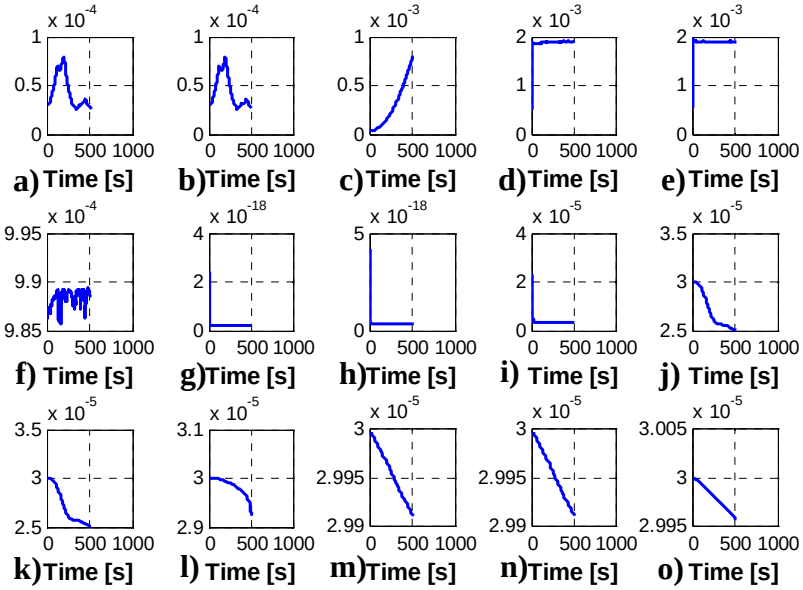

Figure 4.51 P Matrix Convergence Test of Feedback GPS/INS Integration for Initial Errors

Figure 4.51 represents the P matrix convergence test for 50 degrees initial error. As it can be seen from figure, the initial condition error of position is compensated immediately. Figure 4.51 (d), (e) and (f) graphs represent the convergence test results of the latitude, longitude and height. On the other hand, The initial condition error of orientation is not compensated. Figure 4.51 (a), (b) and (c) graphs represent the convergence test results of roll, pitch and yaw angle. Thus, Roll, Pitch and Yaw angles are wrong. Actually, GPS does not provide orientation. So, it can be concluded that orientation initial condition is vital for exact solution of Roll, Pitch and Yaw angle.

4.5 Absence of GPS Data for Fifty Seconds

In this section for feed forward and feedback GPS/INS integration, outputs are examined in case of GPS data absence for about fifty seconds between 200 and 250 seconds. Actually, the GPS receiver gives last known data when the data absence occurs.

4.5.1 Results for Feed Forward GPS/INS Integration for GPS Absence

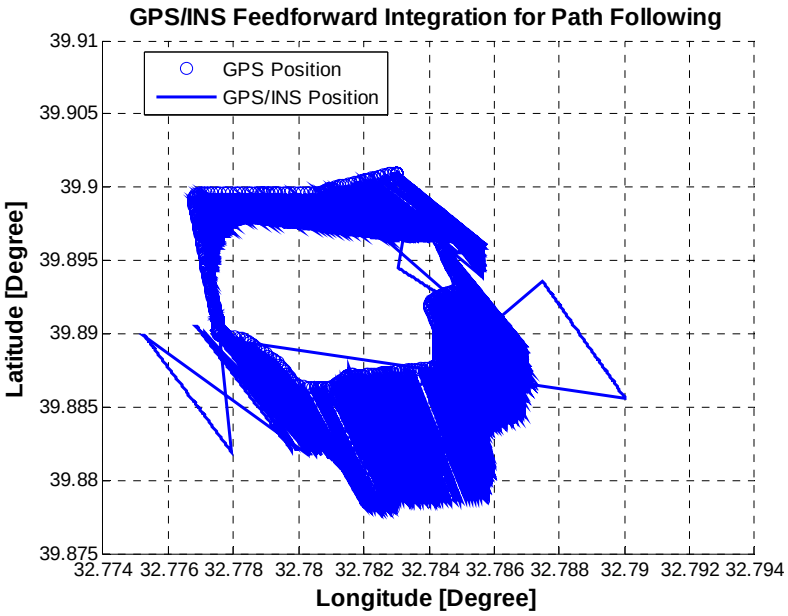

Figure 4.52 Feed Forward GPS/INS Integration Solutions of Latitude and Longitude for GPS Absence

In Figure 4.52, the latitude and longitude values provided by the feed forward GPS/INS integration are shown at the same time. When the Kalman Filter estimation of error states is used, the mechanization equations outputs become almost actual. Otherwise, the mechanization equations outputs become worse. In the figure, the upper bound is the GPS only output and the lower bound is the INS only output. In the absence of GPS the values reach the value of last GPS data. When the GPS data is available, the values of feed forward GPS/INS integration become almost actual.

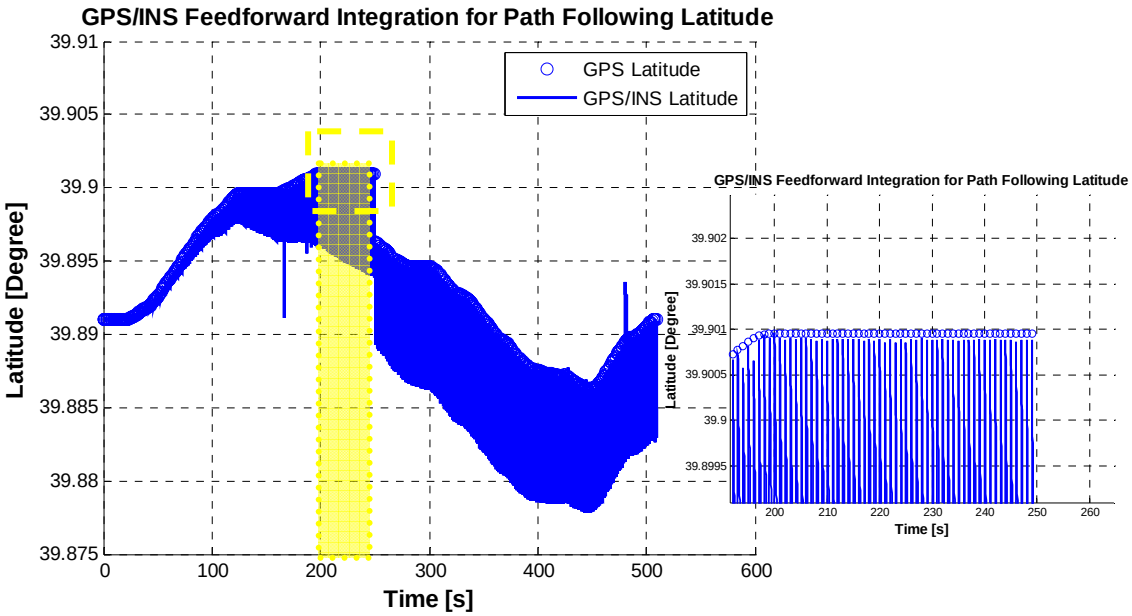

Figure 4.53 Latitude Solution of Feed Forward GPS/INS Integration for GPS Absence

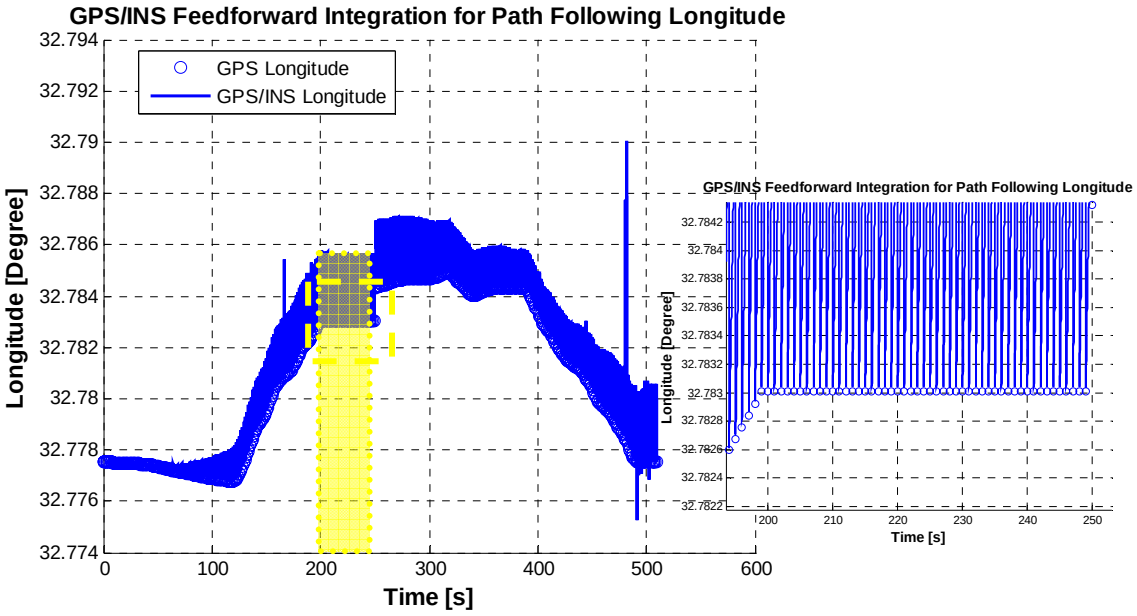

Figure 4.54 Longitude Solution of Feed Forward GPS/INS Integration for GPS Absence

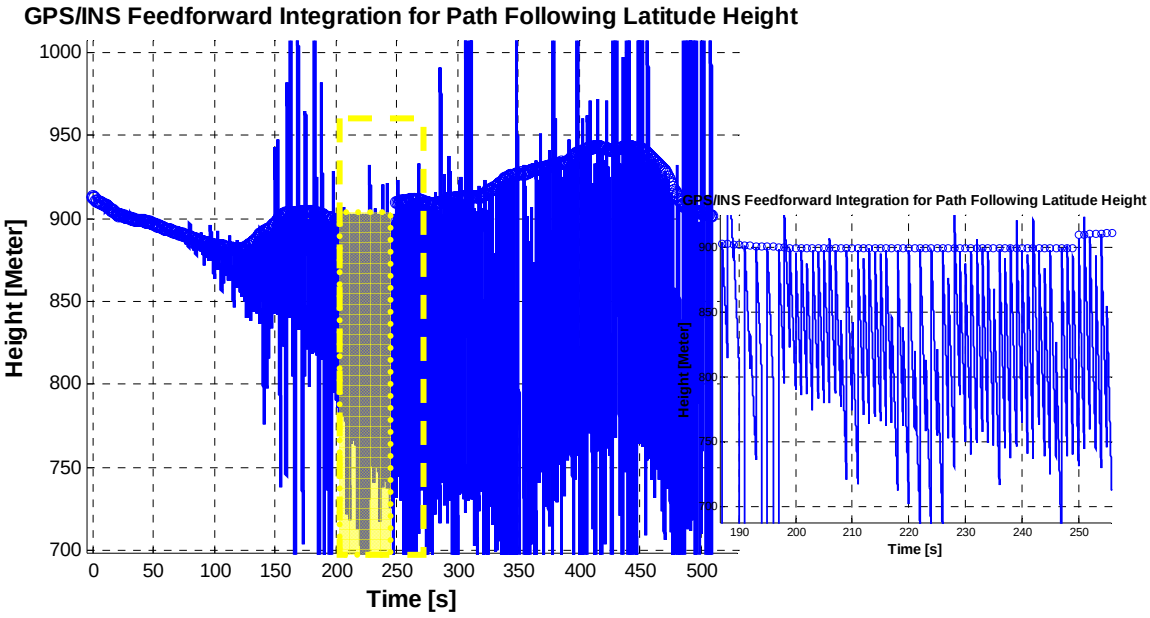

Figure 4.55 Height Solution of Feed Forward GPS/INS Integration for GPS Absence

From the Figures 4.53, 4.54 and 4.55, when the absence of GPS data, the values of Latitude, Longitude and height reach the last value of GPS data.

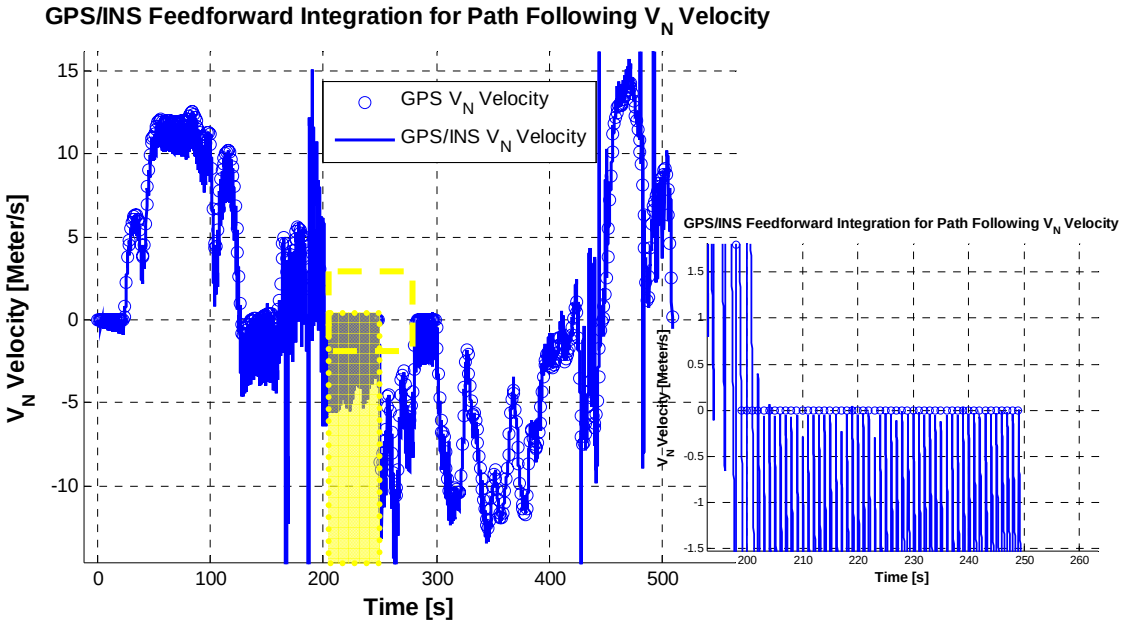

Figure 4.56 North Velocity Solution of Feed Forward GPS/INS Integration for GPS Absence

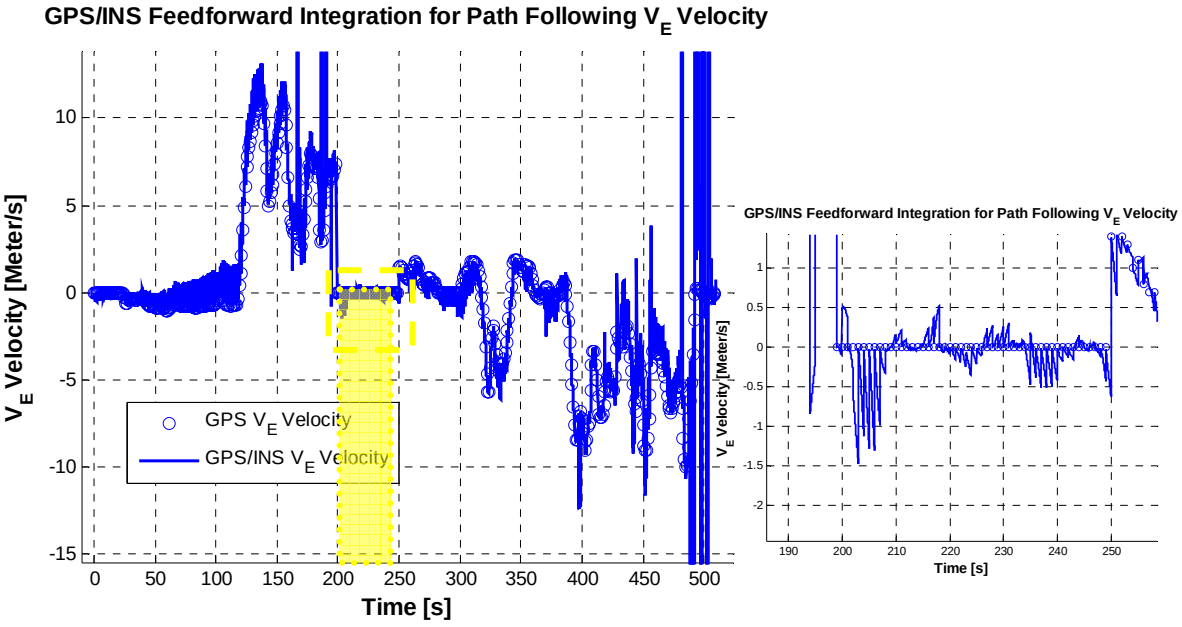

Figure 4.57 East Velocity Solution of Feed Forward GPS/INS Integration for GPS Absence

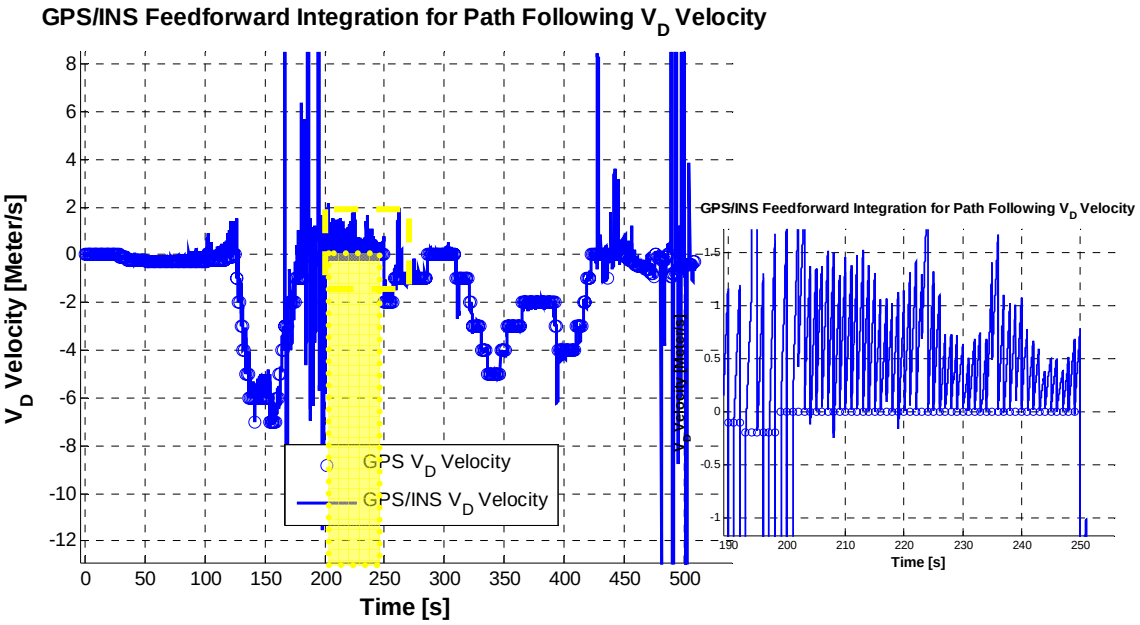

Figure 4.58 Down Velocity Solution of Feed Forward GPS/INS Integration for GPS Absence

From the Figures 4.56, 4.57 and 4.58, when the absence of GPS data, the values of North, East and down velocities reach the last value of GPS data.

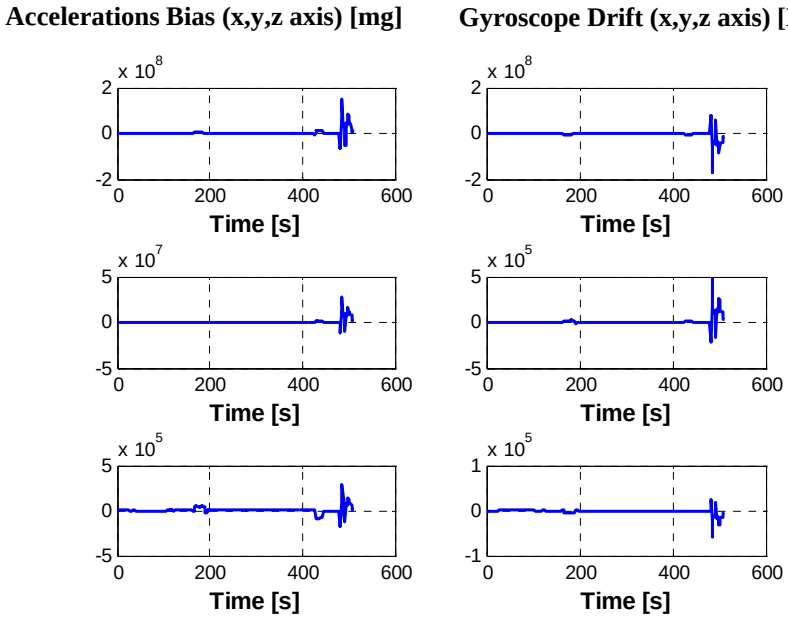

Figure 4.59 Gyro Drifts and Accelerometer Bias Estimation of Feed Forward GPS/INS Integration for GPS Absence

Like feed forward GPS/INS integration following a path case, this result is also anticipated.

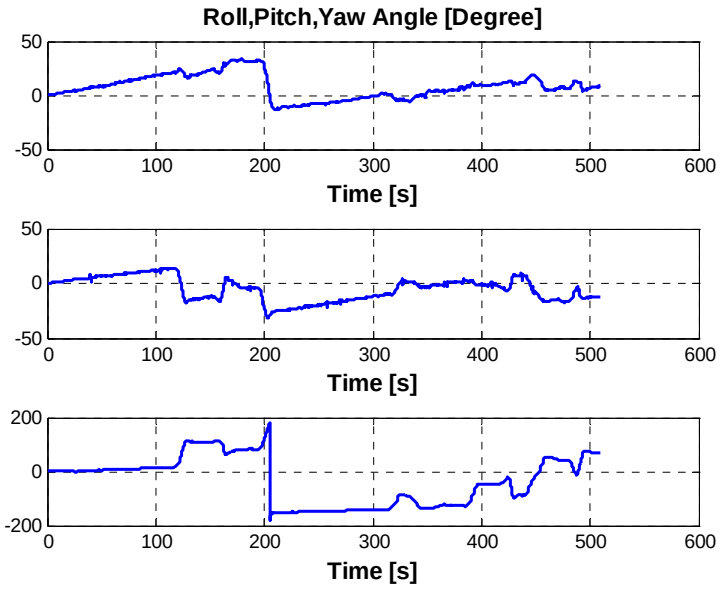

Figure 4.60 Roll, Pitch and Yaw Angles Solution of Feed Forward GPS/INS Integration for GPS Absence

The body frame x, y and z axis angular position with respect to the geographical frame is shown in Figure 4.60. In the loosely coupled feed forward GPS/INS integration, the outputs of the Kalman Filter are added after the mechanization equations are computed. Therefore, the Kalman Filter estimations of orientation errors do not correct the roll, pitch and yaw angles.

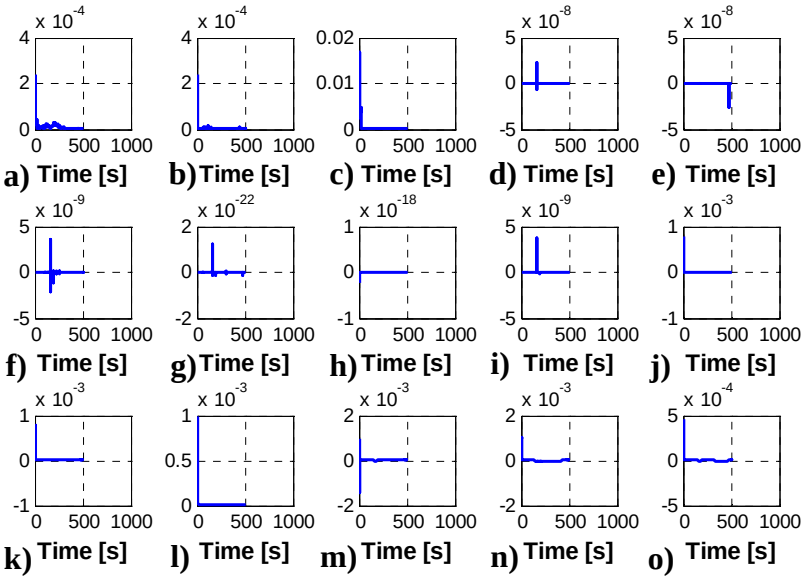

Figure 4.61 P Matrix Convergence Test of Feed Forward GPS/INS Integration for GPS Absence

In Figure 4.61, convergence test results of P matrix are shown. Actually, values of convergence test results should be zero. Yet, as it can be seen from figure, they are not zero. Due to reasons discussed in Section 2.6.5. The estimated corrections tend to grow due to the fact that the mechanization equations are kept being integrated without any interruption.

4.5.2 Results for Feedback GPS/INS Integration for GPS Absence

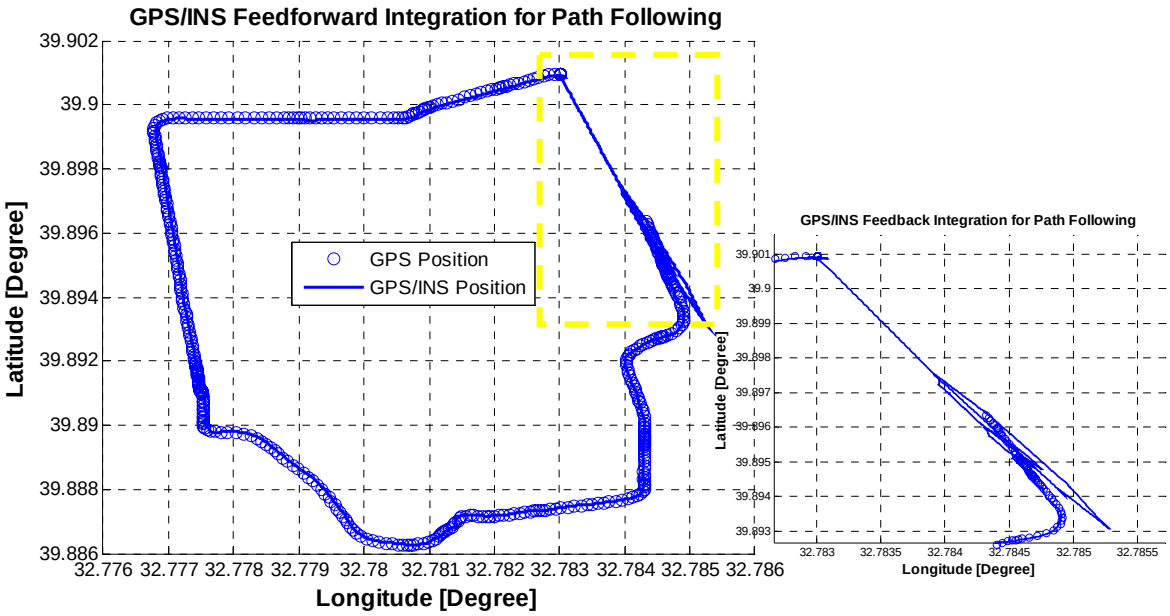

Figure 4.62 Feedback GPS/INS Integration Solutions of Latitude and Longitude for GPS Absence

In Figure 4.62, the latitude and longitude values provided by the feedback GPS/INS integration are shown in the same graph. Feed forward GPS/INS integration reaches the last GPS data, when the GPS lost for 50 seconds. But, feedback GPS/INS integration does not reach the last GPS data.

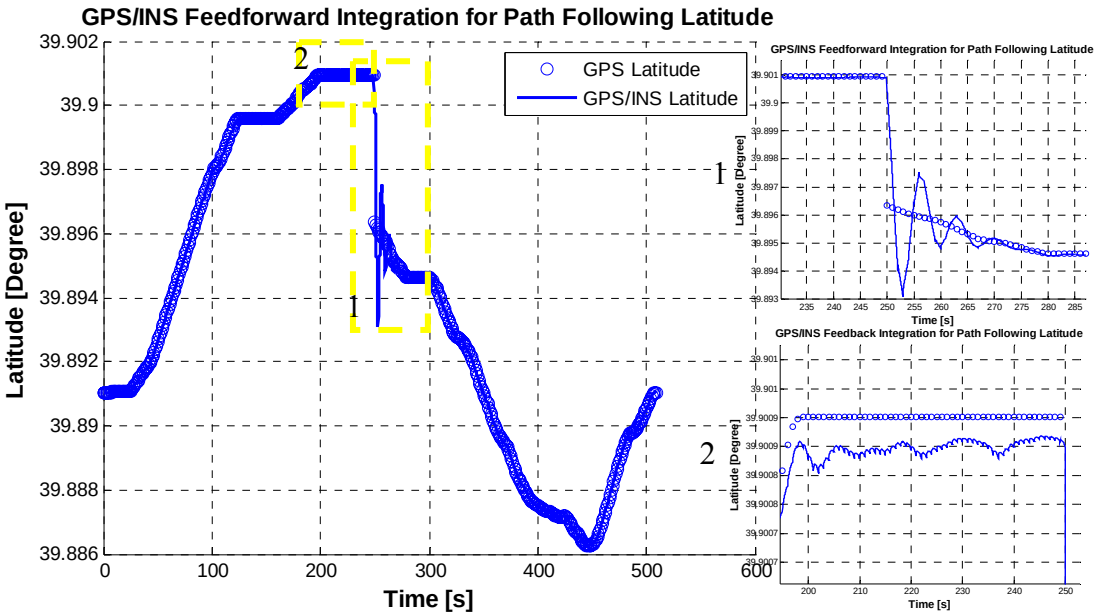

Figure 4.63 Latitude Solution of Feedback GPS/INS Integration for GPS Absence

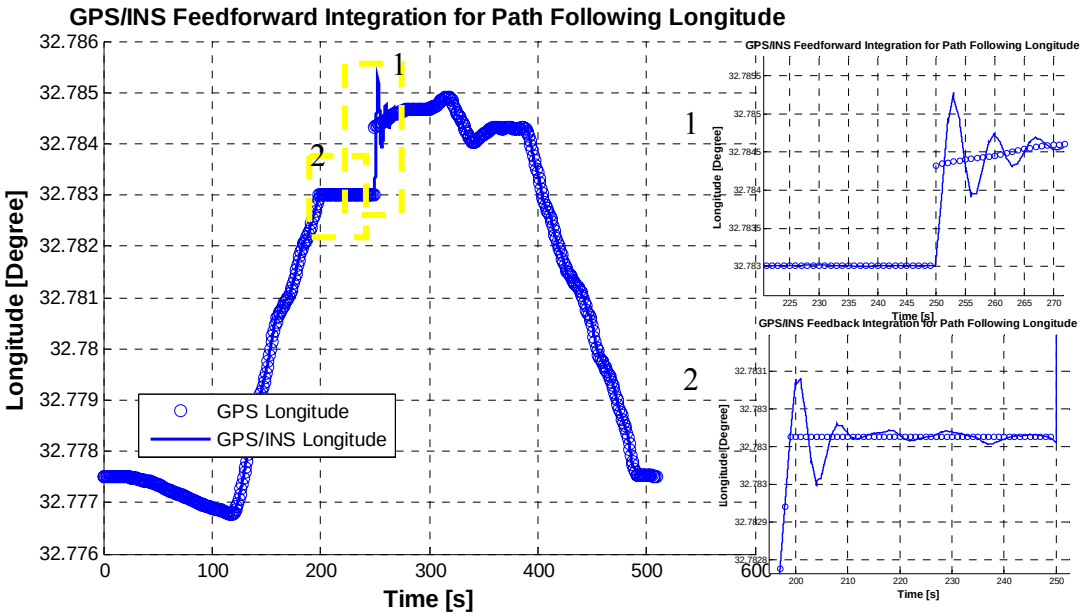

Figure 4.64 Longitude Solution of Feedback GPS/INS Integration for GPS Absence

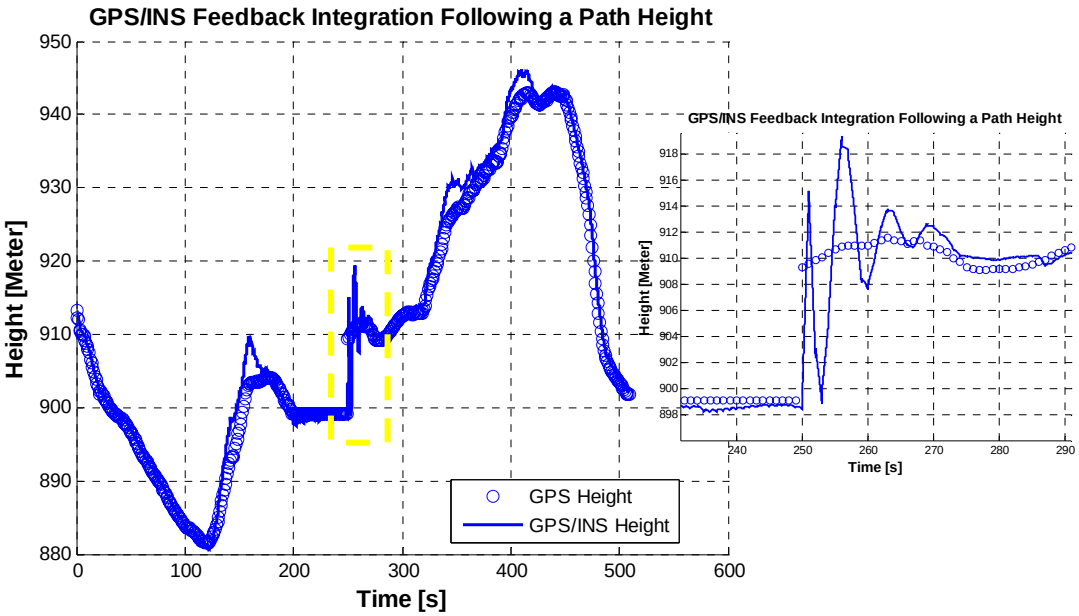

Figure 4.65 Height Solution of Feedback GPS/INS Integration for GPS Absence

From the Figures 4.63, 4.64 and 4.65, when the GPS data is lost for 50 seconds, the values of Latitude, Longitude and height are close the actual value. After the GPS data come up, the values reach the actual values.

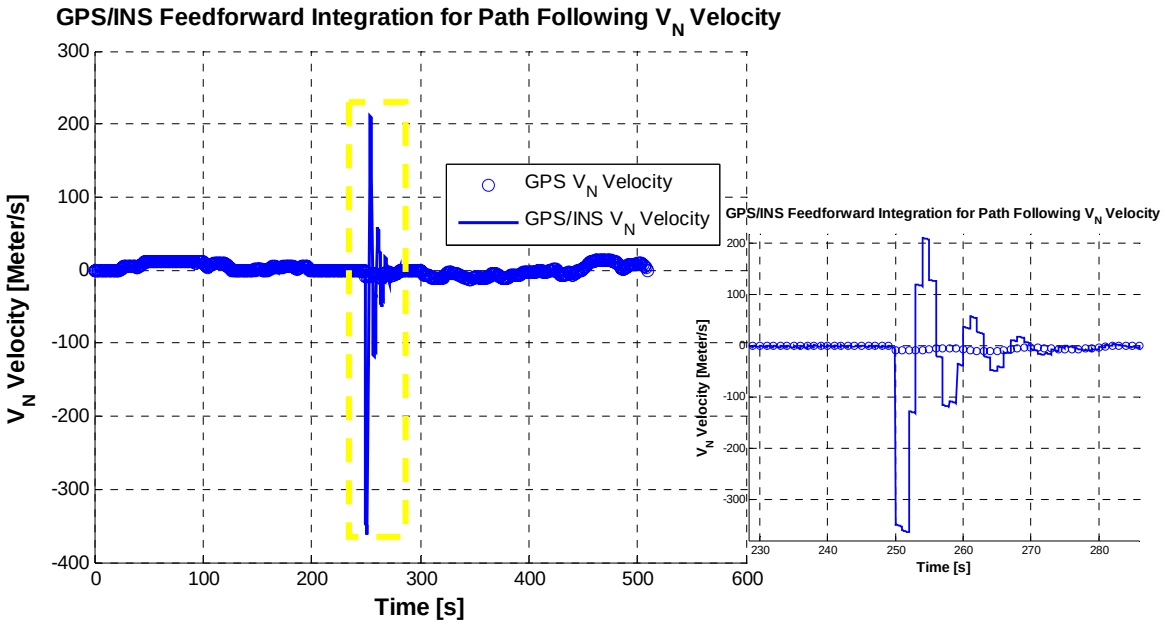

Figure 4.66 North Velocity Solution of Feedback GPS/INS Integration for GPS Absence

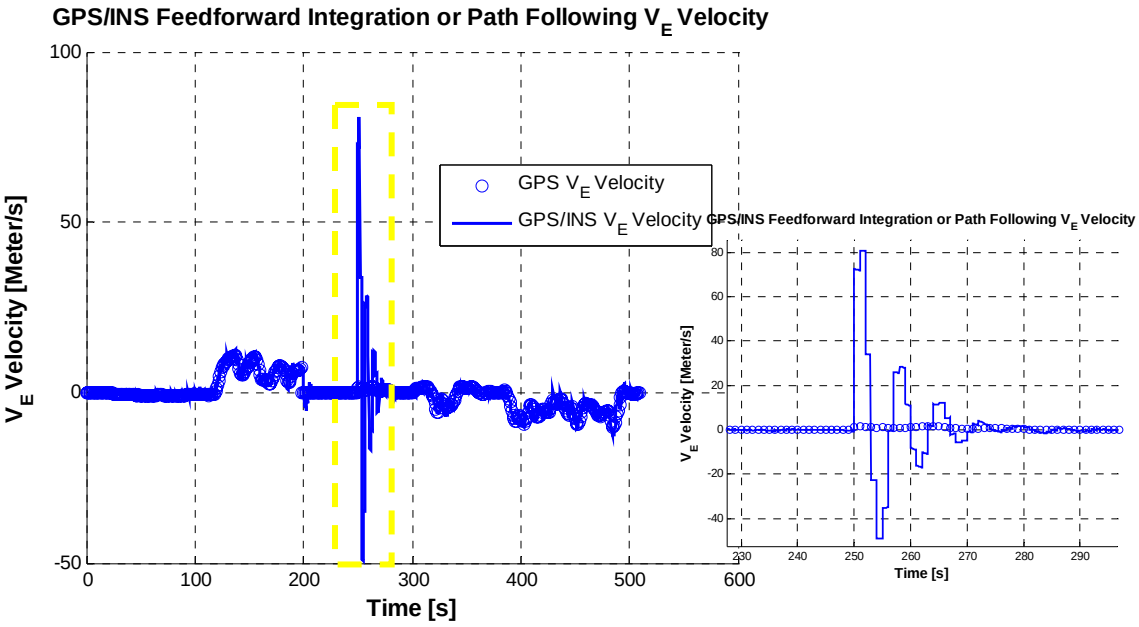

Figure 4.67 East Velocity Solution of Feedback GPS/INS Integration for GPS Absence

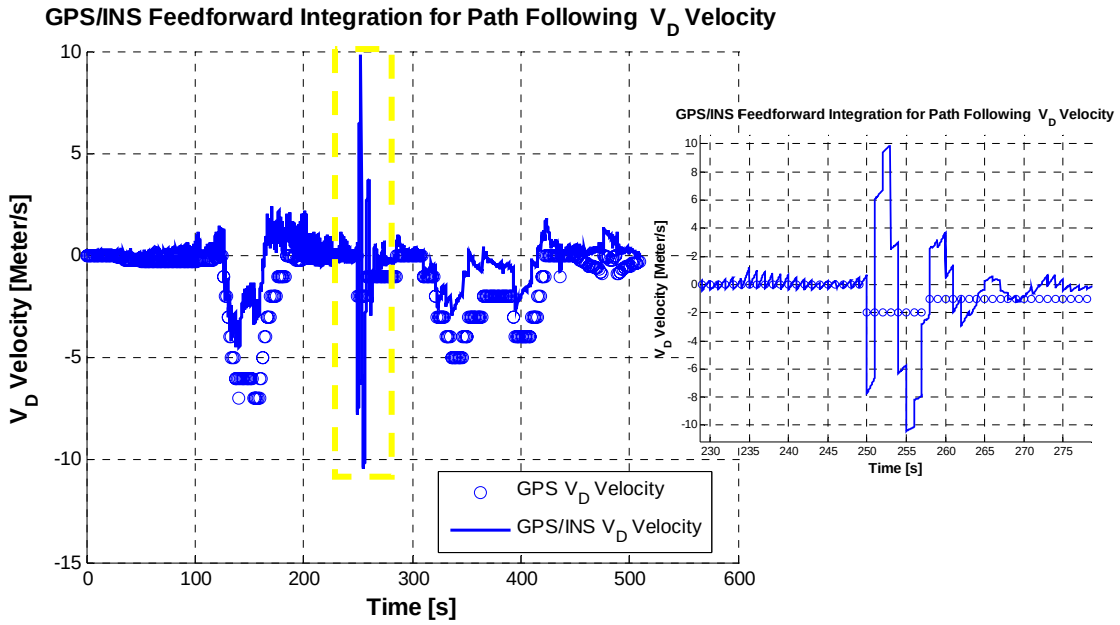

Figure 4.68 Down Solution of Feedback GPS/INS Integration for GPS Absence

From the Figures 4.66, 4.67 and 4.68, when the GPS data lost while 50 seconds, the solutions of North, East and down velocities reach the last GPS data similar to the

solution obtained for position. Owing to the reasons discussed above, these results are also expected.

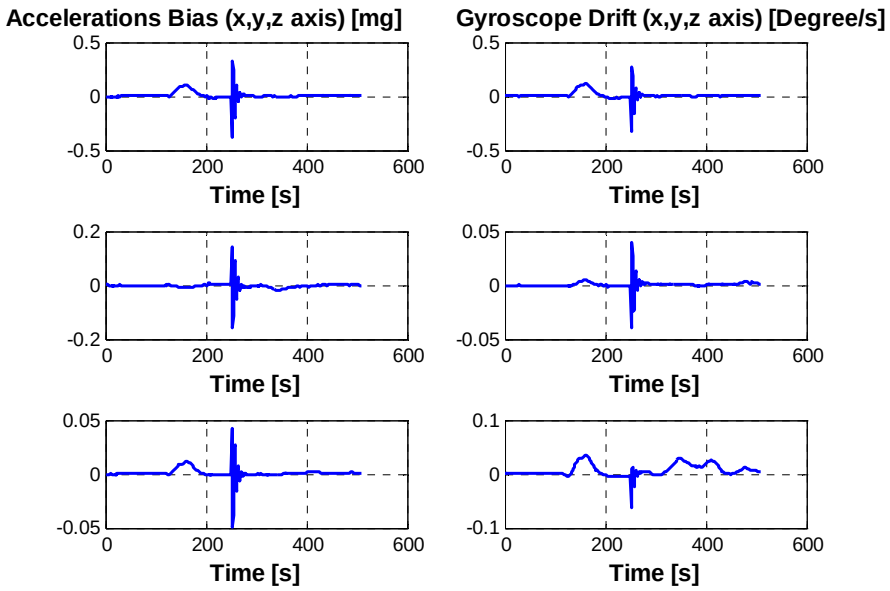

Figure 4.69 Gyro Drifts and Accelerometer Bias Estimation of Feedback GPS/INS Integration for GPS Absence

Figure 4.69 represents the gyros drifts and accelerometers biases. As it can be seen from figure, the values become unstable when the absence of GPS data. After GPS data is available, they converge to the real values.

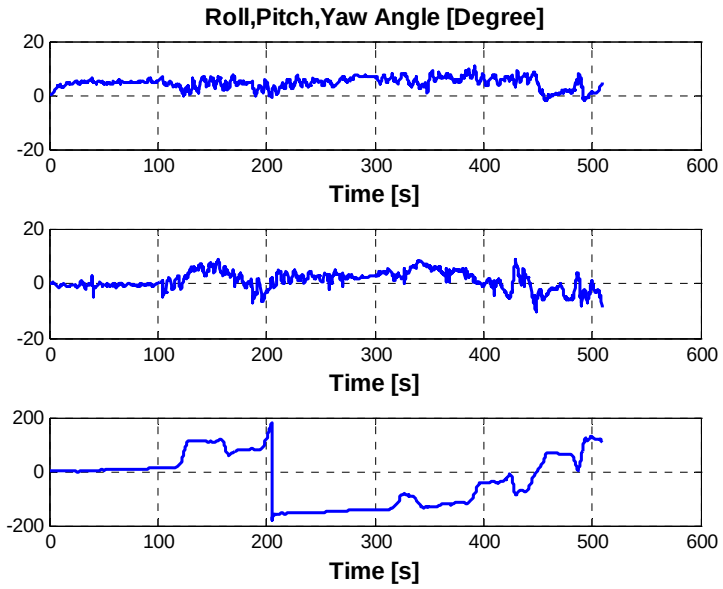

Figure 4.70 Roll, Pitch and Yaw Angles of Feedback GPS/INS Integration for GPS Absence

In Figure 4.70, the roll, pitch and yaw angles error are smaller than feed forward case. Actually, they are acceptable because roll and pitch angle of the vehicle does not exceed 40 degrees. But in feed forward case they exceed 40 degrees.

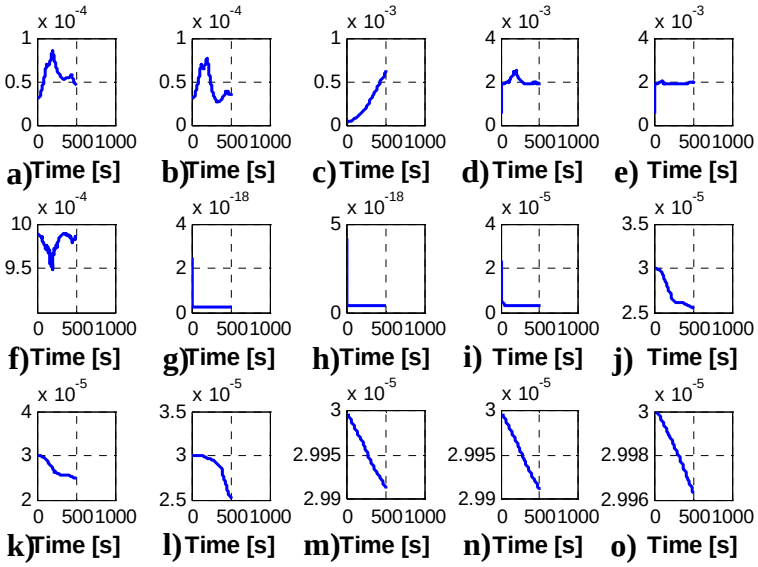

Figure 4.71 P Matrix Convergence Test of Feedback GPS/INS Integration for GPS Absence

Figure 4.71 represents the P matrix convergence test results. As it can be seen from figure, when the absence of GPS data, the position, which is the (d), (e) and (f) elements diverges. After GPS data is available, they converge to the zero value.

CHAPTER 5

CONCLUSION

5.1 Conclusions

In this study, the improvement which of a feed forward and feedback loosely coupled GPS/INS integration system is intended. For this purpose, the mechanization equations are derived for the geographical frame. After this step, an error mathematical model of INS is constructed using the perturbation of the mechanization equations and the IMU's sensor's error mathematical model added to the perturbed mechanization equation. Then, a Kalman filter is constructed based on this error model. As a summary, current navigation data is calculated using IMU data with the help of the mechanization equations, where GPS receiver supplies external measurement data to Kalman filter. Kalman filter estimates the error of INS using the error mathematical model and current navigation data is updated using Kalman filter error estimates.

For the aim of implementing this model, MATLAB Simulink Real Time Windows Target software is used. Subsequently, some real tests are undertaken using an IMU, a GPS receiver.

As expected, feedback GPS/INS system is more accurate and reliable than feed forward GPS/INS integration. Moreover, the test results confirm that with the help of GPS position and velocity aiding system, one can achieve more accurate system from GPS only system or INS only system. In addition, some tests are carried out to observe the results when the GPS receiver's data lost. In this test it is observed that, feedback GPS/INS integration has better performance than feed forward GPS/INS integration.

As a conclusion, the GPS receiver provides position and velocity data of a vehicle. Thus, the outputs of GPS/INS integration reach actual values of position and velocity data of the vehicle. On the other hand, the GPS receiver does not supply orientation data of the vehicle. Therefore, the orientation can be calculated using angular

velocity of the IMU data and the error estimation of the Kalman Filter. The orientation data of feedback GPS/INS integration is accurate compared to the feed forward GPS/INS integration due to the reason discussed in Section 2.6.5. That reason is the Kalman Filter estimations of the error states are subtracted directly from the mechanization equations' outputs. Thus, the integration process of the mechanization equations is not interrupted and the estimations corrections tend to grow in time.

5.2 Future Work

In upcoming studies, providing that the other errors like g depending bias etc. are also taken into consideration, much more accurate results can be attained. In addition, system covariance matrix Q and the measurement covariance matrix R can be arrived at by carrying out more statistical analysis and can be found off-diagonal terms. This can also enhance the integration performance. The Kalman Filter estimates the errors at 1 Hz in this study. On the other hand, mechanization equations run at 100 Hz. The Kalman Filter estimation could be extended to 100 Hz using data extrapolation. Thus, the feedback methodology could be improved with that extrapolation.

REFERENCES

[1] Jay Farrell, Matthew Barth "The Global Positioning System and Inertial Navigation", McGraw-Hill, 1998

[2] Daniel J. Biezad, "Integrated Navigation and Guidance Systems", AIAA Education Series, 1999

[3] C.F. Savant, Fr., R.C. Howard, C.B. Solloway and C.A. Savant, "Principles of Inertial Navigation", McGraw-Hill, 1961

[4] D.H. Titterton, J.L. Weston "Strapdown Inertial Navigation Technology", Process in Astronautics and Aeronautics, Volume 207, second edition, 2004

[5] S. Godha and M. E. Cannon "Development of a DGPS/MEMS IMU Integrated System for Navigation in Urban Canyon Conditions", GNSS -05, December 8-10, 2005, Hong Kong

[6] Francois Caron, Emmanuel Duflos, Denis Pomorski, Philippe Vanheeghe, "GPS/IMU data fusion using multisensor Kalman filtering: introduction of contextual aspects", Elsevier, 2004

[7] Wei Wang , Zong-yu Liu, Rong-rong Xie, "Quadratic extended Kalman filter approach for GPS/INS integration", Elsevier, 2004

[8] Jihua Huang*, Member, IEEE*, and Han-Shue Tan, "A Low-Order DGPS-Based Vehicle Positioning System Under Urban Environment", IEEE/ASME TRANSACTIONS ON MECHATRONICS, VOL. 11, NO. 5, OCTOBER 2006

[9] Alison Brown, Dien Nguyen, Yan Lu, and Chaochao Wang, NAVSYS Corporation, "Testing of Ultra-Tightly-Coupled GPS Operation using a Precision GPS/Inertial Simulator*",* Proceedings of ION GNSS 2005, Long Beach, California, September 2005.

[10] C. Goodall, Z. Syed, N. El-Sheimy, "Improving INS/GPS Navigation Accuracy through Compensation of Kalman Filter Errors", IEEE, 2006

[11] Jau Hsiung Wang, "Intelligent MEMS INS / GPS Integration For Land Vehicle Navigation", Phd thesis, University of Calgary

[12] Rashad Sharaf and Aboelmagd Noureldin "Sensor Integration for Satellite-Based Vehicular Navigation Using Neural Networks" IEEE TRANSACTIONS ON NEURAL NETWORKS, VOL. 18, NO. 2, MARCH 2007

[13] Öztürk, A., "Development, Implementation, and Testing Of A Tightly Coupled Integrated INS/GPS System", Ms. Thesis, ODTU, 2003

[14] Ekütekin,V., "Integration And Error Modelling of Global Positioning System(GPS) And Inertial Navigation System(INS)", Ms. Thesis,ODTU,2000.

[15] Britting, K. R., “Inertial Navigation Systems Analysis”, John Wiley & Sons, 1962

[16] Unsan, Y., Lecture 17: Gyroscopes and Rotation,

http://www.gidb.itu.edu.tr/staff/unsan/D/yleb/experimental/not/sensor/l17/lect_17.html, Last Access Date: 05.02.2009

[17] Jekeli, C., “Inertial Navigation Systems With Geodetic Applications”, Published by Walter de Gruyter, 2001

[18] Lundborg, P. GP&C Press Clip,

http://www.gpc.se/press/wingtip1.htm, Last Access Date: 05.02.2009

[19] GPS Central, What is GPS?

http://www.gpscentral.ca/aboutgps.htm, Last Access Date: 05.02.2009

[20] Ziff Davis Medra,

http://common.ziffdavisinternet.com/util_get_image/21/0,1425,i=212547,00.gif, Last Access Date: 05.02.2009

[21] Ofcom,

http://www.ofcom.org.uk/static/archive/ra/topics/pbr/pbrnews/images1/dgps.jpg, Last Access Date: 05.02.2009

[22] Mohinder S. Grewal, Angus P. Andrews “Kalman Filtering Theory and Practice using MATLAB”, A John Wiley & Sons, Inc. Publication, 2001

[23] Maybeck P., “Stochastic Models, Estimation and Control”, Volume1, Academic Press, 1982

[24] Kaplan, E. D., “Understanding GPS Principles and Applications”, Artech House Publishers, 1996

[24] Zonum Solutions,

http://www.zonums.com/, Last Access Date: 05.02.2009

[25] Google Earth,

http://earth.google.com/, Last Access Date: 05.02.2009

[26] Özgören, M. K. “ME 502 Advanced Dynamics Lecture Notes”, Middle East Technical University, 2005.

APPENDIX A

MATHEMATICAL TOOLS USED IN THIS THESIS

A-1 Skew Symmetric Cross-Product Matrix Corresponding to a Vector

In vector notation cross product is

$$\vec{r} = \vec{l} \times \vec{m} \tag{A.1}$$

Eq.A1 can be resolved in any reference frame such as $\Im_a$. In the frame $\Im_a$, the relevant vectors can be represented by the following column matrices.

$$\overline{r}^{(a)} = \begin{bmatrix} r_1^{(a)} \\ r_2^{(a)} \\ r_3^{(a)} \end{bmatrix} \tag{A.2}$$

$$\overline{l}^{(a)} = \begin{bmatrix} l_1^{(a)} \\ l_2^{(a)} \\ l_3^{(a)} \end{bmatrix} \tag{A.3}$$

$$\overline{m}^{(a)} = \begin{bmatrix} m_1^{(a)} \\ m_2^{(a)} \\ m_3^{(a)} \end{bmatrix} \tag{A.4}$$

Then, the matrix equivalent of Eq. (A.1) will be

$$\begin{bmatrix} r_1^{(a)} \\ r_2^{(a)} \\ r_3^{(a)} \end{bmatrix} = \begin{bmatrix} l_2^{(a)} m_3^{(a)} - l_3^{(a)} m_2^{(a)} \\ l_3^{(a)} m_1^{(a)} - l_1^{(a)} m_3^{(a)} \\ l_1^{(a)} m_2^{(a)} - l_2^{(a)} m_1^{(a)} \end{bmatrix} = \begin{bmatrix} 0 & -l_3^{(a)} & l_2^{(a)} \\ l_3^{(a)} & 0 & -l_1^{(a)} \\ -l_2^{(a)} & l_1^{(a)} & 0 \end{bmatrix} \begin{bmatrix} m_1^{(a)} \\ m_2^{(a)} \\ m_3^{(a)} \end{bmatrix} \tag{A.5}$$

This can be written compactly as

$$\overline{r}^{(a)} = \tilde{l}^{(a)}\overline{m}^{(a)} \tag{A.6}$$

In this equation,

$$\tilde{l}^{(a)} = \begin{bmatrix} 0 & -l_3^{(a)} & l_2^{(a)} \\ l_3^{(a)} & 0 & -l_1^{(a)} \\ -l_2^{(a)} & l_1^{(a)} & 0 \end{bmatrix}$$

Note that $\tilde{l}^{(a)}$ is a skew symmetric matrix and it is defined as the cross-product matrix corresponding to $\overline{l}^{(a)}$

A-2 Transformation Matrix Between Two Reference Frames

In this study, the Euler angles of the yaw-pitch-roll or 3-2-1 sequence is used in order to orient $\Im_{bf}$ with respect to $\Im_{gf}$.

This sequence can be shown as

$$\Im_{gf} \xrightarrow[\vec{u}_3^{(gf)}]{\psi} \Im_p \xrightarrow[\vec{u}_3^{(p)}]{\theta} \Im_q \xrightarrow[\vec{u}_3^{(q)}]{\phi} \Im_{bf}$$

Here, $\Im_p, \Im_q$ are intermediate reference frames and $\Im_{gf}$ is the geodetic reference frame which is defined in Chapter 2. $\Im_{bf}$ is the body frame, which is also defined in Chapter 2.

$\vec{u}_3^{gf}, \vec{u}_2^{p}, \vec{u}_1^{q}$ are the unit vectors of the relevant frames along their respective third, second and first coordinate axes.

As for the Euler angles, they are defined as follows

ψ is the yaw angle about the $\vec{u}_3^{(gf)}$ axis

θ is the yaw angle about the $\vec{u}_2^{(p)}$ axis

ϕ is yaw angle about $\vec{u}_1^{(q)}$ axis

The transformation from $\Im_{gf}$ to $\Im_{bf}$ can be performed using the elementary rotation matrices as indicated below.

$$\hat{C}^{(gf,bf)} = \hat{C}^{(gf,p)}\hat{C}^{(p,q)}\hat{C}^{(q,bf)} \tag{A.7}$$

$$\hat{C}^{(gf,bf)} = \hat{R}_3(\psi)\hat{R}_2(\theta)\hat{R}_1(\phi) \tag{A.8}$$

The elementary rotation matrices are defined as follows.

$$\hat{R}_1(\phi) = \begin{bmatrix} 1 & 0 & 0 \\ 0 & \cos\phi & -\sin\phi \\ 0 & \sin\phi & \cos\phi \end{bmatrix},\ \hat{R}_2(\theta) = \begin{bmatrix} \cos\theta & 0 & \sin\theta \\ 0 & 1 & 0 \\ -\sin\theta & 0 & \cos\theta \end{bmatrix},\ \hat{R}_3(\psi) = \begin{bmatrix} \cos\psi & -\sin\psi & 0 \\ \sin\psi & \cos\psi & 0 \\ 0 & 0 & 1 \end{bmatrix}$$

APPENDIX B

MOTION REFERRED TO DIFFERENTLY MOVING FRAMES

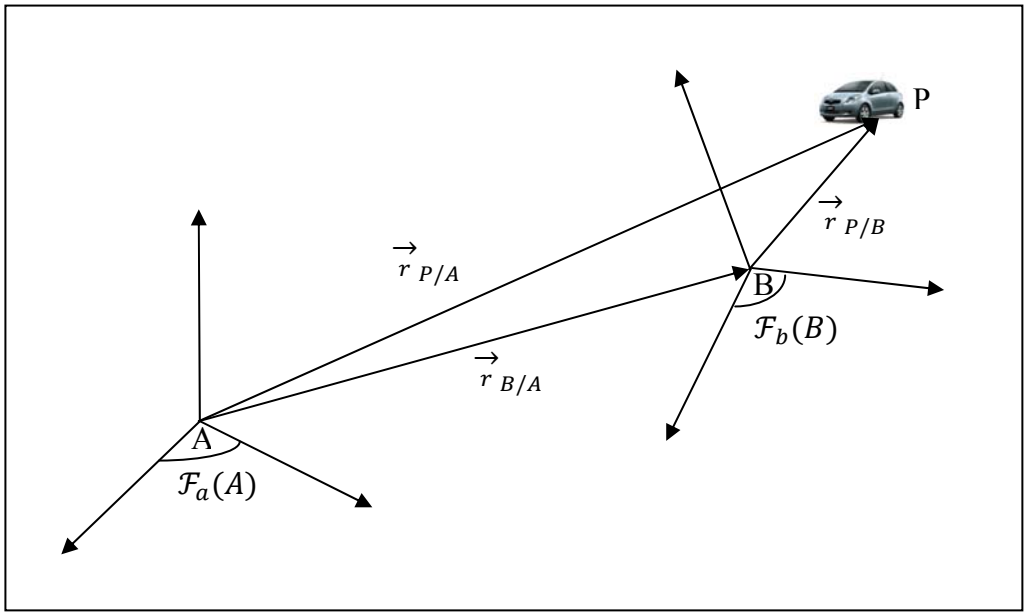

Figure B.1 Differently Moving Frames

In this appendix, the position, velocity and acceleration vectors of a point P with respect to differently moving reference frames are defined. Details are given in reference [26].

B-1 Position Equation

The position vectors of point P with respect to $\mathfrak{I}_a^{(A)}$ and $\mathfrak{I}_b^{(B)}$ can be defined as

$$\vec{r}_{P/A} = \vec{r}_{P/B} + \vec{r}_{B/A} \tag{B.1}$$

B-2 Velocity Equation

The velocity vectors of point P with respect to $\mathfrak{I}_a^{(A)}$ and $\mathfrak{I}_b^{(B)}$ can be defined as

$$\vec{v}_{P/\Im_a(A)} = \vec{v}_{P/\Im_b(B)} + \vec{\omega}_{b/a} \times \vec{r}_{P/B} + \vec{v}_{B/\Im_a(A)} \tag{B.2}$$

Here, the relative velocities of P with respect to $\Im_a^{(A)}$ and $\Im_b^{(B)}$ are derived as follows.

$$\vec{v}_{P/\Im_a(A)} = D_a \vec{r}_{P/A} = \left(\frac{d\vec{r}_{P/A}}{dt} \right)\Bigg|_{\Im_a(A)}$$

$$\vec{v}_{P/\Im_b(B)} = D_a \vec{r}_{P/B} = \left(\frac{d\vec{r}_{P/B}}{dt} \right)\Bigg|_{\Im_b(B)}$$

$\vec{\omega}_{b/a}$ is the relative angular velocity of $\Im_b^{(B)}$ with respect to $\Im_a^{(A)}$

B-3 Acceleration Equation

The acceleration vectors of point P with respect to $\Im_a^{(A)}$ and $\Im_b^{(B)}$ can be defined as

$$\vec{a}_{P/\Im_a(A)} = \vec{a}_{P/\Im_b(B)} + \vec{\alpha}_{b/a} \times \vec{r}_{P/B} + 2\vec{\omega}_{b/a} \times \vec{v}_{P/\Im_b(B)} + \vec{\omega}_{b/a} \times (\vec{\omega}_{b/a} \times \vec{r}_{P/B}) + \vec{a}_{B/\Im_a(A)} \tag{B.3}$$

Here, $\vec{\alpha}_{b/a}$ is the angular acceleration of $\Im_b^{(B)}$ with respect to $\Im_a^{(A)}$. The relative accelerations of P with respect to $\Im_a^{(A)}$ and $\Im_b^{(B)}$ are defined as follows.

$$\vec{a}_{P/\Im_a(A)} = D_a^2 \vec{r}_{P/A} = \left(\frac{d^2\vec{r}_{P/A}}{dt^2} \right)\Bigg|_{\Im_a(A)}$$

$$\vec{a}_{P/\Im_b(B)} = D_b^2 \vec{r}_{P/B} = \left(\frac{d^2\vec{r}_{P/B}}{dt^2} \right)\Bigg|_{\Im_b(B)}$$

APPENDIX C

FORMULATION OF THE ANGULAR VELOCITY OF EARTH

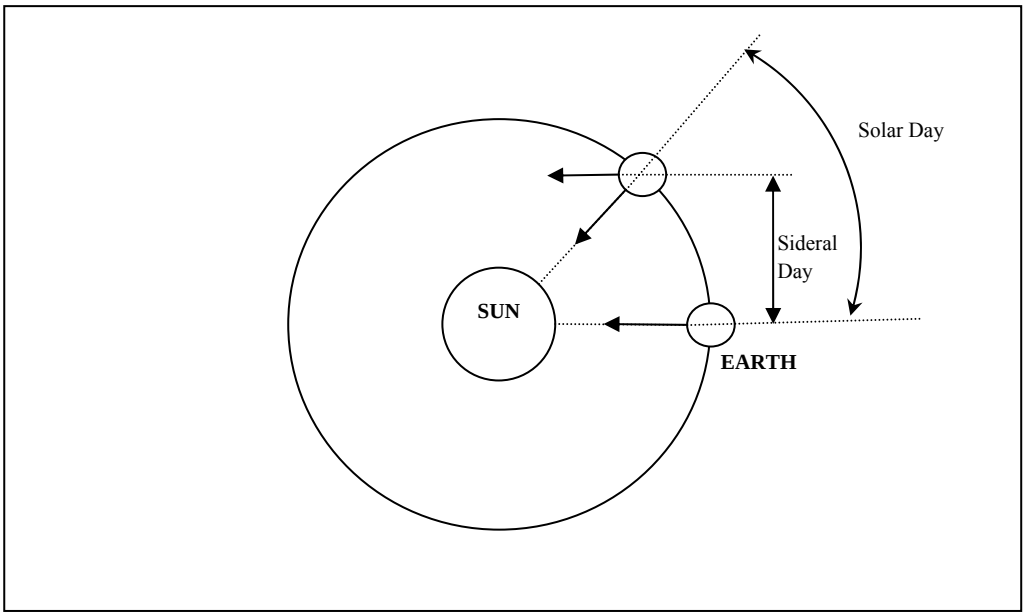

Figure C.1 Sidereal Day

Shown Figure C.1, the sidereal day and the solar day are different. The Solar day is the time taken between successive rotations for an Earth fixed object to point directly to the sun. On the other hand, the sidereal day is the time taken for Earth to rotate to the same orientation in space and this time is slightly shorter than the solar day and the difference between the solar and sidereal days is constant.

In WGS-84 model, the sidereal day is 23 h 56 min 4.1 s.

Using this information, the angular velocity magnitude $\omega_{ecef/if} = \left|\vec{\omega}_{ecef/if}\right|$ can be found as follows.

$\omega_{ecef/if}$ = 1 revolution / sidereal day

The numerical value is

$$\omega_{\text{ecef/if}} = \frac{2\pi}{86164.1} = 7.292115x10^{-5}\ \left[\frac{rad}{s}\right]$$

APPENDIX D

CROSSBOW IMU SPECIFICATIONS

Crossbow

Specification	IMU440CA-200	Remarks
Performance		
Update Rate[1] (Hz)	2-100	Programmable
Start-up Time Valid Data (sec)	< 1	
Angular Rate		
Range: Roll, Pitch, Yaw (°)	± 200	
Bias: Roll, Pitch, Yaw (°/sec)	< ± 0.75	Full temperature range
Scale Factor Accuracy (%)	< 1	
Non-Linearity (% FS)	< 0.5	
Resolution (°/sec)	< 0.06	
Bandwidth (Hz)	25	-3 dB point nominal, programmable
Random Walk (°/hr$^{1/2}$)	< 4.5	
Acceleration		
Input Range: X/Y/Z (g)	± 4	
Bias: X/Y/Z (mg)	< ±15	Full temperature range
Scale Factor Accuracy (%)	< 1	
Non-Linearity (% FS)	< 1	
Resolution (mg)	< 0.6	
Bandwidth (Hz)	25	-3 dB point nominal, programmable
Random Walk (m/s/hr$^{1/2}$)	< 1.0	
Environment		
Operating Temperature (°C)	-40 to +71	
Non-Operating Temperature (°C)	-55 to +85	
Enclosure[2]	IP66 compliant	
Electrical		
Input Voltage (VDC)	9 to 42	
Input Current (mA)	< 350	At 12 VDC nominal
Power Consumption (W)	< 5	
Digital Output Format	RS-232	
Physical		
Size (in)	3 x 3.75 x 2.50	With mounting flanges
(cm)	7.62 x 9.53 x 6.43	With mounting flanges
Weight (lbs)	< 1.3	
(kg)	< 0.58	
Connector	15 pin "D" male	

15 Pin "D" Connector Male Pinout

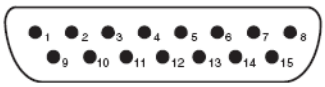

Pin	Signal
1	RS-232 Transmit Data
2	RS-232 Receive Data
3	Positive Power Input (+Vcc)
4	Power Ground
5	Chassis Ground
6	NC – Factory use only
7	NC – Factory use only
8	NC – Factory use only
9	Signal Ground
10	1PPS OUT
11	1PPS IN
12	NC – Factory use only
13	BIT Out
14	NC – Factory use only
15	NC – Factory use only

IMU440 Pin Diagram

Figure D.1 Crossbow IMU 440 Specifications

APPENDIX E

NMEA 0183 SENTENCES TRANSMITTED BY GARMIN GPS 10

Global positioning system fixed data

$GPGGA,<1>,<2>,<3>,<4>,<5>,<6>,<7>,<8>,<9>,M,<10>,M,<11>,<12>*hh<CR><LF>

<1>	UTC time of position fix, hhmmss format
<2>	Latitude, ddmm.mmmm format (leading zeros will be transmitted)
<3>	Latitude hemisphere, N or S
<4>	Longitude, dddmm.mmmm format (leading zeros will be transmitted)
<5>	Longitude hemisphere, E or W
<6>	GPS quality indication, 0 = fix not available, 1 = Non-differential GPS fix available, 2 = Differential GPS (DGPS) fix available, 6 = Estimated
<7>	Number of satellites in use, 00 to 12 (leading zeros will be transmitted)
<8>	Horizontal dilution of precision, 0.5 to 99.9
<9>	Antenna height above/below mean sea level, -9999.9 to 99999.9 meters
<10>	Geoidal height, -999.9 to 9999.9 meters
<11>	Differential GPS (RTCM SC-104) data age, number of seconds since last valid RTCM transmission (null if not an RTCM DGPS fix)
<12>	Differential Reference Station ID, 0000 to 1023 (leading zeros will be transmitted, null if not an RTCM DGPS fix)

Figure E.1 GPS Fixed Data

3D Velocity Information

$PGRMV,<1>,<2>,<3>*hh<CR><LF>

<1>	True east velocity, 514.4 to 514.4 meters/second
<2>	True north velocity, 514.4 to 514.4 meters/second
<3>	Up velocity, 999.9 to 9999.9 meters/second

Figure E.2 3D Velocity Information